UNIVERSITY OF
KWAZULU-NATAL

INYUVESI
YAKWAZULU-NATALI

Moringa oleifera crude aqueous leaf extract induces apoptosis in human hepatocellular carcinoma cells via the upregulation of NF-kB and IL-6/STAT3 pathway

By

Letitia Shunmugam

B. Sc. B. Med. Sc. (Hons) (UKZN)

Submitted in fulfilment of the requirements for the degree of

Master of Medical Science In the

Discipline of Medical Biochemistry and Chemical Pathology

School of Laboratory Medicine and Medical Sciences

College of Health Sciences

University of KwaZulu-Natal

Durban

2016

DECLARATION

This dissertation contains the original work by the author and has not been submitted in any form to another university. The use of work by others has been duly acknowledged in the text. The research described in this study was carried out in the Department of Medical Biochemistry and Chemical Pathology, School of Laboratory Medicine and Medical Science, Faculty of Health Sciences, University of KwaZulu-Natal, Durban, under the supervision of Professor Anil A. Chuturgoon and Dr Charlette Tiloke.

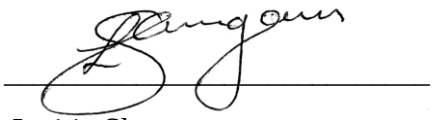

Letitia Shunmugam

21 February 2017

Date

ACKNOWLEDGEMENTS

Firstly, all praises and thanks be to God, without his assistance and grace, nothing can be possible.

I would also like to thank:

My family, for the love, support and patience without which the completion of this thesis would not have been possible. To my **Dad**, I am truly grateful for all the knowledge you have instilled in me, the sacrifices you have made and the wisdom you have imparted upon me. I would not be the person I am today if it had not been for you.

Professor Anil A. Chuturgoon and **Dr Charlette Tiloke** for your unwavering encouragement, support and guidance, throughout the course of this thesis.

Miss Nikita Devnarain, Miss Pritika Ramharack, Miss Denelle Moodley, Miss Terisha Ghazi, Miss Bestinee Naidoo, **Mr Naeem Sheik and the rest of Masters class of 2015/2016** the friends who have become family, thank you for your friendship, support and assistance.

Mrs Rene Myburg for your words of wisdom**,** support, advice and encouragement.

National Research Foundation and **UKZN College of Health Science** for the scholarship that provided financial assistance for completion of this degree.

Staff and **postgraduate students** of Medical Biochemistry and Chemical Pathology for their support and assistance throughout this thesis.

TABLE OF CONTENTS

LIST OF ABBREVIATIONS

%	Percentage
µg	Microgram
µm	Micrometre
ADP	Adenine diphosphate
AFB_1	Aflatoxin B_1
AP-1	Activator protein-1
Apaf-1	Apoptotic protease activating factor-1
APS	Ammonium persulfate
ARE	Antioxidant response elements
ATP	Adenosine triphosphate
BCA	Bicinchoninic acid
Bcl-2	B-cell lymphoma-2
Bcl-x	B-cell lymphoma-2-extra-large
BH	B-cell lymphoma-2 homology domain
BHT	Butylated hydroxytoluene
Bid	Bcl-2 homology domain-3 interacting death domain agonist
BSA	Bovine serum albumin
Caco-2	Colorectal adenocarcinoma cell
CAD	Caspase DNase
CARD	Caspase recruitment domain
CCM	Complete culture medium
cDNA	Complimentary DNA
c-FLIP	Cellular flice inhibitory protein
CO_2	Carbon dioxide
COX-2	Cyclo-oxygenase 2
Cu^+	Cuprous ion
Cu^{2+}	Cupric ion
CYP	Cytochrome P_{450}
DD	Death domain
DED	Death effector domain
Dex	Dexamethasone

DISC	Death inducing signalling complex
DM	Diabetes mellitus
DMSO	Dimethyl sulphoxide
DNA	Deoxyribose nucleic acid
dNTP	Deoxynucleotide triphosphate
EDTA	Ethylenediaminetetraacetic acid
ELISA	Enzyme-linked immunosorbent assay
ER	Endoplasmic reticulum
ETC	Electron transport chain
FAD^{2+}	Flavin adenine dinucleotide
FADD	Fas associated protein with death domain
$FADH_2$	Flavin adenine dinucleotide
Fe^{3+}	Ferric iron
FeO^{3+}	Perferryl FeO^{3+} species
g	Gram
h	Hour
H^+	Hydrogen
H_2O_2	Hydrogen peroxide
HBV	Hepatitis B virus
HBx	Hepatitis B viral proteins
HCC	Hepatocellular carcinoma
HCl	Hydrogen chloride
$HepG_2$	Hepatocellular carcinoma cell
HRP	Horseradish peroxidase
HSC	Hepatic stellate cell
IAP	Inhibitors of apoptosis proteins
IC50	Half maximal inhibitory concentration
ICAD	Inhibitors of caspase DNase
IKB	Inhibitor of Nuclear factor kappa-light-chain-enhancer of activated B-cells
IKK	Inhibitor of Nuclear factor kappa-light-chain-enhancer of activated B-cells complex
IL	Interleukin

iNOS	Inducible nitric oxide synthase
kDa	Kilodaltons
LDH	Lactate dehydrogenase
LMPA	Low melting point agarose
LPS	Lipopolysaccharide
M	Molar
mA	Milliampere
MCF-7	Breast adenocarcinoma cell
Mcl-1	Induced myeloid leukaemia cell differentiation protein-1
MDA	Malondialdehyde
mg	Milligram
Mg^{2+}	Magnesium ion
Min	Minutes
ml	Millilitres
mM	Millimolar
MO	*Moringa oleifera*
MOE	*Moringa oleifera* crude aqueous leaf extract
mRNA	Messenger ribonucleic acid
mt	Mitochondria/mitochondrial
MTT	3-(4, 5-Dimethyl-2-thiazolyl)-2, 5-diphenyl-2H-tetrazolium bromide
Na_2EDTA	Disodium ethylenediaminetetraacetic acid
NaCl	Sodium chloride
NAD^+	Nicotinamide adenine dinucleotide
NADH	Nicotinamide adenine dinucleotide hydrogen
$NADP^+$	Nicotinamide adenine dinucleotide phosphate
NADPH	Nicotinamide adenine dinucleotide phosphate hydrogen
NaOH	Sodium hydroxide
NEDD	N-(1-naphthyl)ethylenediamine
NF-kB	Nuclear factor kappa-light-chain-enhancer of activated B-cells
nm	Nanometres
NO	Nitric oxide

Nrf2	nuclear erythroid factor 2
O_2	Molecular oxygen
$O_2^{\cdot -}$	Superoxide
^oC	Degrees Celsius
OD	Optical density
P53	Protein 53
Panc-1	Pancreatic cancer cells
PARP-1	Poly (ADP-ribose) polymerase-1
PBS	Phosphate buffer saline
pg	Picogram
pH	Potential hydrogen
Pi	Phosphate
PMS	Phenazine melosulfate
PUFAs	Polyunsaturated fatty acids
Q-PCR	Quantitative polymerase chain reaction
RBD	Relative band density
RH	Substrate
RHD	Rel homology domain
RIP	Receptor-interacting protein
RLU	Relative light unit
RNA	Ribose nucleic acid
RNS	Reactive nitrogen species
R-OH	Oxidised xenobiotic metabolite
ROS	Reactive oxygen species
rpm	Revolutions per minute
RT	Room temperature
SA	South Africa
SCGE	Single cell gel electrophoresis
SDS	Sodium dodecyl sulphate
SDS-PAGE	Sodium dodecyl sulphate - polyacrylamide gel electrophoresis
SEC	Sinusoidal endothelial cell
SEM	Standard error of the mean

Smac/DIABLO	Second mitochondria-derived activator of caspases/DIABLO
STAT3	Signal transducer and activator of transcription 3
SULF	Sulphanilamide
TBA	Thiobarbituric acid
TBA/BHT	Thiobarbituric acid/ butylated hydroxytoluene
TBARS	Thiobarbituric acid reactive substances
tBid	Truncated Bcl-2 homology domain-3 interacting death domain agonist
TBST	Tris buffer saline tween 20
TCA cycle	Tricarboxylic acid cycle
TEMED	Tetremethylethylenediamine
TNF-α	Tumour necrosis factor alpha
TNFR1	Tumour necrosis factor-receptor 1
TNF-α	Tumour necrosis factor-α
TRADD	Tumour necrosis factor –receptor 1 associated protein with death domain
TRAIL-1	Tumour necrosis factor-related-apoptosis-inducing-ligand-receptor
UDP	Uridine diphosphate
USA	United States of America
V	Voltage
VCl_3	Vanadium (III) chloride
β-actin	Beta-actin

LIST OF FIGURES

CHAPTER 1

CHAPTER 2

CHAPTER 3

CHAPTER 4

LIST OF TABLES

CHAPTER 3

ABSTRACT

Introduction: *Moringa oleifera* (MO) is a highly nutritional medicinal plant mainly located in Africa and Asia. It is traditionally used to treat a diverse array of illnesses. Hepatocellular carcinoma (HCC) is one of the most common cancers worldwide and the second leading cause of cancer related deaths. This study investigated the antiproliferative and cytotoxic effect of *Moringa oleifera* crude aqueous leaf extract (MOE) in the $HepG_2$ cell line.

Materials and Methods: $HepG_2$ cells were treated with a range of MOE concentrations (0-4 000 µg/ml) over 72 h. An IC_{50} was obtained from the MTT assay and used in all subsequent assays. The cells were then assayed for oxidative stress and membrane damage (TBARS and LDH cytotoxicity), apoptotic induction (ATP levels, 3/7 activities), cytochrome P_{450} 3A4 activity (Luminometry), DNA and nuclear fragmentation (Comet and Hoechst assay). Additionally, cytokine production of IL-6 was quantified (ELISA) and relative protein expression of NF-kB, phospho-STAT3 and cleaved PARP-1 was evaluated (Western Blotting).

Results: MOE caused a dose-dependent decrease in cell viability (IC_{50} of 754.0 µg/ml), a significant increase in ROS-induced lipid peroxidation (1.23-fold, $p < 0.05$), extracellular LDH levels (1.17-fold, $p < 0.0035$) and significant decrease in intracellular ATP levels (1.46-fold, $p < 0.0441$). DNA integrity was compromised as indicated by increased DNA fragmentation ($p < 0.0001$). MOE increased protein expression of NF-kB (1.31-fold, $p < 0.0112$) and p-STAT3 (2.78-fold, $p < 0.0277$) whilst increasing cytokine production of IL-6 (1.20-fold, $p < 0.0292$). MOE induced apoptosis by significantly increasing caspase 3/7 activity (2.83-fold, $p < 0.0469$). Furthermore, MOE induced PARP-1 cleavage (1.11-fold, $p < 0.0354$) and apoptotic body formation in $HepG_2$ cells.

Conclusion: MOE does not act via the inflammatory pathway in $HepG_2$ cells however it exerts its antiproliferative, cytotoxic and genotoxic effects in human $HepG_2$ cancer cells by affecting mitochondria activity, DNA and membrane integrity and induces apoptosis in a ROS-mediated manner.

CHAPTER 1

1.1 Introduction

Moringa oleifera (MO) is an edible plant, native to Northern Indian subcontinents but is now commonly distributed throughout Asia and Africa (Ramachandran *et al.*, 1980; Anwar *et al.*, 2007; Mbikay, 2012;). It is a highly nutritious plant consumed in many countries and is also utilised in traditional medicine but in western societies, MO remains a relatively novel food substance (Anwar *et al.*, 2007; Shanker *et al.*, 2007).

Almost every part of the MO plant from the leaves to the fruit, bark and seeds can be used to treat a diverse array of ailments. The leaves are the most widely cultivated part of MO due to its phytochemical composition and their associated medicinal properties. MO leaves are a rich source of kaempferol, quercetin, alkaloids, gallic acid, tannins, saponins, vitamins and minerals (Ferreira *et al.*, 2008; Kasolo *et al.*, 2010; Leone *et al.*, 2015), all of which contribute to the anticancer, antiproliferative, antioxidant and anti-inflammatory properties of MO. In previous studies MO aqueous crude leaf extracts has expressed anticancer effects in both A549 lung cancer cells and SNO oesophageal cancer cells (Tiloke *et al.*, 2013, 2016) as well as KB tumour cells (Sreelatha *et al.*, 2011) in a ROS-dependent manner.

Inflammation is an important physiological process required to protect against infection and restore injuries sustained by tissues. Nevertheless, chronic inflammation can trigger a variety of inflammatory-associated diseases. One such disease is hepatocellular carcinoma (HCC), which is the fifth most frequent neoplasm worldwide and the second leading cause of cancer-related mortality. Primary liver malignancies account for approximately 7% of all cancers and HCC signifies more than 90% of all primary cancers (Yan *et al.*, 2015). Chronic hepatitis B virus (HBV) infection and prolonged exposure to dietary fungal toxin, aflatoxin B_1 (AFB_1) are prominent factors influencing the development of HCC amongst sub-Saharan black Africans (Kew, 2010). Other factors contributing to HCC development includes alcohol consumption, westernised diets and genetic predispositions (Sherlock and Dooley, 2008). Despite the development of new treatment modalities, HCC still remains an escalating burden in many developing countries such as South Africa and is becoming widespread throughout wealthy westernised nations (Fan *et al.*, 2014).

This study investigated the antiproliferative and cytotoxic effects of *Moringa oleifera* crude aqueous leaf extract and its effect on inflammation in the $HepG_2$ cell line after 72 hour (h) chronic exposure.

1.2 Aims and Objectives

The ***null hypothesis*** of this study is stated that MOE does not have an antiproliferative and cytotoxic effect on $HepG_2$ cells following a chronic exposure (72 h).

The ***aim***:

To determine the antiproliferative and cytotoxic effects of MOE on human hepatocellular carcinoma ($HepG_2$) cells by investigating the biochemical molecular mechanisms contributing to cell death following chronic exposure.

The ***objectives*** of the study were to investigate the effects of MOE on:

- Cell viability and metabolic activity in $HepG_2$ cells using the MTT assay.
- Cytochrome P_{450} activity and drug metabolism using luminometric quantification.
- The magnitude of ROS-induced lipid peroxidation and RNS in $HepG_2$ cells exposed to MOE by quantification of the biomarker, malondialdehyde (MDA) using the TBARS assay and the Nitrates and nitrites assay.

- Cell membrane integrity using the lactate dehydrogenase (LDH) cytotoxicity detection assay to determine the presence of extracellular LDH and intracellular luminometric quantification of adenosine triphosphate (ATP).
- The regulation, induction or inhibition of inflammatory mediators using western blotting to determine protein expression of transcription factors (NF-kB and STAT3) and ELISA to quantify cytokine production (IL-6, TNF-α, IL-10 and IL-1β).
- The apoptotic pathways induced using luminometric quantification of intracellular caspase (8, 9 and 3/7) activities.
- DNA integrity by assessing DNA fragmentation via the comet (SCGE) assay and DNA repair enzyme PARP-1 protein expression using western blotting.
- Cellular and nuclear morphological features using Hoechst nucleic stain assay.

Experimental approach:

The human hepatocellular carcinoma $HepG_2$ cell line was used as cell toxicity model to investigate the antiproliferative and cytotoxic effects of MOE against liver cancer. Cells were treated over a 72 h period with a range of concentrations to determine cell viability. This resulted in a concentration-dependent decrease in viability and the concentration which was half the maximum inhibition (IC_{50}) was deduced. This concentration was used to test the mechanisms underlying the biochemical effects of MOE.

1.3 Literature Review

1.3.1 Moringa oleifera

1.3.1.1 Botanical characterisation

The monogeneric *Moringaceae* plant family consists of a single Genus and 13 species (Dangi *et al.*, 2002; Leone *et al.*, 2015). *Moringa oleifera* (MO) is the most well-known and extensively studied member of the family (Ramachandran *et al.*, 1980; Sakpere, 2016) and is commonly referred to as the "Drumstick", "Horse radish" or "Ben oil" tree (Fahey, 2005; Spandana and Srikanth, 2016). This medium-sized, deciduous tree is rapid growing, often reaching heights between 10 to 12 metres. The thick, softwood bark appears whitish grey, branches are brittle and wide spread, surrounded by feathery greenery of tripinate leaves. It also bares bisexual yellow-white flowers in lateral clusters and pensile linear fruits (Figure 1.1) (Parrotta, 1993; Amabye and Tadesse, 2016).

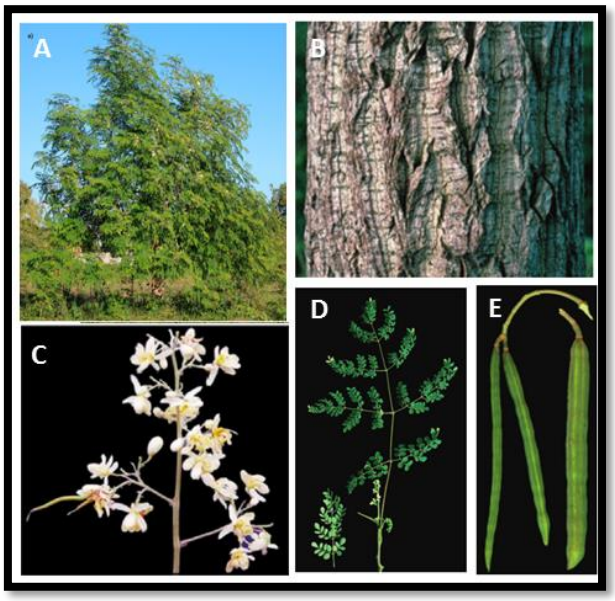

Figure 1.1: A. *Moringa oleifera* tree, **B.** Mature bark, **C.** Flower cluster, **D.** Leaves and **E.** Fruit [Adapted from (Roloff *et al*., 2009; Leone *et al*., 2015)].

1.3.1.2 Distribution

Classified as a perennial tree, MO has a life span greater than two years and favourably grows in tropical and subtropical geographical locations that experience dry to moist climate conditions (Leone *et al.*, 2015). The MO tree is indigenous to the sub-Himalayan areas of India, Afghanistan, Bangladesh and Pakistan. Once utilised by ancient Egyptians, Greeks and Romans, it has now become naturalised in many tropical locations and is an important crop cultivated throughout North and South America, Asia and Africa (Ramachandran *et al*., 1980; Anwar *et al*., 2007; Mbikay, 2012).

1.3.1.3 Traditional uses

The entire MO plant can be implemented in non-medicinal practises. The honey collected from the nectar of the flowers can be consumed, seeds are crushed and used as coagulants for water treatment and the oils are extracted and used as machine lubrication or in the production of

cosmetic products. The leaves are commonly crushed and used as organic domestic cleaning agents or as gaseous fuels (Fahey, 2005; Pereira *et al*., 2016). Worldwide, MO has mainly been associated with traditional medicine, with the leaves being utilised the most. MO leaves have high nutritional status and are therefore used as a nutritional supplement incorporated within food in developing countries plagued by malnutrition (Kasolo *et al.*, 2010). They can also be used to treat fever, malaria, skin diseases (Stevens *et al.*, 2013), wounds (Rathi *et al.*, 2006), diarrhoea (Lakshminarayana *et al.*, 2011), indigestion and eye infections (Muthu *et al.*, 2006).

1.3.1.4 Phytochemistry

Several bioactive phytochemical compounds have been positively identified in MO leaves including vitamins, flavonoids, alkaloids, tannins, saponins, oxalates and phytates (Kasolo *et al.*, 2010; Leone *et al.*, 2015).

Fresh MO leaves are a rich source of vitamin A, B, C and E. Vitamin A (βeta-carotene) has major roles in several physiological processes such as cell proliferation, differentiation, apoptosis, embryonic growth and development, vision, immune proficiency and brain function (Kidmose *et al.*, 2006). In developing countries, vitamin A deficiency is a common occurrence and may be responsible for mortality amongst women and children (Álvarez *et al.*, 2013). Among group B vitamins, only biotin, niacin, riboflavin, thiamine and pyridoxine appear to be present in MO leaves. These vitamins principally act as enzyme cofactors involved in energy production and nutrient metabolism (Moyo *et al.*, 2011; Leone *et al.*, 2015). Vitamin C is a mediator of synthesis and metabolism of many compounds, like lysine, proline, glycine hydroxylation, tryptophan, folic acid and tyrosine. Additionally, it increases gastrointestinal iron absorption by reducing ferric to ferrous state and it expedites the conversion of cholesterol into bile acids to reduce blood cholesterol levels. Vitamin C serves as an antioxidant in a bid to protect the body from various destructive effects of free radicals, toxins and pollutants (Chambial *et al.*, 2013). Vitamin E predominately functions as a lipid soluble antioxidant and modulates expression of genes. It also has an inhibitory role during cell proliferation, monocyte adhesion, platelet aggregation and bone mass regulation (Borel *et al.*, 2013). An important component of vitamin E is α-tocopherols, an antioxidant that prevents lipid peroxidation caused by the generation of free radicals. Peroxides damage cell membranes, tocopherols metabolise peroxides thus maintaining the redox state within cells. Disruption of intracellular redox state promotes oxidative stress resulting in diseases such as cancer and atherosclerosis. Elevated levels of tocopherols are found throughout the plant (Ferreira *et al.*, 2008).

Flavonoids are omnipresent, polyphenolic plant compounds containing a benzo-γ-pyrone structure and are synthesized in response to microbial infections (Kumar and Pandey, 2013). Epidemiological studies have shown that high flavonoid intake has protective effects against cancers, cardiovascular diseases and viral and bacterial infections (Pandey and Rizvi, 2009; Kumar and Pandey, 2013). The two main flavonoids found in MO leaves are quercetin and kaempferol (Leone *et al.*, 2015). Both flavonoids contain phenolic hydroxyl groups, possess antioxidant activities and provide protection against damage caused by radiation, inhibition of prostaglandin synthesis and cell cycle progression as well as mutations and carcinogenesis (Ferreira *et al.*, 2008).

Alkaloids are a group of basic plant chemical compounds existing in nature containing oxygen, nitrogen, hydrogen and carbon atoms (Goss, 2012). A great interest has been generated with regards to alkaloids due their pharmacological activities; these plant products exert antimicrobial effects through intercalation with the DNA of microorganisms. The presence of alkaloids has been positively identified in MO leaves (Sreelatha and Padma, 2009; Kasolo *et al.*, 2010).

Phenolic acids are a sub-group of naturally occurring phenol compounds derived from hydroxycinnamic and hydroxybenzoic acid (Prakash *et al.*, 2007). Gallic acid and tannins are two important phenolic compounds present in MO leaves. Gallic acid (GA) (3,4,5-tri-hydroxybenzoic acid) is a natural triphenolic compound. It provides defence against reactive oxygen species (ROS)-induce oxidative damage and is considered to be the main contributing component responsible for antioxidant properties of MO (Prakash *et al.*, 2007; Badhani *et al.*, 2015). Tannins, an important water soluble phenolic compound, bind and precipitate alkaloids and a wide variety of proteins. They have been shown to exhibit anti-hepatotoxic, anti-inflammatory and anti-cancer properties (Kancheva and Kasaikina, 2013).

Saponins are a group of natural bioactive glycoside compounds that consist of an isoprenoidal-derived aglycone, designated genin or sapogenin, linked covalently to one or more sugar molecules (Leone *et al.*, 2015). They have anti-inflammatory, antioxidant, anticancer and immunostimulatory properties (Moses *et al.*, 2014). Previous studies by Bauman *et al.* (2000) indicated saponins induced cytotoxicity in human erythrocytes by forming complexes with cholesterol present in the cell membrane leading to pore formation and permeabilisation of the cell (Baumann *et al.*, 2000; Devisetti *et al*., 2016). MO leaves also possess a rather high content of oxalates and phytates, these compounds are anti-nutritional and inhibit minerals reabsorption in the intestines (Leone *et al.*, 2015).

1.3.1.5 Pharmacological activities

Earlier studies have confirmed the pharmacological activities associated with MO such as its hypoglycaemic (Jaiswal *et al.*, 2009), hypolipidemic (Mehta *et al.*, 2003; Yadav and Srivastava, 2016), hypotensive (Dangi *et al.*, 2002; Stohs and Hartman, 2015), hepato and kidney protective abilities , all of which are mainly attributed to its leaves (Leone *et al.*, 2015).

A study by Coppin *et al.* (2013) confirmed the anti-inflammatory activity of three randomly selected samples of MO leaves and found that two samples actively attenuated the production of nitric oxide (NO) by bacterial lipopolysaccharide (LPS)-stimulated macrophage cells whilst the third sample was found to be non-active. The authors credited this variance to the plants chemical composition and genotype which can vary within the species (Coppin *et al.*, 2013). An experimental study carried out by Waterman *et al.* (2014) utilised concentrated MO leaf derived isothiocyanates on macrophages and observed a significant decrease in the gene expression of interleukin-1 beta (IL-1β) and inducible nitric oxide synthase (iNOS). In addition, the production of NO and tumour necrosis factor alpha (TNF-α) was also inhibited by both isolates (Waterman *et al.*, 2014). Kooltheat *et al.* (2014) identified that the ethyl acetate extract of MO leaves prohibited interleukin-6 (IL-6), interleukin-8 (IL-8) and TNF-α cytokine production by human macrophages (Kooltheat *et al.*, 2014). Fard *et al.*, (2015) evaluated the anti-inflammatory effect of MO hydroethanolic bioactive leaves extract and showed that it significantly inhibited the production of NO, TNF-α, IL-6, and IL-1β. The bioactive compound had induced interleukin-10 (IL-10) production in a dose-dependent manner. Additionally, the extract had efficiently inhibited the expression of nuclear factor kappa-light-chain-enhancer of activated B-cells p65 (NF-kB p65), iNOS and cyclooxygenase 2 (COX-2) in LPS-induced RAW264.7 macrophages in a dose-dependent manner (Fard *et al.*, 2015).

MO leaves also possess the capability to protect an organism against oxidative DNA damage associated with cancer. Numerous studies analysed the anticancer properties of ethanolic and water extracts of MO leaves on different types of cancer cells. The intracellular activity of MO leaves aqueous extract was a subject of interest in human KB tumour cell lines. Sreelantha and co-workers showed that MO leaves inhibit cell proliferation in a dose dependent manner (Sreelatha *et al.*, 2011). The antiproliferative effect was accompanied by apoptosis induction, morphological cellular alterations and fragmentation of DNA. In 2013, Tiloke *et al.* observed a

significant increase in ROS concurrent with diminished intracellular glutathione levels in human A549 lung cancer cells treated with MOE (166.7 μg/ml) brought about by the reduced expression and activation of antioxidant protein, Nrf-2. The apoptotic inducing properties of MO leaves was confirmed by significant increases in the activity of initiator caspase 9, effector caspase 3/7, p53 protein and elevated Smac/DIABLO expression in MO treated cells. MO leaves extract has also been pin pointed in the proteolytic cleavage and subsequent activation of poly (ADP-ribose) polymerase 1 (PARP-1) into 24 kDa and 89 kDa fragments. Hence, MOE exerts antiproliferative effects in A549 lung cells through the upregulation of oxidative stress, DNA fragmentation and apoptosis induction (Tiloke *et al.*, 2013). A study carried out by Jung *et al.* (2015) not only confirmed the antiproliferative and apoptotic induction of tumour cell but also revealed MO leaves heightened cytotoxicity on tumour cells in comparison to normal healthy cells (Jung *et al.*, 2015). In pancreatic cancer cells (Panc-1), MO leaves inhibited cell survival through cumulative cell apoptosis partially due to the down-regulation of NF-KB key signalling proteins (Berkovich *et al.*, 2013). The ethanolic extract of MO leaves inhibited cell survival and proliferation of colon cancer cell lines, hepatocellular carcinoma ($HepG_2$) , acute lymphoblastic leukaemia and acute myeloid leukaemia cells (Khalafalla *et al.*, 2010; Pamok *et al.*, 2012). A relatively recent cytotoxicity study by Charoensin demonstrated the cytotoxic effect of the dichloromethane extract of MO against several human cancer cell lines including breast adenocarcinoma (MCF-7), colorectal adenocarcinoma (Caco-2) and $HepG_2$. It was also established that the dichoromethane extract had a greater potency than the methanolic extract but both extracts were deemed non-toxic when tested on human fibroblast (Charoensin, 2014).

1.3.2 Liver

1.3.2.1 Structure and function

The liver is the largest organ of the human anatomy, it has a functional purpose in essential biological processes including bile secretion, iron and vitamin storage, plasma protein synthesis and degradation, regulation of hormones, amino acid, lipid and xenobiotic metabolism (Baynes and Dominiczak, 2007; Akhter, 2013). The human liver is comprised of four lobes and several lobules containing bile ducts, blood sinusoids and hepatocytes. The central hepatic vein passes through each lobule, surrounded by the hepatic portal vein and artery which promotes a tightly regulated communication between the liver and both the lymphatic and vascular system (Malarkey *et al.*, 2005; Zatloukalová, 2008).

1.3.2.2 Cells of the liver

Hepatocytes are the primary cell population located within the liver, other cells include hepatic stellate cells, Kupffer cells and Sinusoidal endothelial cells (Malarkey *et al.*, 2005). Hepatocytes are parenchymal cells representing 80% of all liver cells (Akhter, 2013). They actively partake in the hepatic production of bile as well as in the metabolism of vitamins, metals, lipids, glycides and proteins. Furthermore, these cells assist in energy storage, detoxification and excretion processes (Zatloukalová, 2008). Hepatic stellate cells (HSC) are storage cells for fats and vitamin A. In response to liver damage, HSC participate in the commencement and progression of hepatic fibrosis and thus may contribute toward hepatic carcinogenesis (Kmieć, 2001; Akhter, 2013). Kupffer cells are hepatic macrophages activated by gastrointestinal endotoxins. These cells are known to have high secretory, endocytic and phagocytic activities (Kmieć, 2001; Choi *et al.*, 2011). Sinusoidal Endothelial cells (SEC) are non-parenchymal cells and function as the communication mediator between the inner sinusoidal space and hepatocytes (Kmieć, 2001; Akhter, 2013). Endothelial cells also prevent the hepatic parenchymal infiltration of pathogens.

Additionally sinusoidal cells participate in the regulation of blood flow, degradation of toxic agents and in metabolic exchanges between the hepatocytes and plasma (Akhter, 2013).

1.3.2.3 Xenobiotic metabolism

The liver plays a pivotal role in xenobiotic metabolism. This mechanism of detoxification facilitates excretion of foreign chemicals from the body, however this process may lead to the unintentional rise in reactive metabolite production (Zatloukalová, 2008). Pollutants present in the environment, toxins, additives in food and drugs are just a few xenobiotics that may be encountered daily through absorption via the skin or inhalation, which leads to multiple organs being exposed to toxic xenobiotic metabolites. Xenobiotics gain access to cells by either specialised protein or passive transport. Once inside the cell, the xenobiotic is metabolised by phase I and II enzymes. Phase I enzymes include cytochrome P_{450} enzymes(Zatloukalová, 2008), which catalyses peroxidation, epoxidation, dehalogenation, deamination and hydroxylation reactions. Phase II enzymes also known as conjugation enzymes, catalyse the conjugation of phase I metabolites for the sole purpose of creating a water soluble complex which can be efficiently excreted from the body. Glutathione, adenosine-3´- phosphate-5´-phosphosulfate and uridine diphosphate (UDP)-glucuronate serve as conjugation donors (Nebert and Dalton, 2006; Zatloukalová, 2008).

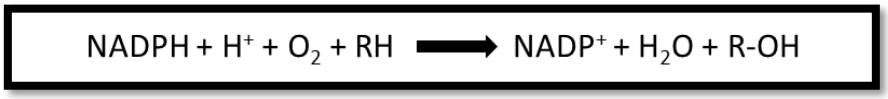

Figure 1.2: Cytochrome P_{450} catalysed chemical reaction (Kalra, 2007). RH, O_2, nicotinamide adenine dinucleotide phosphate ($NADP^+$) and R-OH represents the xenobiotic compound, oxidant, reducing agent and oxidised xenobiotic metabolite respectively.

1.3.2.4 Cytochrome P_{450}

Cytochrome P_{450} (CYP) proteins are a superfamily of heme-containing mono-oxygenases and they have a well-established role in drug discovery and development (Guengerich, 1999; Zangar *et al.*, 2004). CYP enzymes are dynamically involved in regulating the synthesis and metabolism of eicosanoids, retinoic acid hydroxylation, bile acids, cholesterol, vitamin D_3, biogenic amines and steroids (Nebert and Russell, 2002; Nebert and Dalton, 2006). Phase I reactions involved in the mechanism of detoxification are catalysed by CYP enzymes whereby they facilitate the addition of functional groups or modify existing functional groups located on the xenobiotics in order to create a more polar compound to aid phase II reactions (Westerink and Schoonen, 2007). In humans, the distribution of CYPs is widespread. They can be located in the vascular smooth muscle tissues, nasal mucosa, lungs, intestine and liver. Intestinal and hepatic CYPs play fundamental roles in oxidation of xenobiotics (Zanger *et al*., 2004; Mukherjee *et al.*, 2011; Pillay *et al.*, 2013). These enzymes also have a major role in pro-carcinogen metabolic activation and the subsequent activation to carcinogens that contribute to tumorigenesis or are capable of inducing mutations within the DNA. Thus mutations arising in CYP enzymes or dysregulation of CYP associated signalling pathways may contribute toward cancer development and disorders in organs such as the liver (Nebert and Russell, 2002; Nebert and Dalton, 2006).

1.3.2.4.1 *CYP3A4*

The CYP3A enzyme subfamily is the most abundantly expressed CYP and comprises of three isoforms, CYP3A7, CYP3A5 and CYP3A4. The most highly expressed CYP is CYP3A4 within the liver and small intestine where it represents 50% of the CYP total content and it plays a significant role in the metabolism of xenobiotic and drugs (Guengerich, 1999; Basheer and Kerem, 2015). The CYP3A4 enzyme is expressed to a lesser extent in extrahepatic tissues such as the lung (Pillay *et al.*, 2013). The CYP catalytic cycle involves molecular oxygen (O_2) reduction and oxidation. The enzyme, nicotinamide adenine dinucleotide phosphate hydrogen (NADPH)-P_{450} reductase provides electrons for the oxidation of NADPH. Generally, the cycle is initiated by the binding of substrate (RH) to the CYP's active heme-centre. The ferric iron (Fe^{3+}) is reduced, followed by the binding of O_2, reduction of O_2 and cleavage of O_2 at the O-O bond leading to the formation of water. The substrate undergoes reaction with the active perferryl FeO species (FeO^{3+}) and finally the product is released, as seen in Figure 1.3 (Guengerich, 1999; Pillay *et al.*, 2013). The CYP catalytic cycle produces ROS as a by-product. Electrons are leaked out during the cycle at various steps causing the continuous formation of ROS. Puntarulo and Cederbaum (1998) conducted a study investigating CYPs ability to generate ROS and found that CYP3A4 was the most active CYP isoform in catalysing NADPH oxidation and producing superoxide ($O_2^{\cdot -}$) (Puntarulo and Cederbaum, 1998; Pillay *et al.*, 2013).

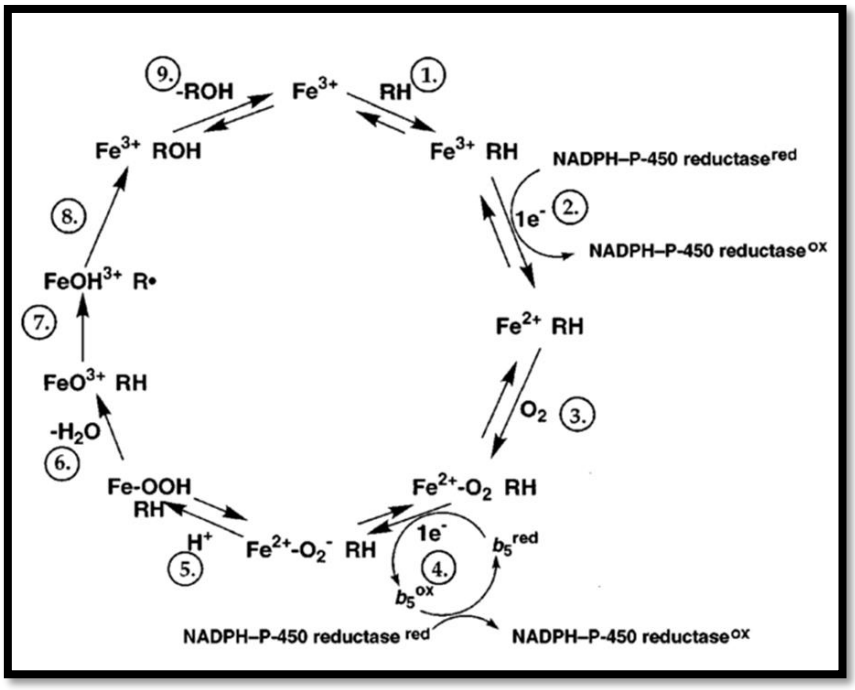

Figure 1.3: The catalytic cycle of cytochrome P_{450} 3A4 (Guengerich, 1999)**.**

Drug-drug interactions that alter the activity of CYP3A4 have been extensively studied. Consumption of drugs in combination may lead to one drug proficiently controlling the metabolism of the second drug through CYP3A4 induction or inhibition. This may result in either toxic levels of the drug or sub-therapeutic levels. In the same way, phytochemical compounds found in medicinal plants may inhibit or induce CYP3A4 and are therefore vulnerable to alterations arising in co-administered drug metabolism which may contribute to the risk of severe adverse reactions (Mukherjee *et al.*, 2011; Pillay *et al.*, 2013). On the other hand, CYP3A4 induction may lead to amplified drug elimination resulting in reduced drug plasma concentrations, diminished efficiency and effectiveness and failure of treatment (Mukherjee *et al.*, 2011).

Another possibility that may arise is increased xenobiotic metabolism such as carcinogens. This may lead to the bioactivation and transformation of substances resulting in toxic and highly reactive metabolites being formed (Westerink and Schoonen, 2007; Pillay *et al.*, 2013).

1.3.3 Cancer

1.3.3.1 Hepatocellular carcinoma

Cancer is defined as "a group of diseases characterised by unregulated division and spread of abnormal cells" (Auyang, 2006). Solid malignant tumours are a common occurrence and develop within various bodily tissues including the prostrate, breast, colon and liver. Usually malignant tumours can be treated or removed if it remains localised however they often tend to metastasise. Metastasis is a process involving the evasion of the cancer cells from the immune response, in doing so, the cancer cells survive and migrate away from the parent mass, gaining access to the blood or lymphatic circulation. They invade surrounding tissues and organs where they form lethal secondary tumours (Auyang, 2006).

In spite of the liver's detoxification and regenerative capacity, it remains the main target for toxin-induced liver damage by xenobiotic agents. Congenital and genetic predispositions, drugs, hepatitis viruses, diabetes mellitus type 2, westernised diets, alcohol and chronic inflammation are a few main factors that facilitate the development and progression of hepatic diseases ranging from fibrosis and cirrhosis to acute liver failure (Sherlock and Dooley, 2008; Koh *et al.*, 2013). These hepatic diseases are prominent predispositions for the development of hepatocellular carcinoma (HCC) (Figure 1.4). Worldwide, HCC is the most common occurring cancer and is mainly associated with hepatic cirrhosis and hepatitis B viral infections. Several cellular mechanisms and molecular pathways are evidently modified during hepatic carcinogenesis (Zatloukalová, 2008). Chronic viral infections such as hepatitis B virus (HBV) and continuous long term exposure to dietary fungal toxin, aflatoxin B_1 (AFB_1) are eminent factors in development of HCC amongst sub-Saharan black Africans (Kew, 2010). HBV association with HCC development is through its various mechanism some of which include gene expression deregulation of important cell survival (p53), differentiation (E-cadherin) and proliferation (AP-1, NF-κB and Wnt/β-catenin) genes. It also has the ability to activate or deactivate of retinoic acid β-receptor or cyclin A. additionally, HBV prompts epigenetic modifications and causes instability of chromosomes which arises from the insertion or deletion of provirus or by the direct effects exerted by the viral HBx proteins (Zatloukalová, 2008). AFB_1 exerts is tumorigenic effect through inactivation of cell cycle regulation, gene expression of p53 protein and by directly reacting with DNA molecules ultimately resulting in the formation of DNA adduct and tumour initiation (Zatloukalová, 2008). Even though the pathogenesis of HCC has been extensively studied, the molecular mechanisms underlying the aetiology of HCC remain poorly understood, particularly in regard to the role and influence of xenobiotics in the initiation of hepatic carcinogenesis (Zatloukalová, 2008).

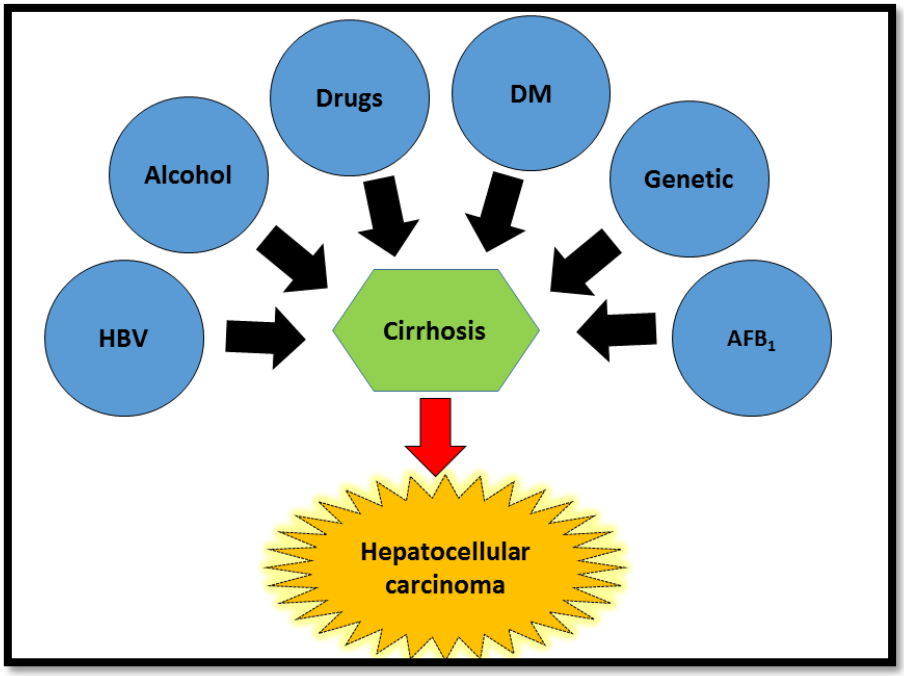

Figure 1.4: Risk factors of HCC development (Prepared by author).

1.3.3.2 In-vitro model

The attenuation of prospective drugs during the late stages of drug development is commonly attributed to drug-induced hepatic injury. Accordingly, early detection of drug-induced hepatotoxicity is a necessity prior to compounds being tested in animals and clinical trials in effort to save resources and time (Gerets *et al.*, 2012). *In vitro* model systems are often utilised in toxicity studies as it allows the study of dose-response relationships, enzyme kinetics, mechanisms of toxicity and chemical metabolism (Soldatow *et al.*, 2013). *In vitro* models have many advantages including reduced time requirements, small quantities of reagents are needed, number of animal test subjects are reduced as well as the minimised cost of animal care and maintenance (Soldatow *et al.*, 2013).

Hepatocellular carcinoma ($HepG_2$) cells are endothelial cells derived from the liver of a 15 year old Caucasian male. They are highly differentiated cells that exhibit many of the genotypic characteristics of normal hepatocytes. Hence, $HepG_2$ cells are considered as a good cell model system for studies pertaining to drug design and development, mechanisms underlying hepatocarcinogenesis, xenobiotic metabolism, cytotoxicity and genotoxicity (Soldatow *et al.*, 2013).

1.3.4 Inflammation

1.3.4.1 Mediators of inflammation

Inflammation is a fundamental part of wound healing in response to hepatic injury. Acute inflammation is beneficial as it promotes regeneration following traumatic injuries to the liver or induces the immune response to target and eradicate abnormal cells. However chronic inflammation is pernicious as persistent hepatic injury and its associated regenerative wound healing responses lead to the sequential development of fibrosis, cirrhosis and eventually

hepatocellular carcinoma (Luedde and Schwabe, 2011; Hoesel and Schmid, 2013; Bishayee, 2014). The three distinct mediators of inflammation are nuclear factor kappa-light-chain-enhancer of activated B cells (NF-kB), interleukin-6 and signal transducer and activator of transcription 3 (STAT3).

1.3.4.1.1 Nuclear factor kappa -light-chain-enhancer of activated B cells (NF-kB)

NF-kB is a dimeric complex consisting of subunits belonging to the Rel family of DNA binding proteins: p105/p50, p100/p52, RelB, c-Rel and p65 (RelA) which regulates the transcription of genes involved in cell survival, growth and differentiation, immune responses and inflammation (Beinke, 2004). NF-kB proteins have the Rel homology domain (RHD) enabling binding to DNA, dimerisation and nuclear localisation. Under normal physiological conditions, subunits p50 and RelA of dimerised NF-kB are cloistered in the cytoplasm by binding to the inhibitor of NF-kB (I-kB) proteins which consists catalytic subunits, IKKα and IKKβ and a regulatory subunit IKK γ/NEMO (Ben-Neriah and Karin, 2011). Upon a specific stimulation such as chemotherapeutic agents, stress inducers or cytokines, I-kB is phosphorylated thereby triggering its ubiquitination and degradation by the 26S proteasome. Liberated NF-kB dimer translocates to the nucleus to initiate gene transcription by binding to the kB site also identified as the consensus DNA sequence 5'-GGGRNNYYCC-3' where N is any base, Y indicates cytosine or thymine and R indicates adenine or guanine (Antonaki *et al.*, 2011). NF-kB dimerised complex is further regulated by protein phosphorylation as well as post translational modifications including protein acetylation. It also is responsible for activation of genes involved in cell death inhibition, promotion of migration and invasion of transformed cells and tumorigenesis associated mesenchymal stem cell formation (Figure 1.5) (Ben-Neriah and Karin, 2011). A possible link between cancer and NF-kB first became evident during the cloning of the p65 encoding gene, RelA. It was identified to be homologous to v-Rel, a viral oncogene. Constitutively activated NF-kB is observed in most lymphoid and solid tumours. In majority of cancer cells, NF-kB activation is maintained as a response to extracellular stimulus within the tumour microenvironment or through mutations of signalling molecules upstream of active NF-kB (Ben-Neriah and Karin, 2011). The RelA and p50 NF-kB heterodimeris crucial in the induction of inflammatory response and NF-kB -mediated pro-oncogenic activities (Yu *et al.*, 2009).

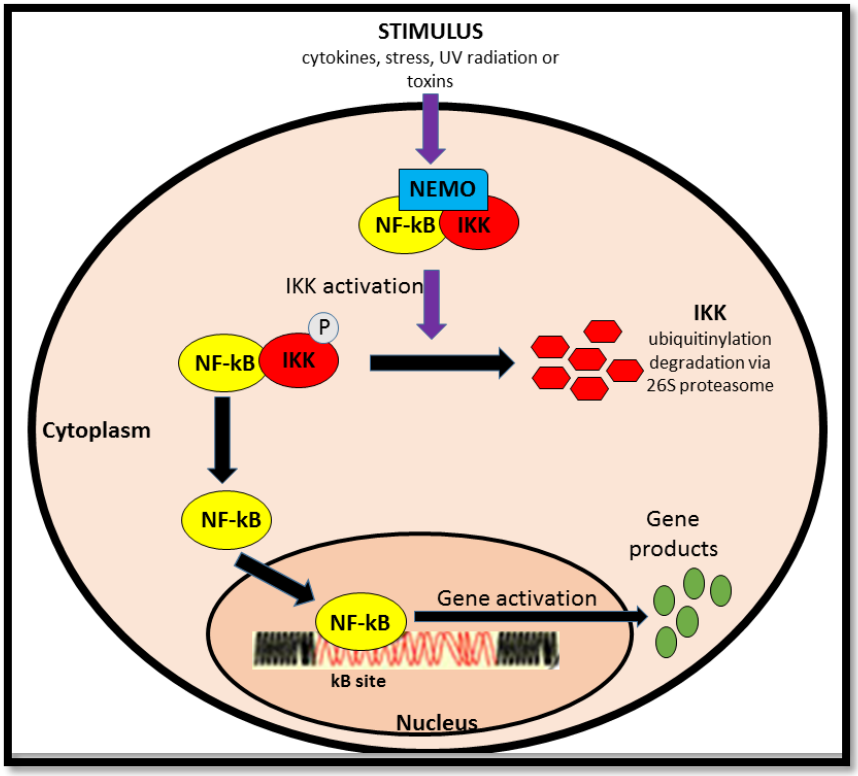

Figure 1.5: The pathway of NF-kB activation (Prepared by author).

1.3.4.1.2 Interleukin-6

Within the tumour microenvironment, STAT3 activation is dependent on NF-kB. As in most tumours, persistent activation of RelA requires continuous STAT3 signalling. Thus STAT3 signalling increases NF-kB activity. This reciprocal relationship existing between STAT3 and RelA stems from the fact that growth factors and cytokines encoded by RelA are activators of STAT3. The most crucial and important STAT3 activator downstream of NF-kB is interleukin-6 (IL-6) (Yu *et al.*, 2009; Wang *et al.*, 2011). Interleukin-6 is a pleiotropic cytokine exhibiting both pro and anti-inflammatory characteristics. This cytokine is able to exert its effects on different cell populations within the inflammatory and immune systems. IL-6 is functionally involved in B cell differentiation, T-cell activation, malignancy development and progression and chronic inflammation (Choi *et al.*, 1994; Hunter and Jones, 2015).

1.3.4.1.3 Signal transducer and activator of transcription 3 (STAT3)

STAT proteins have a central role in cytokine signalling pathways involved in cellular growth, proliferation and differentiation. The STAT family comprises of seven members: STAT1, STAT2, STAT3, STAT4, STAT5a, STAT5b, and STAT6. A distinguishable feature of STAT proteins is their dual role: in the nucleus they function as transcription factors and transduce signals through the cytoplasm (Yu *et al.*, 2009). Among the STAT members, STAT3 has garnered great interest in regard to its role in oncogenic signalling pathways and its influence in the regulation of signal transduction pathways of pro-inflammatory cytokines functional in hepatic damage and repair mechanisms (Bishayee, 2014). Inflammation and cancer are interconnected through both the intrinsic and extrinsic pathway of STAT3 activation. In transformed cells, the intrinsic pathway also known as the oncogenic pathway is activated by epigenetic or genetic

alterations such as persistent activation or overexpression of cytokine receptors with accompanying Janus kinase (JAK) family of tyrosine kinases and growth factor receptors with intrinsic activity of tyrosine kinase. Inducers of the extrinsic or environmental pathway include cigarette smoking, stress, UV radiation or carcinogens (Schmidt-Arras and Rose-John, 2016). The IL-6-STAT3 signalling pathways is initially activated by the ligation of IL-6 to its corresponding receptor. Signalling is then activated upon IL-6/IL-6R complex association with glycoprotein receptor, GP130. The GP130 receptor undergoes dimerisation and in doing so, activates tyrosine kinase JAK1 causing the phosphorylation of STAT3 protein (Schmidt-Arras and Rose-John, 2016). Phosphorylated STAT3 forms dimers and then translocates to the nucleus for direct regulation of gene expression cell proliferation, survival, invasion and metastasis. Additionally STAT3 induces the expression of inflammatory mediators including cyclo-oxygenase 2, IL-10 and IL-6, the latter of which results in further activation of STAT3 thus forming an autocrine and paracrine feedback mechanism ultimately resulting in alterations of the genetic programme and advancement of cancer associated inflammation (Figure 1.6) (Yu *et al.*, 2009).

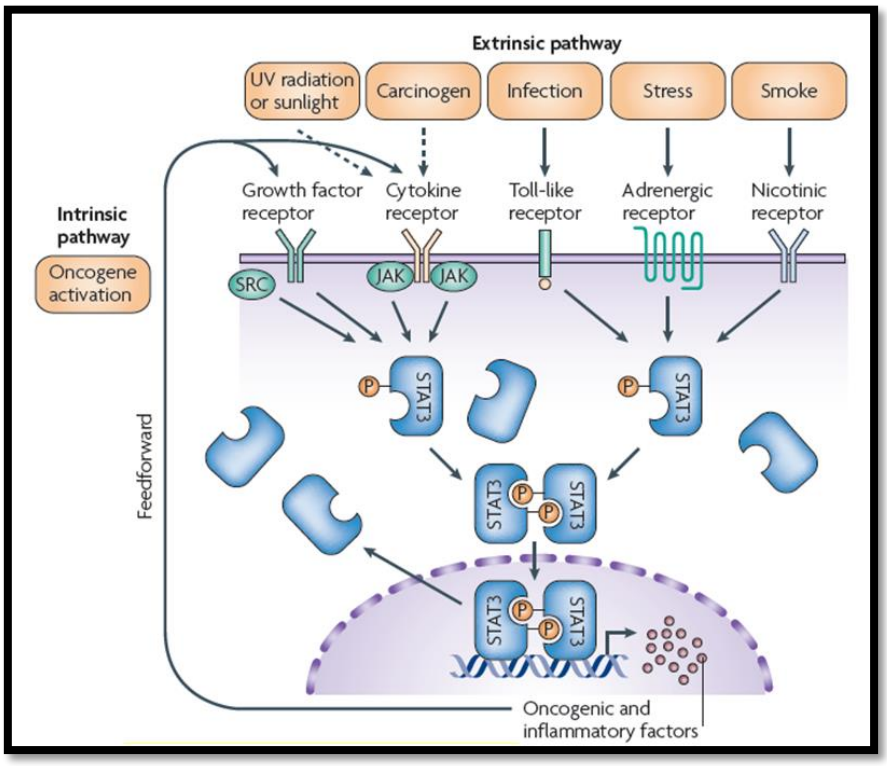

Figure 1.6: The intrinsic and extrinsic pathway of STAT3 activation linking inflammation and cancer (Yu *et al.*, 2009).

Hepatocellular carcinoma as the result of chronic inflammation is mainly induced by viral exposures, environmental pollutants, cigarette smoking and alcohol consumption (Aggarwal *et al.*, 2006). It has been established that although inflammation aids in immune responses, on a chronic level, it appears to have pro-oncogenic properties (Grivennikov *et al.*, 2010). Chronic inflammation is responsible for the overproduction of ROS, reactive nitrogen species (RNS), and inflammatory cytokines. This excessive production of ROS and RNS can eventually lead to oxidative stress and cellular DNA damage (Zhang, 2011).

1.3.5 Oxidative stress

1.3.5.1 *Reactive oxygen and nitrogen species*

ROS typically exist at low levels in aerobic cells and is formed during the metabolism of molecular oxygen (Waris and Ahsan, 2006). However, ROS can also be generated during exposure to ultraviolet (UV) radiation, reactions catalysed by metals or produced by phagocytes during inflammation (Waris and Ahsan, 2006; Rahman, 2007).

Mammalian cells depend on the mitochondria to generate energy in the form of ATP through oxidative phosphorylation, a process involving the transfer of electrons through the electron transport chain (ETC) (Martinou and Youle, 2011). The ETC is made up of enzyme-dependent complexes: complex I (NADH-Q oxidoreductase), II (succinate-Q reductase), III (Q- cytochrome c oxidoreductase), IV (cytochrome c oxidase) and V (mitochondrial ATP synthase) (Berg *et al.*, 2002). Briefly, nicotinamide adenine dinucleotide (NADH) donates a free proton to complex I which then transfers it to flavin mononucleotide (FMN) to produce flavin mononucleotide (reduced form), during this process electrons are released from NADH. Complex I transfers electrons to Flavin-adenine dinucleotide (FAD) from succinate. Electrons from both complexes are transferred to complex III via ubiquinone (co-enzyme Q). Ubiquinone carries electrons to complex III through redox reactions together with the generation of a proton gradient across the inner mitochondrial membrane. Complex IV produces a proton gradient against the transmembrane by receiving electrons from cytochrome c. Electrons are received at the active sites of complex IV with molecules of iron, copper and haem. Using the proton gradient provided, oxygen is reduced to two molecules of water by complex IV and ATP is synthesised from adenosine diphosphate (ADP) and orthophosphate (Pi) through complex V(Figure 1.7) (Berg *et al.*, 2002).

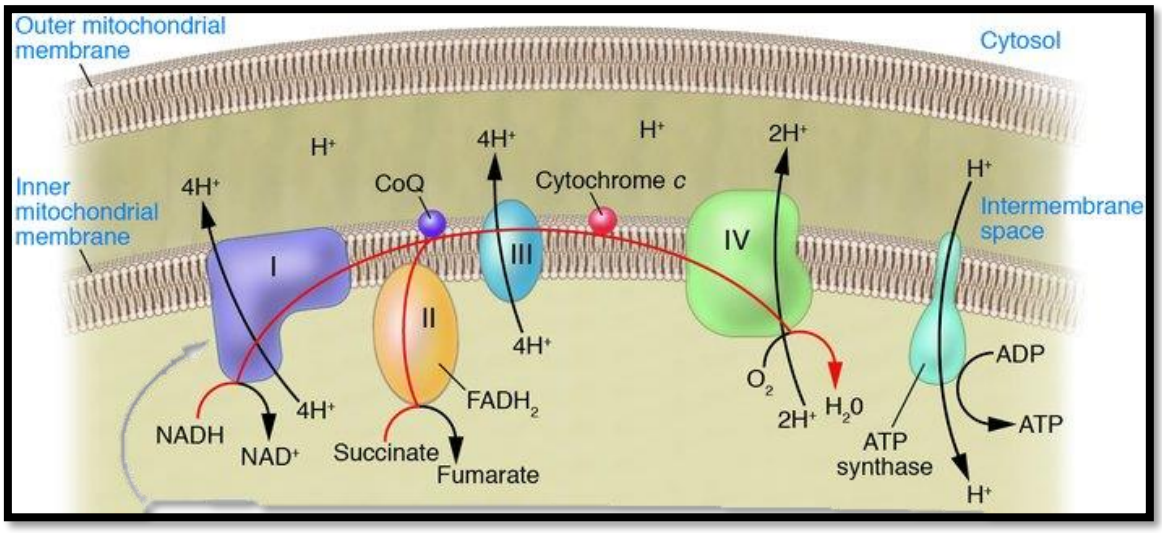

Figure 1.7: Representation of the mitochondrial electron transport chain (Nussbaum, 2005).

Within living cells, the main source of ROS is superoxide anion and hydrogen peroxide, both of which are produced as by-products of mitochondrial respiration (Waris and Ahsan, 2006). These highly reactive molecules have a dual effect as they can either be beneficial or harmful. When tightly regulated, ROS can provide added defence against infectious substances and is a functional component of cell to cell communication systems, however during adverse conditions, the balance between ROS and their elimination may be disrupted causing a significant increase in the level of

ROS, mediating damage to cellular membranes, lipids and proteins. This damage is classified as "oxidative stress" (Wei *et al.*, 2000; Rahman, 2007). DNA damaged induced by ROS has been widely recognised as a major cause of cancer (Waris and Ahsan, 2006).

Reactive nitrogen species (RNS) is another variation of oxidants derived from nitric oxide (NO), which include nitrogen dioxide (NO_2), peroxynitrite (ONOO-), nitrosoperoxycarbonate ($ONOOCO_2$-) (Nash *et al.*, 2012). A reaction between O_2- and NO_2 actively generates ONOO- and is deemed the most highly reactive RNS. It is primarily responsible for the oxidative and nitrative damage to biological cellular components including proteins, lipids and DNA (Dedon and Tannenbaum, 2004).

1.3.5.2 *Consequence of oxidative stress*

In pathological conditions, ROS and RNS are generated at a substantially higher rate than in the normal physiological state, and as a consequence, lipid peroxidation occurs. Lipid peroxidation is initiated by abstraction of hydrogen atoms from lipids containing two or more carbon atoms or by the addition of oxygen radicals resulting in undue oxidative damage towards polyunsaturated fatty acids (PUFAs) (Halliwell, 2006; Repetto *et al.*, 2012; Ayala *et al.*, 2014). This results in a single unpaired electron on the carbon atom forming a "carbon-centred radical" (Repetto *et al.*, 2012). The lipid radical firstly undergoes a molecular rearrangement to stabilise the double carbon bonds and then subsequently reacts with O_2 to form peroxyl radicals. The peroxyl radical by itself, is capable of removing a hydrogen atom from another PUFA and so starts a chain reaction (Repetto *et al.*, 2012). Peroxyl radicals readily attack adjoining side-chains and mediate the oxidation of proteins within the cell membrane (Halliwell, 2006) leading to the eventual destruction of the lipid membrane accompanied with the generation of a variety of decomposition products including ethers, aldehydes ketones and hydroperoxides which exerts genotoxic and cytotoxic effects (Esterbauer, 1993; Niki *et al.*, 2005; Repetto *et al.*, 2012). Lipid peroxidation, is thus the main molecular mechanism responsible for cellular oxidative damage and through the toxicity process, it is capable of inducing cell death (Repetto *et al.*, 2012; Ayala *et al.*, 2014).

1.3.6 Fate of the cell

1.3.6.1 *Poly (ADP-ribose) polymerase*

DNA damage is repaired by numerous proteins including those that cause cell death to prevent the future transmission of mutations or disrupt the cell cycle. Poly (ADP-ribosyl)ation is a post-translation modification of nuclear proteins consisting of the synthesis of ADP-ribose polymers on target proteins, in response to DNA damage. Synthesis of poly (ADP-ribose) is solely carried out by members of the poly (ADP-ribose) polymerase family but majority is by the most active and abundant member, poly (ADP-ribose) polymerase-1 (PARP-1). PARP-1 is a 113 kDa, zinc fingered protein consisting of 1014 amino acids. It has been implicated in several biological cellular processes including genome stability, DNA transcription, replication and repair, signalling for degradation of protein, energy source required for base excision repair and regulation of telomerase activity. Typically, in the absence of DNA damage, poly (ADP-ribosyl)ation levels are relatively low in the absence of DNA damage however in response to double or single stranded DNA breaks, PARP-1 becomes rapidly activated. In response to DNA strand breaks, PARP-1 becomes active and subsequently prompts poly (ADP-ribose) synthesis at the expense of nicotinamide adenine dinucleotide (NAD^+) which is cleaved into nicotinamide and ADP-ribose. On the target acceptor protein, PARP-1 catalyses ADP-ribose binding at the glutaminic residue thereby facilitating the elongation and branching of the protein. Inversely, decreased levels of NAD^+ results in an unbalanced NAD^+/NADH ratio which affect the Kreb's cycle, pentose shunt and glycolysis due to aberrant activation of enzymes. The redox state of cells

are also significantly altered as the cell attempts to revive the NAD^+ stores by recycling nicotinamide with two ATP molecules. However during this process, excessive PARP-1 activation leads to the depletion of intracellular ATP and NAD^+. As a result, majority if not all energy-dependent cellular processes are suddenly disrupted. Therefore, in incidences of widespread DNA damage, excessive poly(ADP-ribose) synthesis drives the cell to its death (Bouchard *et al.*, 2003). During apoptosis, executioner capase 3/7 cleaves PARP-1 into two fragments, an 89 kDa and 24 kDa fragment. This cleavage prevents the repair of DNA strand breaks, ultimately resulting in cell death (Erener *et al.*, 2012).

1.3.6.2 *Apoptosis: Programmed cell death*

Multicellular organisms maintain their functionality through the regulation of homeostasis and developmental processes by maintaining the appropriate balance between cell proliferation and death. Billions of cells on a daily basis undergo programmed cell death as it allows the cell numbers to be closely regulated (Hengartner, 2000; Sreelatha *et al.*, 2011; Govender, 2012).

Apoptosis is a process by which cells are extracellularly or intracellularly signalled to their demise as a cellular defence mechanism used to eliminate cells damaged by toxic agents, normal metabolic processes or disease (Elmore, 2007; Sreelatha *et al.*, 2011). Apoptotic cell death is energy-dependent and consists of an orchestrated set of events involving multiple caspase activation and a multiplex cascade that relates the initial stimuli to the death of the cell (Elmore, 2007). Intracellular caspases are cysteine-rich proteases that govern programmed cell death (Circu and Aw, 2010; Govender, 2012). They are synthesised as procaspases and require proteolytic cleavage for activation (Ashe and Berry, 2003). In humans, more than twelve caspases have been identified and about two thirds have been involved in the function of apoptosis (Hengartner, 2000). Caspases are classified into two groups: initiators and executioners (Govender, 2012). Both of the caspase groups, the initiator caspases (caspases 8 and 9) become activated through homodimerisation and they subsequently cleave and activate the executioner caspases (caspase 3 and 7). Caspase 3/7 are responsible for the morphological changes characteristic of apoptotic cell death, such as shrinkage of cells, chromatin condensation, DNA fragmentation, membrane blebbing and apoptotic body formation (Hengartner, 2000; Circu and Aw, 2010; Govender, 2012).

Apoptosis is divided into two pathways: extrinsic and intrinsic but ultimately both pathways converge to execute the final phase of cell death (Elmore, 2007). The extrinsic apoptotic pathway is activated through death receptor-ligand binding. The intrinsic pathway initiates apoptosis through a variety of stimuli including hypoxia, radiation, growth factor deprivation, DNA damage or oxidative stress (Mukhopadhyay *et al.*, 2014).

1.3.6.2.1 Extrinsic apoptosis: Death-receptor mediated pathway

The extrinsic pathway is induced by the interaction between the Tumour necrosis factor (TNF) superfamily and a specific associated ligand. FAS (CD-95), TNF receptor 1 (TNFR1), TNF-related apoptosis-inducing ligand-receptor 1 and 2 (TRAIL 1 and 2) are the most understood and best characterised members of the TNF superfamily (Ashe and Berry, 2003). Ligation of TNFR1 and TNF- α causes the trimerisation of the death receptor followed by the clustering of the death domains (DD) (Ashe and Berry, 2003; Elmore, 2007). The DD transmits a death signal from the cellular surface to the signalling pathways within the cell. TNFR1- associated death domain (TRADD) is recruited and binds to the DD followed by FAS-associated death domain (FADD) and receptor-interacting protein (RIP). FADD contains a death effector domain (DED) that associates with procaspase 8 via dimerization and the death inducing signalling complex (DISC) is then formed. This results in procaspases 8 being auto-catalytically cleaved for activation thereby triggering the execution step of apoptosis involving the cleavage and activation of

executioner caspases 3 and 7 (Figure 1.8). Caspase 8 also relays a signal to the mitochondria via BH3- only protein, cytosolic Bid. Caspase 8 cleaves Bid to form truncated Bid (tBid) which then translocates to the mitochondria from the cytosol and induces the release of cytochrome c (Wang, 2001). Cellular flice inhibitory protein (c-FLIP) binds to FADD and procaspase 8 rendering them inept, DISC is ineffective and apoptosis is thus inhibited (Elmore, 2007).

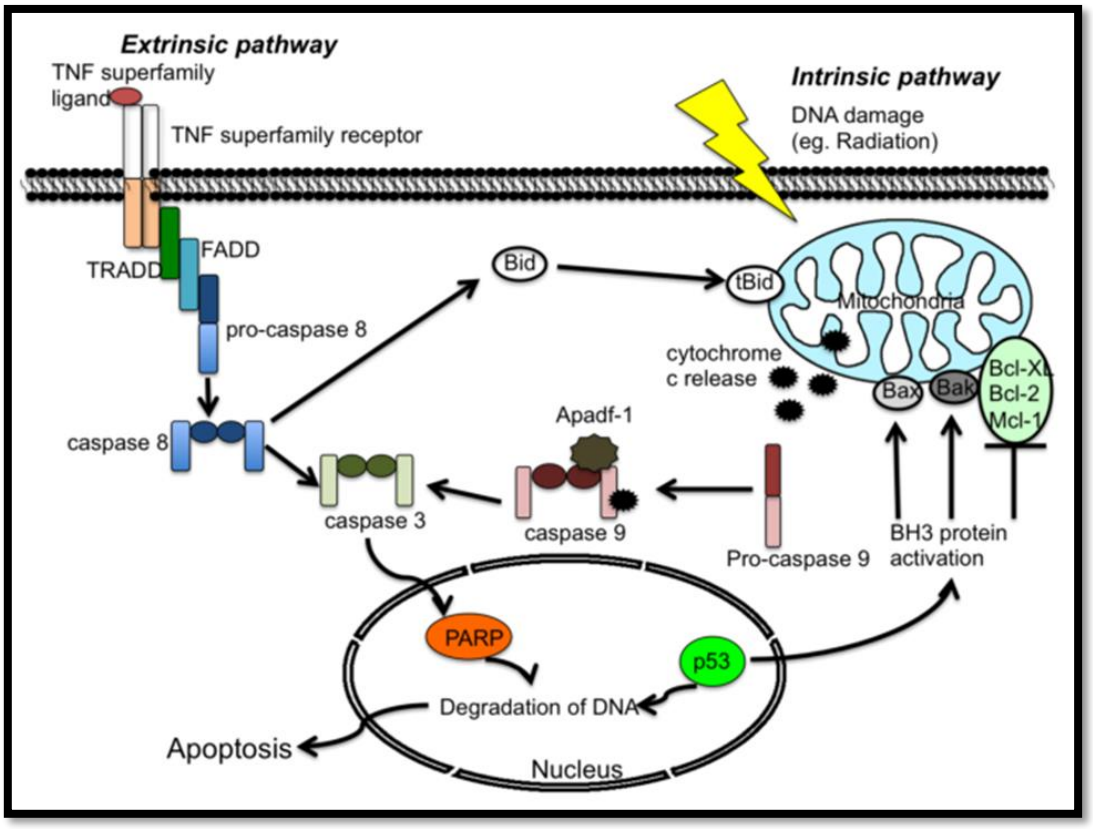

Figure 1.8: Extrinsic and intrinsic induction of apoptosis (Yuan *et al.*, 2012).

1.3.6.2.2 Intrinsic apoptosis: Mitochondrial- mediated pathway

The intrinsic pathway is initiated through several stimuli that generate intracellular signals which act specifically on targets within the cell, which is mediated by the mitochondria (Elmore, 2007). The mitochondria have a fundamental role in apoptotic cell death as it releases key proteins functional in apoptosis from its intermembrane space (Kuwana and Newmeyer, 2003). The Bcl-2 family of proteins regulate apoptosis through mitochondrial permeabilisation. Bax and Bak are apoptotic proteins that belong to the Bcl-2 family. Once a death stimulus is received, Bax experiences conformational modifications and incorporates itself into the outer mitochondrial membrane (Figure 1.8). Oligomerisation of Bak and Bax permeabilises the outer mitochondrial membrane to facilitate the release of the pro-apoptotic proteins from the mitochondria. Bcl-2, Bcl-xL and Mcl-1 are anti-apoptotic proteins also belonging to the Bcl-2 family (Hunter *et al.*, 2007). The initiating stimuli cause the inner mitochondrial membrane to change its morphology resulting in the mitochondrial permeability transitional pores opening, membrane potential is reduced and two groups of pro-apoptotic proteins are released from the mitochondria into the cytosol. The first group includes cytochrome c and second mitochondria-derived activator of caspases/DIABLO (Smac/DIABLO) both of which activates the intrinsic pathway. Cytochrome c binds to the adaptor protein apoptotic protease activating factor-1 (Apaf-1) in the cytosol, numerous procaspase 9 molecules are recruited to the caspase recruitment domain (CARD) of Apaf-1 resulting in

apoptosome formation (Wang, 2001; Elmore, 2007). Apaf-1 undergoes conformational changes and activation by ATP hydrolysis (Kim *et al.*, 2005). Apoptosis is promoted by Smac/DIABLO's ability to inhibit inhibitors of apoptosis proteins (IAP). Procaspase 9 homodimerisation leads to the activation of caspase 9. Apoptotic-inducing factor (AIF), endonuclease G and caspase DNase (CAD) form part of the second group of pro-apoptotic proteins released from the mitochondria during the latter stages of apoptosis. AIF translocates to the nucleus for the induction of peripheral nuclear chromatin condensation and chromosomal cleavage. Endonuclease G translocates to the nucleus where it induces nuclear chromatin cleavage resulting in fragmentation of DNA. Mitochondrial-released CAD translocates to the nucleus and is subjected to cleavage by caspase 3 after which it actively participates in advanced chromatin condensation and DNA fragmentation (Elmore, 2007).

1.3.6.2.3 Execution of cell death

The extrinsic and intrinsic pathways come together to activate the execution phase of apoptosis. Caspase 3 and 7 activates the cytoplasmic endonuclease and proteases for the degradation of cytoskeletal proteins and nuclear material (Figure 1.8). Caspase 3 is considered the most important of all executioner caspases. In normal dividing cells, CAD forms a complex with an inhibitor of CAD (ICAD), caspase 3 releases CAD in apoptotic cells by cleaving ICAD. Furthermore caspase 3 causes reorganisation of the cytoskeletal structure and the disintegration of cellular contents into apoptotic vesicles (Elmore, 2007).

CHAPTER 2

Materials and Methods

2.1 Materials:

MO leaves were obtained from the KwaZulu-Natal region (Durban, South Africa (SA)) and verified by the KwaZulu-Natal herbarium (Genus no. 3128). The $HepG_2$ cells were purchased from Highveld Biologicals (Johannesburg, SA). Cell culture reagents were purchased from Lonza Biotechnology (Basel, Switzerland). Western blot reagents were purchased from Bio-Rad (Hercules, CA, USA). CellTiter-Glo®, P_{450}-Glo™ and Caspase-Glo® 3/7, 8 and 9 luminometry assays were purchased from Promega. Western blot reagents were purchased from Bio-Rad (USA). All other reagents and consumables were purchased from Merck (Darmstadt, Germany).

2.2 Leaf extract preparation

To prepare the MO leaf extract (MOE), 10 g of air-dried leaves was crushed and 100 ml de-ionised water was added. The mixture was then boiled with continuous stirring for 20 min. The mixture was transferred to 50 ml conical tubes and centrifuged (720 × g, 10 min, room temperature (RT)). The upper aqueous layer (MOE) was aspirated, lyophilised and stored (4°C) until use. MOE stock solution was prepared (1 mg of MOE was dissolved in 1 ml of CCM) and filter sterilised (0.45 μM filter (Millipore).

2.3 Cell culture and treatment

The $HepG_2$ cells were cultured (37°C, 5%, CO_2) in 25 cm^3 culture flasks in complete culture media (CCM) comprised of Eagle's minimum essential medium supplemented with 1% L-glutamine, 1% *penicillin-streptomycin-fungizone* and 10% fetal bovine serum. Cell growth was monitored and CCM was changed as necessary. Confluent flasks were trypsinized using 1 ml trypsin and cell numbers were enumerated using trypan blue. Following the determination of the concentration of half maximum inhibition (IC_{50}), all treatments for subsequent assays were conducted in 25 cm^3 cell culture flasks for duration of 72 hours (h). For the 72 h exposure, treatment culture medium was replenished every 24 h.

2.4 MTT Assay

2.4.1 Introduction

The 3-(4,5-Dimethylthiazol-2-yl)-2,5-Diphenyltetrazolium Bromide (MTT) assay is a colorimetric method used to assess cell viability and proliferation. This technique is based on the reduction of MTT, a water-soluble yellow tetrazolium dye by viable cells to an insoluble formazan product. MTT enters the cell and it is reduced by NAD(P)H-dependent mitochondrial dehydrogenases resulting in the formation of an intracellular purple formazan product and reducing equivalents NAD^+/ $NADP^+$/ FAD^+. The purple formazan product is then solubilised using an organic solvent and quantified with an absorbance of 570 nm (Figure 2.1). The amount of formazan produced is directionally proportional to the number of viable cells (Mosmann, 1983; Bernhard *et al.*, 2003; Riss *et al.*, 2015).

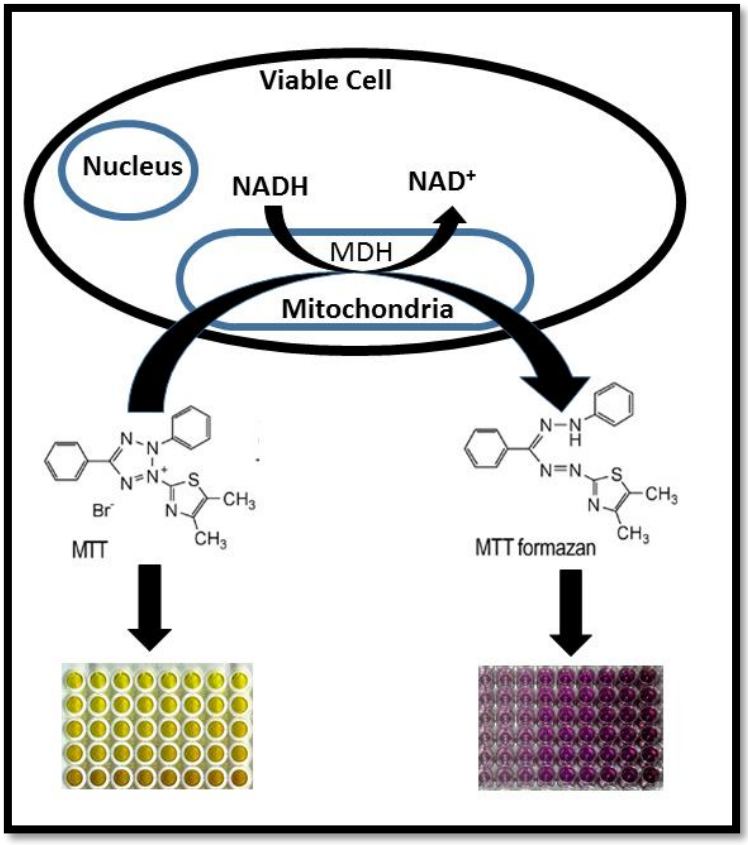

Figure 2.1: Reduction of MTT yellow salt to insoluble purple formazan by metabolically active cells [Adapted from (Riss *et al.*, 2015)]. MDH: mitochondrial dehydrogenase.

2.4.2 Protocol

The cytotoxicity of MOE in $HepG_2$ cells was measured by the MTT assay. Cells (10 000 cells/well) were seeded in a 96-well microtitre plate and allowed to attach overnight (37°C, 5% CO_2). Cells were then incubated with varying MOE concentrations (0, 250, 500, 1 000, 1 500, 2 000, 3 000, 4 000 µg/ml) in triplicate (300 µl/well) and incubated (37°C, 5% CO_2) for 72 h. Following incubation, cells were rinsed once with 0.1M phosphate buffer saline (PBS) and incubated with a MTT salt solution (5 mg/ml in 0.1 M PBS) and CCM (120 µl/well) for 4 h. Thereafter, supernatants were removed and cells were incubated in dimethyl sulphoxide (DMSO; 100µl/well) for 1 h. The optical density (OD) of the formazan product was measured at 570 nm, with a reference wavelength of 690nm by an enzyme-linked immunosorbent assay (ELISA) plate reader (BioTek µQuant, USA). The cell viability percentage was calculated by utilising the equation below and a concentration-response curve was plotted using GraphPad Prism V5.0 software (GraphPad Software Inc., La Jolla, USA). Each experiment was conducted twice on separate occasions to determine the IC_{50}. For all subsequent assays, $HepG_2$ cells were treated at 70% confluency with the determined IC_{50}.

$$\% \text{ Cell viability} = \frac{\text{mean absorbance of treated cells}}{\text{mean absorbance of control cells}} \times 100$$

2.5 ATP assay

2.5.1 Introduction

Adenosine triphosphate (ATP) is a nucleoside triphosphate, functional in energy exchange within biological systems. All metabolically active cells require ATP for survival and to appropriately execute cellular functions thus quantification of ATP serves as a useful tools in determining cell viability and cytotoxicity (Crouch *et al.*, 1993). ATP is produced via cellular respiration and glycolysis however it can also be generated through the electron transport chain, Kreb's cycle and pyruvate oxidation. It is already well established that the main contributor to ATP production is the electron transport chain via oxidative phosphorylation within the mitochondria (Riss *et al.*, 2015).

The ATP quantification assay adapts bioluminescence to determine ATP levels in cells. The assay is based on the ATP dependent conversion of a luciferase-inactive derivative in the presence of Mg^{2+} to a luciferase substrate, D-luciferin. D-luciferin readily reacts with the enzyme luciferase to produce oxyluciferin whilst in the process energy is released in the form of luminescence. The concentration of ATP is directly proportional to the luminescent signal (figure 2.2) (Crouch *et al.*, 1993).

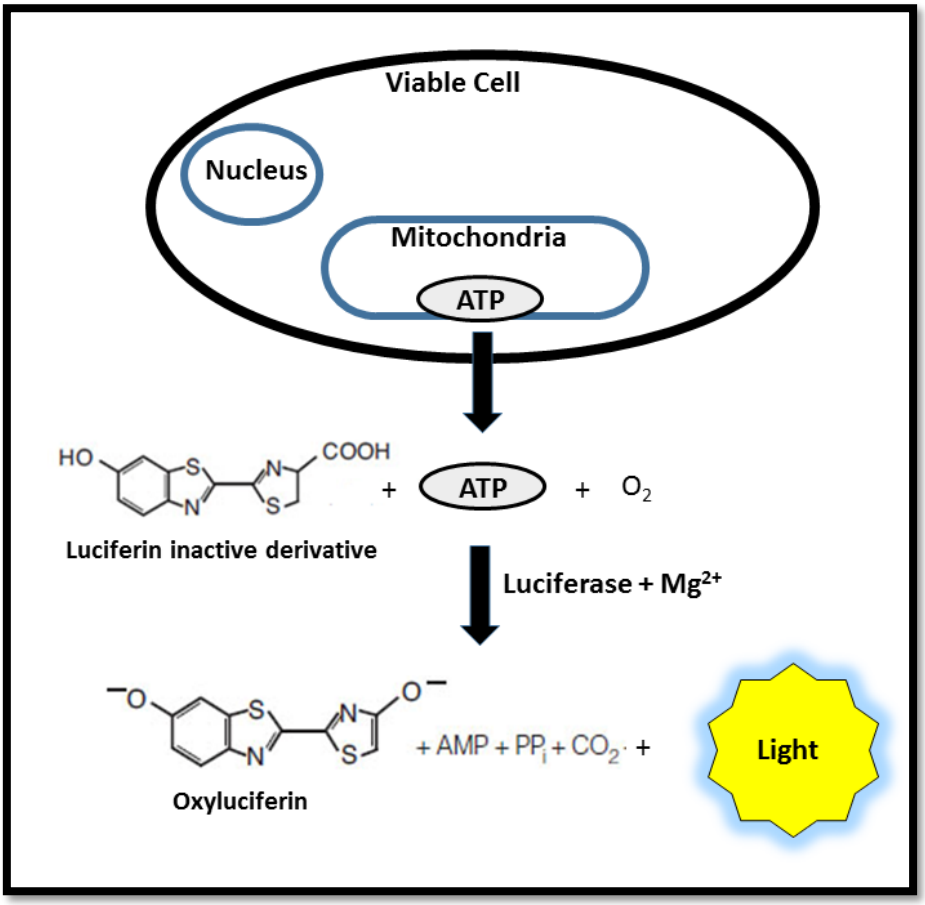

Figure 2.2: Bioluminescent reaction catalysed by luciferase in the presence of ATP, magnesium and molecular oxygen [Adapted from (Riss *et al.*, 2015)].

2.5.2 Protocol

Adenosine triphosphate (ATP) levels were quantified by the CellTiter-Glo® luminescent assay (Promega, Madison, Wisconsin, USA). Reagents were prepared according to manufacturer's instructions. Following treatment, cells were washed (3x), trypsinised and seeded into a white 96-well luminometer plate in triplicate (20,000 cells/well), followed by the addition of 20 µl of the CellTiter-Glo® reagent. The plate then incubated in the dark (RT; 30 min). Following incubation, luminescence was measured on a Modulus™ microplate luminometer (Turner BioSystems, Sunnyvale, California, USA). Data obtained was expressed as relative light units (RLU).

2.6 Cytochrome P_{450} 3A4 activity

2.6.1 Introduction

Cytochrome P_{450} enzymes are a superfamily consisting of hemeproteins, responsible for metabolism of xenobiotics and endogenous compounds. CYP3A4 is the most abundantly expressed member of the superfamily and is the main enzyme involved in hepatic drug metabolism, approximately 60% of all pharmaceutical drugs (Basheer and Kerem, 2015).

The P_{450}-Glo™ 3A4 assay utilises luminescence to provide a simple method for CYP3A4 activity quantification. The assay is based on the conversion of CYP3A4 substrate, a luciferase-inactive D-luciferin derivative, by CYP3A4 to D-luciferin. Released D-luciferin reacts with luciferase to generate a luminescent signal. The luminescent signal is directly proportional to CYP3A4 activity (Figure 2.3) (Cali *et al.*, 2006).

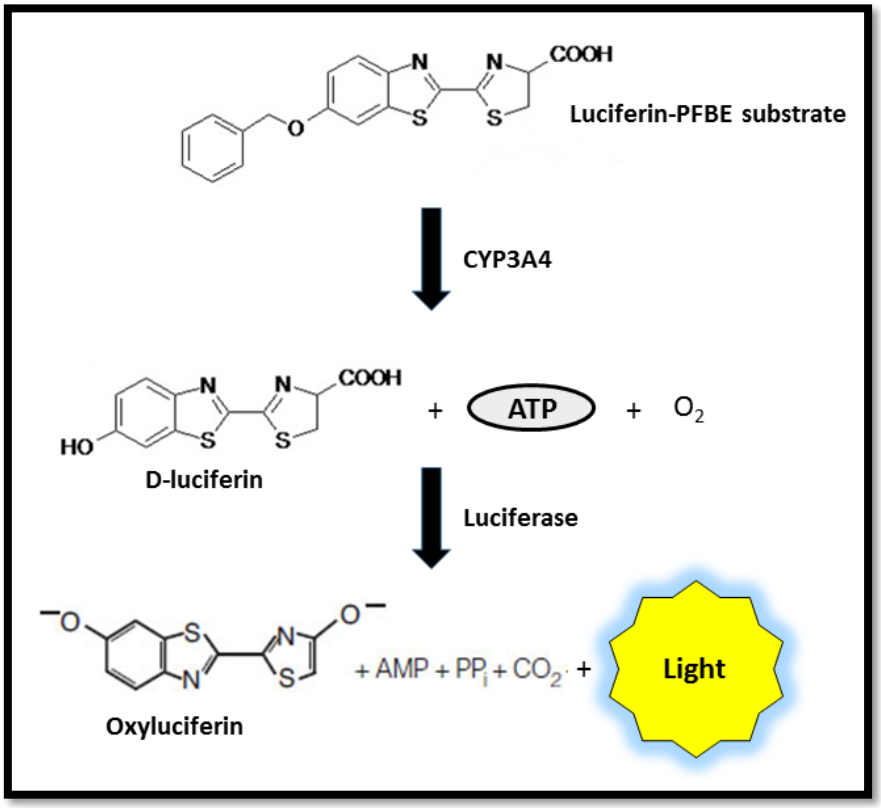

Figure 2.3: Bioluminescent assessment of CYP3A4 activity [Adapted from (Cali *et al.*, 2012)].

2.6.2 Protocol

The P_{450}-Glo™ assay kit was obtained from Promega (Madison, USA). Dexamethasone [Sigma-Aldrich (St. Louis, MO, USA)] is a known inducer of CYP3A4 activity and was used as a positive control according to manufacturer's guidelines. The luciferin-PFBE substrate and luciferin detection reagent were prepared prior to the assay according to the manufacturer's guidelines. Following MOE treatment, cells were washed (3x), trypsinised and seeded into a white 96-well luminometer plate (20,000 cells/well) in triplicate with 5 µl luciferin-PFBE substrate and incubated (37 °C; 4 h). Thereafter, 50 µl of luciferin detection reagent was added and the plate was incubated in the dark (RT; 20 min). Luminescence was measured on a microplate luminometer (Turner Biosystems, USA). Results were expressed as RLU.

2.7 Lipid peroxidation

2.7.1 Introduction

Lipid peroxidation is a process in which oxidants including non-radical and free radical species react with lipids that contain one or more carbon-carbon double bond, particularly susceptible to such reactions are polyunsaturated fatty acids (PUFAs) (Yin *et al.,* 2011). The overall process of lipid peroxidation consists of three steps: initiation, propagation and termination. Initiation results in the generation of lipid free radicals. The free radicals react with PUFAs to yield a second free radical. The free radicals are then free to react with the surrounding PUFAs leading to propagation of the chain reaction. Propagation will take place until two free radicals conjugate with one another, producing an end product to terminate the chain reaction (Repetto *et al.,* 2012). One end product commonly used as the biomarker for lipid peroxidation is Malondialdehyde (MDA) (Ayala *et al.,* 2014).

The thiobarbituric acid reactive substances assay provides a quantitative method to measure MDA concentration. It is fundamentally based on the reaction between MDA and thiobarbituric acid (TBA) butylated hydroxytoluene (BHT). MDA readily reacts with TBA to produce a red, fluorescent 1:2 MDA:TBA compound (Janero, 1990).

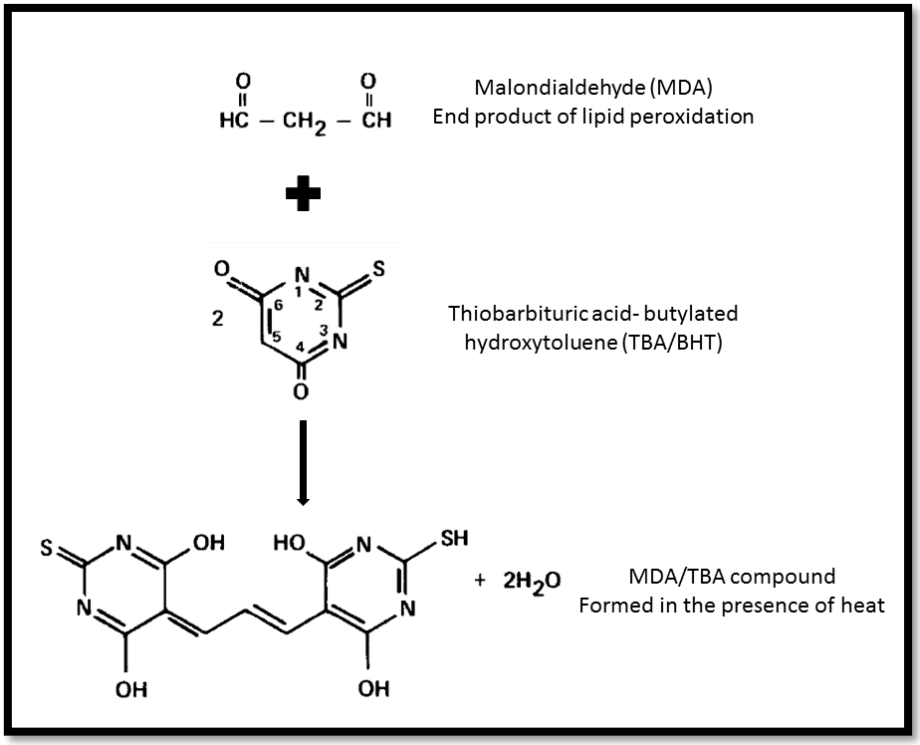

Figure 2.4: Schematic representation of TBARS reaction between MDA and TBA/BHT [Adapted from (Janero, 1990)]**.**

2.7.2 Protocol

The Thiobarbituric Acid Reactive Substances (TBARS) assay was used to assess the oxidative damage incurred by MOE on $HepG_2$ cells. TBARS measures MDA, an end product of lipid peroxidation. Following MOE treatment, supernatant from samples (200 µl) were aliquoted, in duplicate, into clean glass test tubes, followed by the sequential addition of 2% phosphoric acid (200 µl), 7% phosphoric acid (400 µl) and TBA/BHT solution (400 µl). MDA served as a positive control. All samples were adjusted to pH 1.5 and boiled for 15min to allow for the reaction occur (Figure 2.4). Once cooled to RT, butanol (1.5 ml) was added to each test tube, vortexed and allowed to separate into distinct phases. The upper butanolic phase (800 µl) was transferred into micro-centrifuge tubes and centrifuged (13200 rpm, 6 min, RT). Each sample was aliquoted into a 96-well microtitre plate in triplicate (100 µl/well). Optical density was measured using a spectrophotometer at 532 nm with reference wavelength of 600 nm (BioTek µQuant, USA). The assay was completed on three separate occasions to determine MDA levels. The sample means were calculated and divided by the absorption coefficient, 156 mM^{-1} to yield the mean MDA concentration (µM).

2.8 Nitrates and nitrites assay

2.8.1 Introduction

Endogenous Nitric oxide (NO) is produced from L-arginine by nitric oxide synthases (NOS) and plays important role in the modulation of inflammation, immune response and cell communication. NO is an unstable diatomic free radical with an extremely short half-life. It undergoes rapid oxidative degradation to form stable metabolite products, nitrate (NO_3^-) and

nitrite (NO_2^-). NO is shortly lived and therefore cannot be appropriately and efficiently quantified, so its metabolites are used for the colorimetric indirect determination of NO. This allows for an accurate and sensitive method of identifying the overall NO status in the sample of interest (Bryan and Grisham, 2007).

In the colorimetric assay, vanadium (III) chloride (VCl_3) is used to catalyse the reduction of NO_3^- to NO_2^- which is then quantified by the Griess reaction (Figure 2.5).

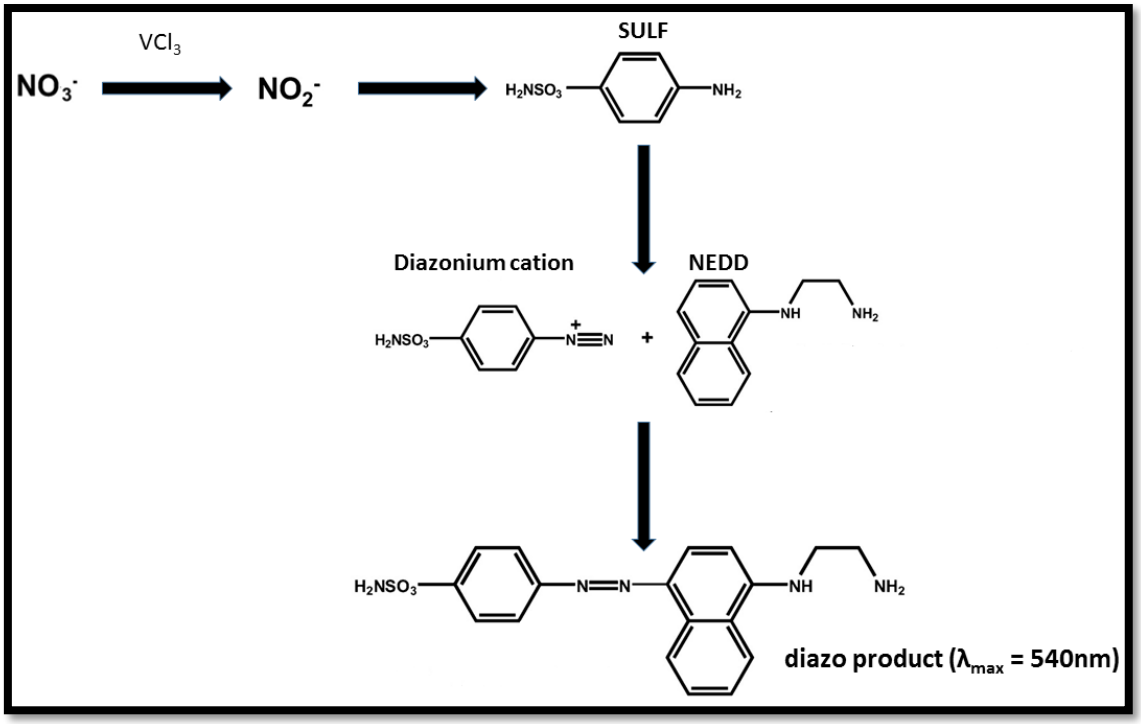

Figure 2.5: The Griess Reaction [Adapted from (Tarpey *et al.*, 2004)]. This involves a two-step diazotisation reaction, NO_2^- reacts with sulphanilamide (SULF) to produce a diazonium cation which couples to N-(1-napthyl)ethylenediamine (NEDD) to form a red-violet chromophoric diazo product (Tsikas, 2007).

2.8.2 Protocol

The nitrates and nitrites assay was used to quantitate the effect of MOE on NO production in $HepG_2$ cells. Proceeding MOE treatment, supernatant from samples and standards (0, 3.125, 6.25, 12.5, 25, 50, 100, 200 µM) (50 µl) were aliquoted, in triplicate, into a 96 well microtitre plate, VCl_3 (50 µl), SULF (25 µl) and NEDD (50 µl) were sequentially added to all wells and the plate incubated (dark, 30 min, 37ºC). Absorbance was measured at 540 nm with reference wavelength 690 nm. Standard means were used to generate a standard curve which was used to determine the nitrates and nitrite levels in the samples. Data was represented as µM.

2.9 LDH Assay

2.9.1 Introduction

Lactate dehydrogenase (LDH) is a stable cytosolic enzyme present in almost all mammalian cell types (Chan *et al*., 2013). During anaerobic glycolysis, lactate is subjected to an oxidation

reaction catalysed by cytosolic LDH and co-enzyme nicotinamide-adenine dinucleotide (NAD^+) to form pyruvate and NADH. The re-oxidation of NAD+ is very important as it ensures the concentration of NAD^+ is adequately high to sustain the glycolytic flux. Cell damage due to intercellular signals, stress or injuries results in the rapid release of LDH from the cell membrane into the extracellular medium (Figure 2.6). Thus, measurement of the extracellular LDH levels serves as a biochemical marker for cytoxicity and cell death (Fiume *et al.*, 2014).

The LDH assay consists of a two-step process involving the enzymatic reaction whereby NAD^+ is reduced to $NADH/H^+$ by the oxidation of lactate to pyruvate. Thereafter, phenazine methosulphate (PMS) or diaphorase catalyst transfers H/H+ from $NADH/H^+$ to a tetrazolium salt to yield a formazan product (Chan *et al.*, 2013).

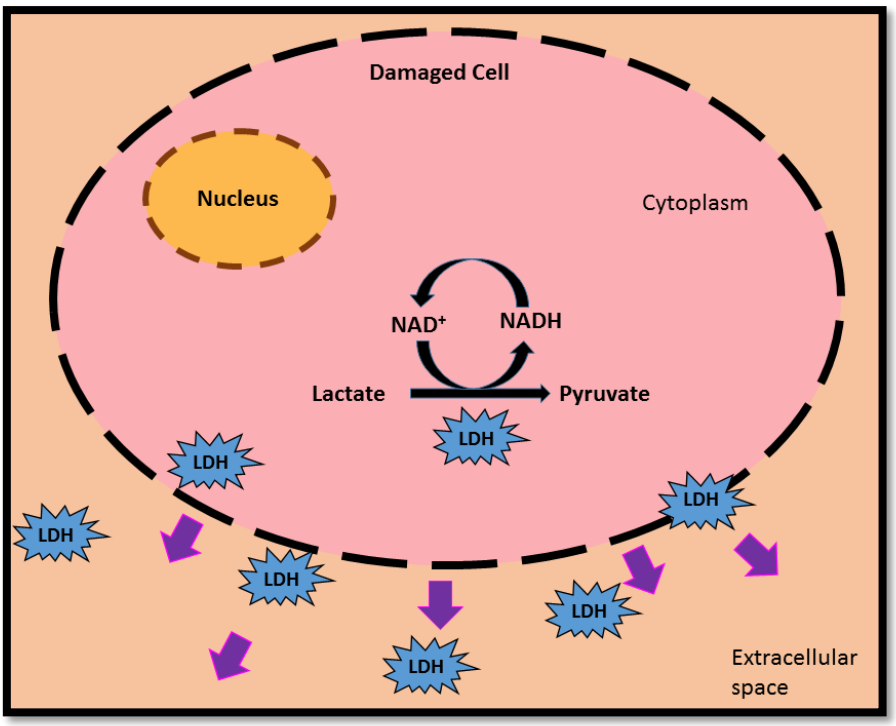

Figure 2.6: Schematic representation of LDH release from a damaged cell [Adapted from (Forest *et al.*, 2015)].

2.9.2 Protocol

LDH activity was measured using the Lactate Dehydrogenase (LDH) cytotoxicity detection kit (11644793001) (Roche, Mannheim, Germany). Sample supernatants (100µl) were transferred, in triplicate, into a 96-well microtitre plate. Thereafter, substrate mixture (100µl) containing catalyst (diaphorase/NAD^+) and dye solution (INT/sodium lactate) was added into each well and allowed to react (25 min, RT). A formazan product was formed and optical density was measured at 500nm with an ELISA plate reader (BioTek µQuant, USA). The data obtained was represented as mean optical density.

2.10 ELISA assay

2.10.1 Introduction

The Enzyme-Linked Immunosorbent Assay (ELISA) is a biochemical method for the qualitative or quantitative detection of analytes such as cytokines. This assay is based on the specific binding between an antigen and its antibody (Cox *et al.*, 2014). The sandwich ELISA was used to quantify cytokine concentrations.

Briefly, wells of an ELISA microtitre polystyrene plate are coated with cytokine antibodies. When the sample is added, the cytokines interact with their corresponding antibodies and form complexes. Once the enzyme-conjugate secondary antibodies are added, they bind to the cytokine. The Streptavidin-HRP working solution is responsible for the substrate that ultimately produces colour (Figure 2.7). The colour intensity is directly proportional to the amount of cytokines present in the samples (Cox *et al.*, 2014).

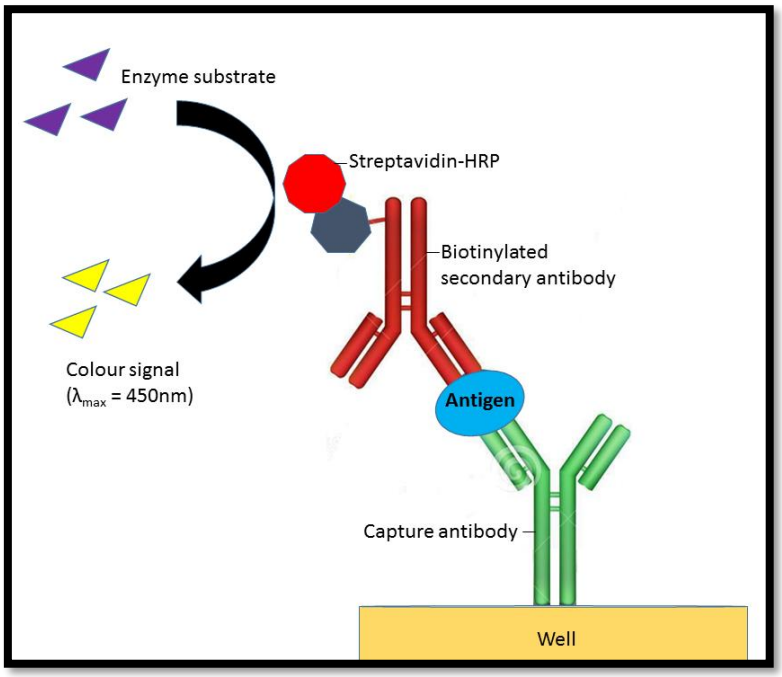

Figure 2.7: Sandwich ELISA [Adapted from (Cox *et al.*, 2014)]. Post coating of wells, analytes binds to their respective antibodies, the biotinylated secondary antibodies are added and bind to the analytes. This is followed by the interaction of the streptavidin labelled enzyme to the biotin molecule. Lastly, an enzyme substrate is added and subsequently converted to generate a colour directly proportional to the cytokine concentration (Cox *et al.*, 2014).

2.10.2 Protocol

The sandwich ELISA was used for the detection of the following cytokines IL-6, IL-10, TNF-α and IL-1β. A 96-well ELISA plate was coated with 100 µl Capture Antibody (cytokine antibody) diluted in Coating Buffer and incubated overnight (4°C). Coated wells were aspirated, washed thrice with 300 µl wash buffer and blocked with 200 µl Assay Diluent (RT, 1 h). After blocking, wells were aspirated and washed thrice with wash buffer (300 µl). Sample and standard dilutions were prepared in Assay Diluent and 100 µl of each was subsequently added to the wells and incubated (RT, 2 h). Wells were aspirated and washed five times (300 µl), 100 µl Working Detector was then added into each well and the plate incubated (RT, 1 h). The Working Detector

was aspirated and the plate washed seven times (300 µl). After the seventh wash, 100 µl of Substrate Solution was added and incubated (dark, RT, 1 h). Finally, 50 µl Stop Solution was added to each well and the optical density (OD) was measured at 450 nm, with a reference wavelength of 570 nm by an enzyme-linked immunosorbent assay (ELISA) plate reader (BioTek µQuant, USA). Data was represented as picograms per ml (pg/ml).

2.11 Caspase activity

2.11.1 Introduction

Caspases are a family of cysteine proteases that have a central role in the initiation and execution of programmed cell death. Caspases are expressed in all types of cells and are initially produced as inactive zymogens, only once an apoptotic signal is received, does activation occur (McIlwain *et al.*, 2013).

Luminometric caspase activity assay is used to quantify caspase activation. This assay involves luminogenic substrate conjugated aminoluciferin cleavage by the caspase. The aminoluciferin serves as the luciferase substrate, upon its release; it reacts with luciferase in the presence of ATP and molecular oxygen to generate a luminescent signal (Figure 2.8). This luminescent signal is directly proportional to the level of caspase activity in the sample (Brunelle and Zhang, 2010).

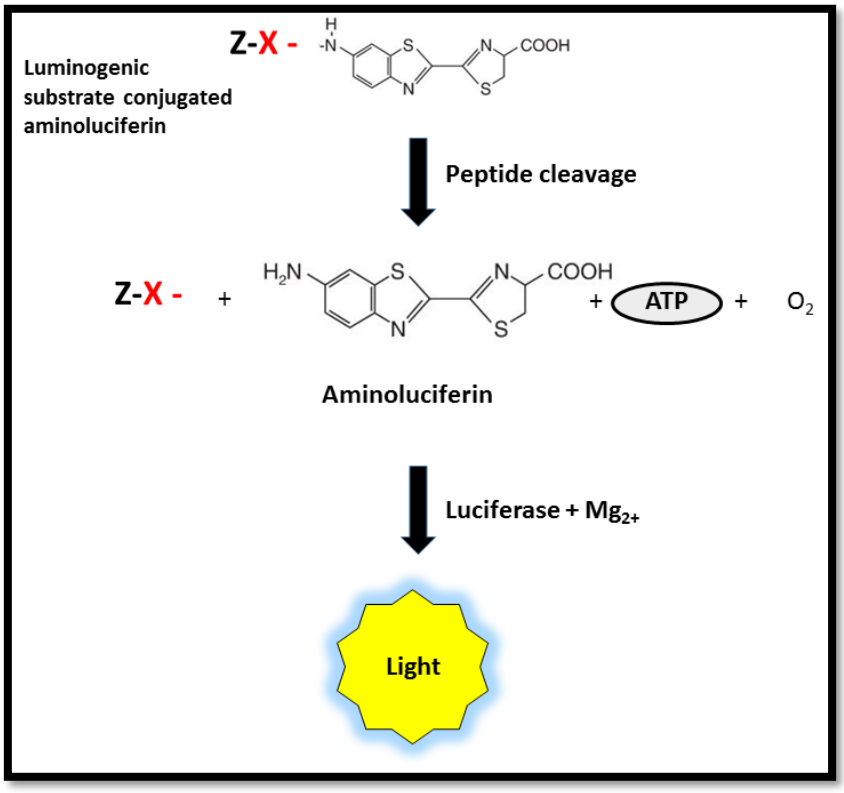

Figure 2.8: Bioluminescent quantification of caspase 8, 9 and 3/7 activity [Adapted from (Brunelle and Zhang, 2010; Riss *et al.*, 2015)]. X represents the peptide sequence: LETD (caspase 8), LEHD (caspase 9) or DEVD (caspase 3/7).

2.11.2 Protocol

Caspase-Glo® 8 (G88201) and Caspase-Glo® 9 (CG8211) and Caspase-Glo® 3/ 7 (G8092) was used to assess apoptosis (Promega, Madison, USA). Reagents were prepared according to manufacturer's guidelines. MOE treated and untreated cells were added to wells of a white 96-well microtitre plate in triplicate (20,000 cells in 50 µl 0.1M PBS/well). Caspase reagent (20 µl) was added and incubated in the dark (30 min, RT). The luminescent signal was measured on a Modulus™ microplate luminometer. The assay was conducted on three separate occasions to determine caspase activities and results were expressed as relative light units (RLU).

2.12 Single cell gel electrophoresis (SCGE) assay

2.12.1 Introduction

Single cell gel electrophoresis (SCGE), best known as the comet assay, is a simple, rapid technique used to detect DNA damage in cells in response to genotoxic stimuli (Collins, 2004; Liao *et al.*, 2009). The comet assay is based upon the quantification of DNA fragments migrating from the cell's nucleus during electrophoresis. DNA fragmentation is regarded as a biochemical hallmark of late apoptosis and is facilitated by proteins induced downstream of the apoptotic cascade (Matassov *et al*., 2004; Olive and Banáth, 2006). Initially, it could only be used to detect double stranded DNA breaks however in 1988, Singh *et al.* optimised the protocol in alkalinic conditions to not only allow for the detection of double stranded DNA breaks but also DNA single stranded breaks and alkali-labile sites (Singh *et al*, 1988; Liao *et al.*, 2009). The alkalinic comet assay involves cells embedded in agarose gel which thereafter are immersed in lysis buffer. The damaged DNA strands released during cell lysis yield the comet tail following electrophoresis. Undamaged DNA does not migrate and remains intact in the comet head (Figure 2.9) (Choucroun *et al.*, 2001).

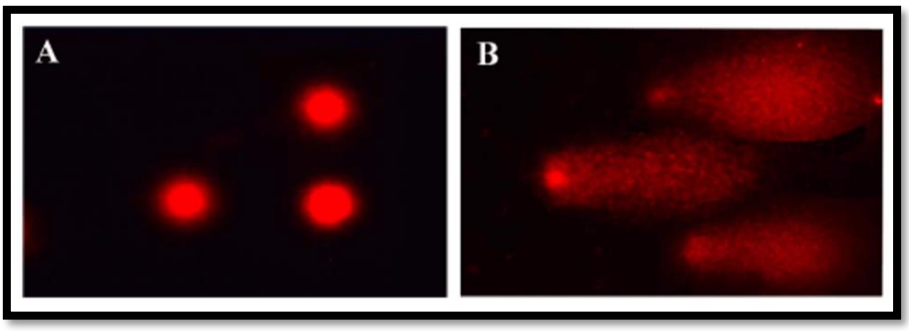

Figure 2.9: Formation of comet tails after electrophoresis (Kumar *et al.*, 2012). **A.** The head of the comet contains intact, undamaged high molecular weight DNA. **B.** If breaks are present in the DNA, the DNA supercoil becomes relaxed allowing the smaller DNA fragments to migrate out of the nucleus during an applied current thus forming a 'tail'. Comet tail length indicates extent of DNA damage (Olive and Banáth, 2006).

2.12.2 Protocol

The comet assay was used to determine DNA fragmentation in MOE treated cells. Briefly, three microscope slides were prepared per control and treatment with a first layer containing 700 µl of 2% low melting point agarose (LMPA, 37°C) which were incubated (10 min, 4°C), a second layer of 25 µl of cell suspension (20,000 cells suspended in 0.1 M PBS) from each sample with 175 µl 1% LMPA (37°C), and 1 µl GelRed ™ Nucleic Acid Gel Stain (Biotium, California, 41003)

which was allowed to solidify (10 min, 4°C). A third layer containing 200 µl of 1% LMPA (37°C) was then added and incubated (10 min, 4°C). Cover slips were removed and slides were submerged in cold cell lysis buffer (2.5 M NaCl, 100 mM EDTA, 1% Triton X-100, 10 mM Tris (pH 10) and 10% DMSO) (4°C, 1 hr). The slides were equilibrated in electrophoresis buffer (300 mM NaOH, 1 mM Na_2EDTA, pH 13; 20 min) then electrophoresed (300 mA, 25 V, 35 min) after which slides were washed three times (0.4 M Tris, pH 7.4, 5 min). Cover slips were placed onto slides and viewed using a fluorescent microscope (Olympus IX51 inverted microscope 510-560 nm excitation and 590 nm emission filters). Images were captured and comet tails of 50 cells were measured using Life Science-Soft Imaging System (analySIS® v5). The results were expressed as mean comet tail length (µm).

2.13 Hoechst assay

2.13.1 Introduction

Hoechst 33342 is a permeable blue fluorescent nucleic dye that's used extensively in fluorescent microscopy. Hoechst has the ability to pass through intact cell membranes and bind to the minor grooves in the DNA double helix, specifically to adenine-thymine-rich regions (Figure 2.10). The nucleic dye aids in the visualisation and identification of morphological characteristics associated with normal cell cycle and apoptosis using fluorescent microscopy (Chazotte, 2011).

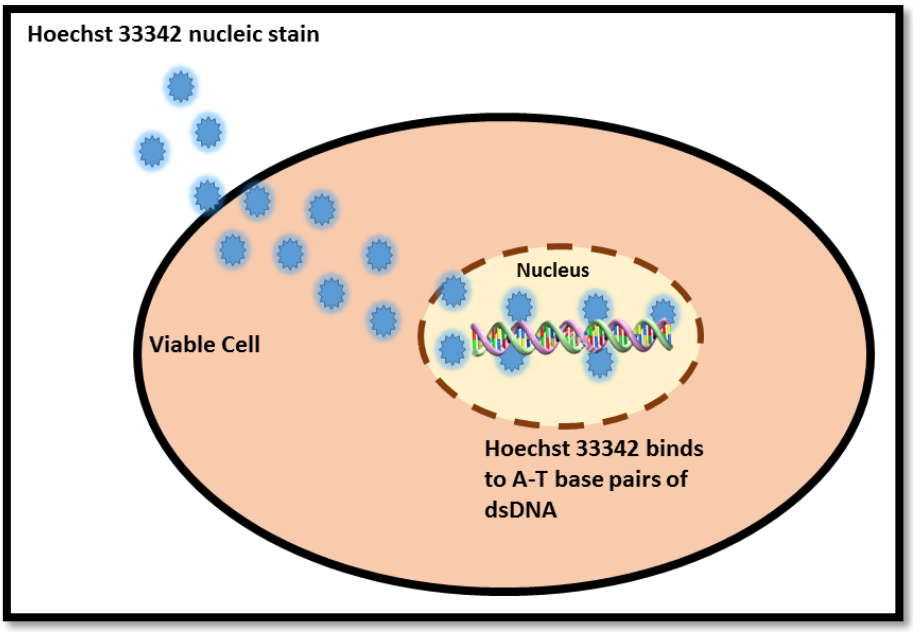

Figure 2.10: Nuclear staining of metabolically active cell using Hoechst 33342 (Prepared by author).

2.13.2 Protocol

Hoechst 33342 stain was used to assess the effect of MOE on nuclear material. Cells were seeded (300 000 cells/well) into a 6 well plate and treated in triplicate for 72 h. Cells were washed 3 times with 0.1 M PBS and fixed with 10% paraformaldehyde for 5 min. After fixation, cells were washed with 0.1 M PBS and the Hoechst working solution was added (5 µg/ml, Molecular probes,

Eugene, OR) and incubated (15 min, 37°C) Images were captured using a fluorescent microscope (Olympus IX51 inverted microscope using 350 nm excitation and 450 nm emission filters). Three images per treatment replicate were captured at 20x and 40x magnification.

2.14 Western Blot

2.14.1 Protein preparation

Protein from cells was isolated using Cytobuster™ reagent (Novagen) supplemented with phosphatase and protease inhibitors (Roche, 04906837001 and 05892791001respectively). Cytobuster (200 µl) was added to the cells and incubated on ice (30 min) and subsequently centrifuged (10 000 xg; 4°C, 10 min) to obtain a crude protein extract. Following protein isolation, crude extracts were quantified and standardised using the bicinchoninic acid (BCA) assay (Sigma, Germany). The BCA assay principle is based on the Biuret reaction. The Biuret reaction measures the conversion of Cu^{2+} to Cu^{+}. In alkaline conditions, Cu^{2+} ions reacts with peptide bonds to form Cu^{+}, which in turn reacts with BCA to produce an intense purple coloured product quantified at 562 nm. Protein quantification is necessary in order to determine the concentration of proteins present within the samples. Protein standards (0; 0.2; 0.4; 0.6; 0.8, 1 mg/ml) were prepared using bovine serum albumin (BSA). Both the protein standards and samples were plated (25 µl). The plate was then incubated (30min, 37°C) and the absorbance was measured using the ELISA plate reader (BioTek µQuant, USA). The absorbance generated from the standards was used to create a standard curve to determine protein concentrations of the samples which were subsequently standardised to 1.5 mg/ml in Cytobuster. Standardisation of proteins is essential, as it ensures each well contains the same concentration and volume of sample thereby providing an accurate comparison of the protein expression. Once the proteins were standardised, samples were prepared with Laemmli buffer containing Tris-HCl, SDS, bromophenol blue, β-mercaptoethanol and glycerol. Tris-HCl is used as buffer to maintain correct pH range of the sample. Sodium dodecyl sulphate is an anionic detergent capable of protein denaturation through the formation of micelles around the polypeptide. A negative charge is generated which enables the migration of the protein in the gel, during an applied electric field, toward a positive electrode. Bromophenol blue is a tracker dye used to monitor protein migration during electrophoresis, β-mercaptoethanol breaks disulphide bonds to facilitate band separation in accordance to molecular size and weight and lastly, glycerol adds density to the sample allowing the sample to sink to the bottom of the well, reducing the occurrence of sample dissemination between wells. Samples were then denatured by boiling for 5min at 100 ºC with a 1:4 dilution of 5 x Laemmli sample buffer [0.5 M Tris-HCL (pH 6.8); 10% SDS; 2% bromophenol blue; 12% β-mercaptoethanol and 3% glycerol in dH_2O].

2.14.2 Electrophoresis and Transfer

After sample preparation, Sodium dodecyl sulphate polyacrylamide gel electrophoresis (SDS-PAGE) is used to separate the proteins based on molecular size. SDS-PAGE gels were prepared using a gel cassette with glass plates. The higher concentration resolving gel is added first followed by the lower concentration stacking gel. A 10% SDS-polyacrylamide resolving gel and a 4% stacking gel was prepared [10% SDS, Tris, Bis-Acrylamide, dH_2O, 10% Ammonium persulfate (APS), TEMED]. TEMED activates bis-acrylamide, which acts as a cross linking agent that facilitates the polymerisation of the acrylamide gel to create a porous matrix through which the proteins can migrate. APS is an oxidising agent used in conjunction with TEMED to facilitate bis-acrylamide polymerisation. This migration allows the proteins to be separated by molecular weight, whereby smaller proteins migrate a further distance through the polyacrylamide gel in comparison to the larger proteins. Samples were loaded onto the gel (25 µl/well) and

electrophoresed (150 V, 1 h). Thereafter, protein bands present in the gel were transferred to a nitrocellulose membrane. The transfer method involves stacking the electrophoresed polyacrylamide gel, nitrocellulose membrane and fibre pads in a cassette, submerged in tank buffer and an external electric current is applied (400 mA, 1 h) (Figure 2.11). The electric current allows the transfer of the protein bands from the gel to the membrane.

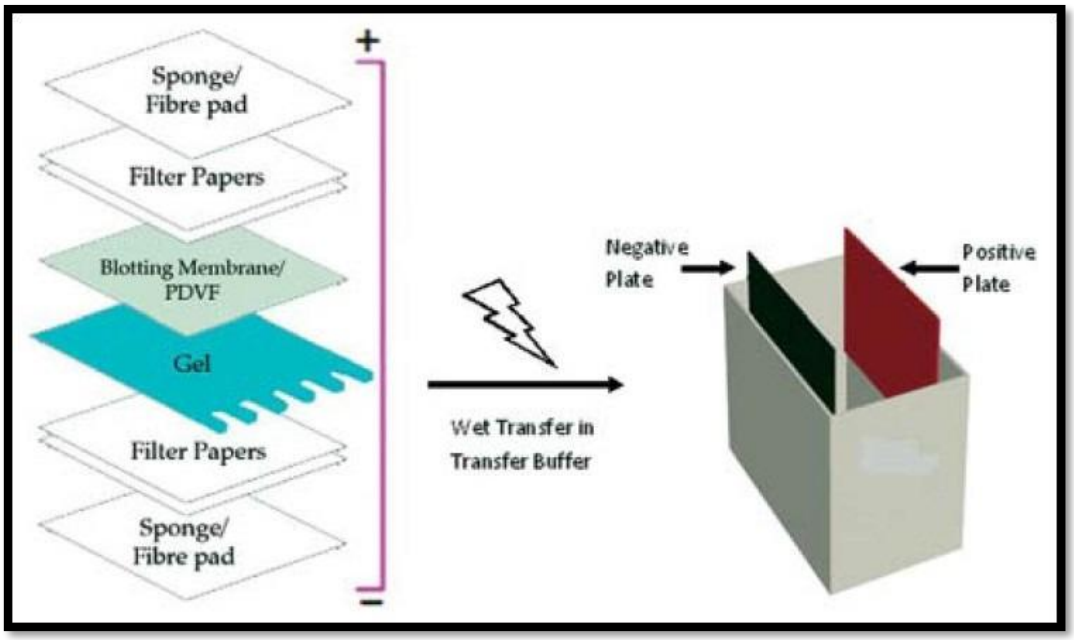

Figure 2.11: Transfer of proteins from the SDS gel to the nitrocellulose membrane (Mahmood and Yang, 2012).

2.14.3 Immunodetection

Immunodetection is a multistep process. The nitrocellulose membrane containing the transferred protein bands were incubated with a protein solution which covers the entire surface of the membrane to prevent non-specific binding of proteins. Membranes were blocked with 5% BSA in Tris buffer saline (20 mM Tris-HCl (pH 7.4), 500 mM NaCl and 0.01% Tween 20 (TBST)) for 2 h. An indirect method of immunodetection was implemented whereby two different antibodies were used in succession, as depicted in Figure 2.12. The membranes were probed with primary antibodies: NF-kB p65 (ab3033, Cell Signalling), phospho-STAT3 (ab9145, Cell Signalling), total-STAT3 (ab4904, Cell Signalling) and PARP-1 (ab110915, Cell Signalling), diluted to 1:1000 in 5% BSA. The membranes were then incubated for 2 h on a shaker at RT followed by overnight incubation at 4°C. After incubation, membranes were equilibrated to RT, washed 5 times (10 ml TTBS, 10 min) and incubated with horse radish peroxidase (HRP)-conjugated secondary antibody (goat anti-rabbit: 1:10,000 in 5% TTBS, RT, 1 h).

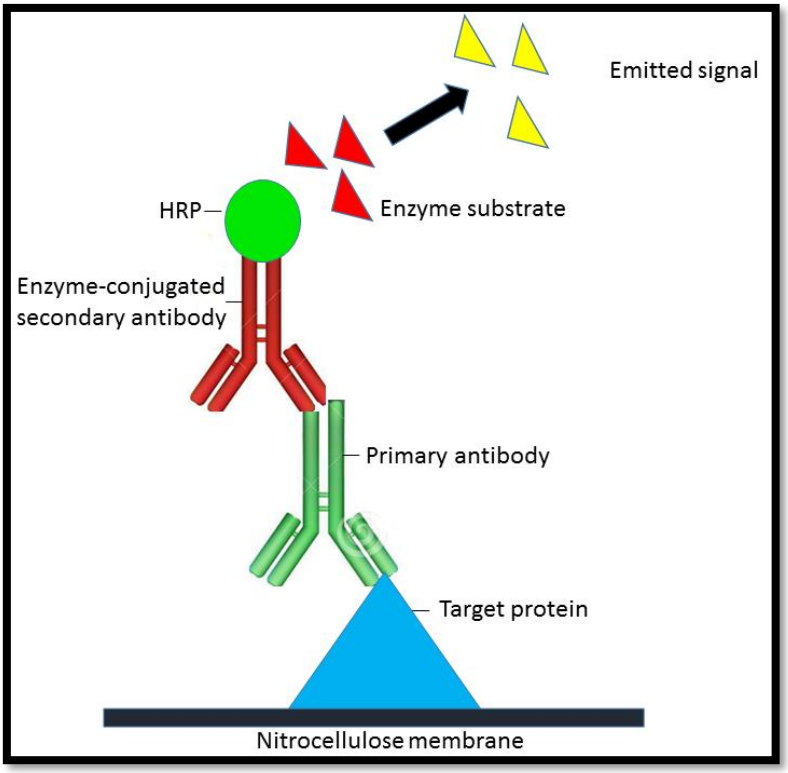

Figure 2.12: Overview of indirect immunodetection involving antigen-antibody interactions (Prepared by author).

Membranes were washed 5 times (TTBS, 10 min). A Clarity Western luminal/enhancer solution and peroxide substrate solution (catalog no. 1705061, Bio-Rad) was added onto each electro-blotted nitrocellulose membrane to form the antigen-antibody complex. The generated signal was detected using the Chemidoc™ Imaging System (Bio-Rad) and protein expression was analysed with Image Lab™ Software (Bio-Rad). The membranes were then quenched with 5% H_2O_2, rinsed thrice (10 min, TTBS), blocked in 5% BSA (2 h; RT) and probed with β-actin (ab8226) (Sigma, St Louis, Missouri, USA) in a 1:5 000 dilution with 5% BSA (30 min) for protein normalisation and loading control. The data was expressed as fold change (FC).

2.15 Statistical Analysis

Data was expressed as mean optical density with standard deviations for the MTT assay and IC_{50} was determined using the dose-response inhibition equation (Log inhibition versus variable slope). For the data obtained from subsequent assays, an unpaired t-test with Welch's correction was performed. The data was represented as means ± standard deviations. A *p* value of 0.05 was considered to be statistically significant. These statistical tests are available on GraphPad prism version 5.0 software.

CHAPTER 3

Results

3.1 Metabolism

3.1.1 MTT assay

MOE toxicity in $HepG_2$ cells was determined using the MTT assay. A dose-response was determined using MOE concentrations in the range 0 to 4 000 µg/ml for 72h (95% Cl= 30.52 to 40.77) (Figure 3.1). Analysis of the curve showed that 754.0 µg/ml MOE caused 50% cytotoxicity in $HepG_2$ cells. This IC_{50} concentration was used in all subsequent assays (Appendix A).

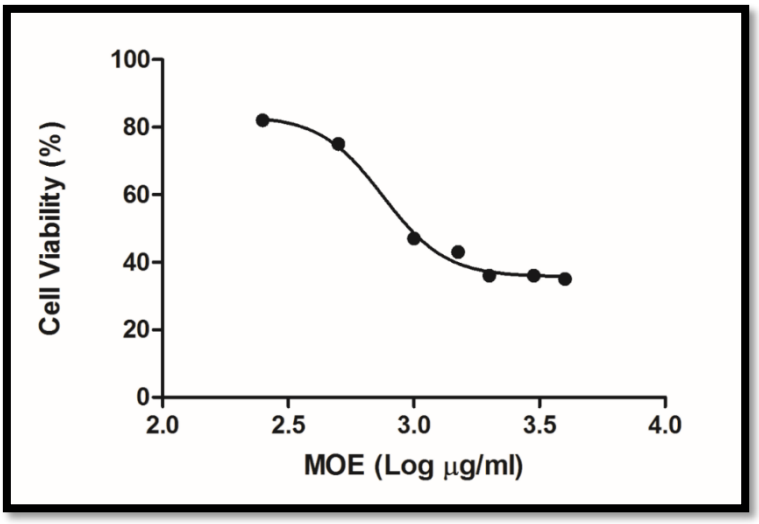

Figure 3.1: Cell viability of $HepG_2$ cells treated with MOE for 72h. Data is represented as viable cell percentage relative to the untreated control. A dose-dependent decline was observed in $HepG_2$ cell viability after MOE treatment.

3.1.2 ATP Assay:

Cellular ATP levels were quantified using the Cell Titre-Glo® assay. MOE significantly reduced ATP levels 1.46-fold (3 507 000 ± 201 700 RLU) compared to the control (4 982 000 ± 96 820 RLU, $p < 0.0441$) (Figure 3.2).

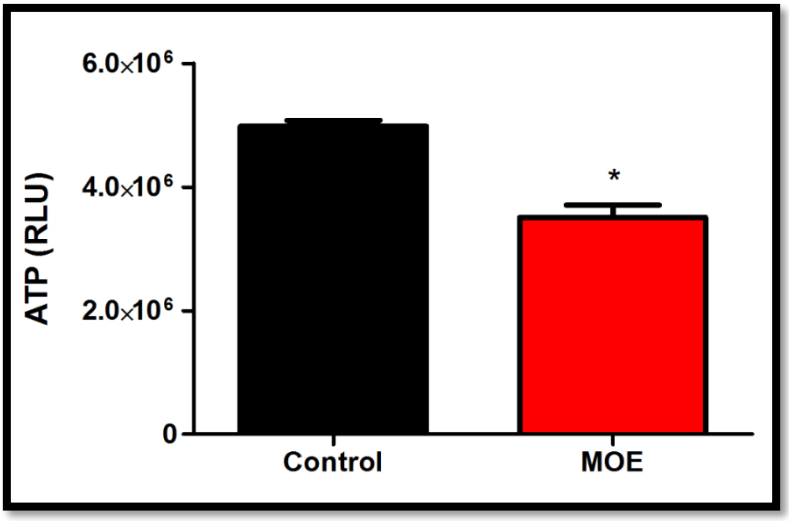

Figure 3.2: Intracellular ATP levels were significantly depleted in MOE treated cells after 72 h (* $p < 0.0441$). RLU: relative light units.

3.1.3 Cytochrome P_{450} 3A4 activity

P_{450}-Glo™ assay was used to determine CYP3A4 catalytic activity. A significant 1.38-fold decrease was seen in CYP3A4 activity in MOE treated cells (1 020 ± 1.155 RLU) compared to the control cells (1 411 ± 46.19 RLU, $p < 0.0004$). Dexamethasone was used as a positive control (6730 ± 875.9 RLU, $p < 0.0012$) (Figure 3.3).

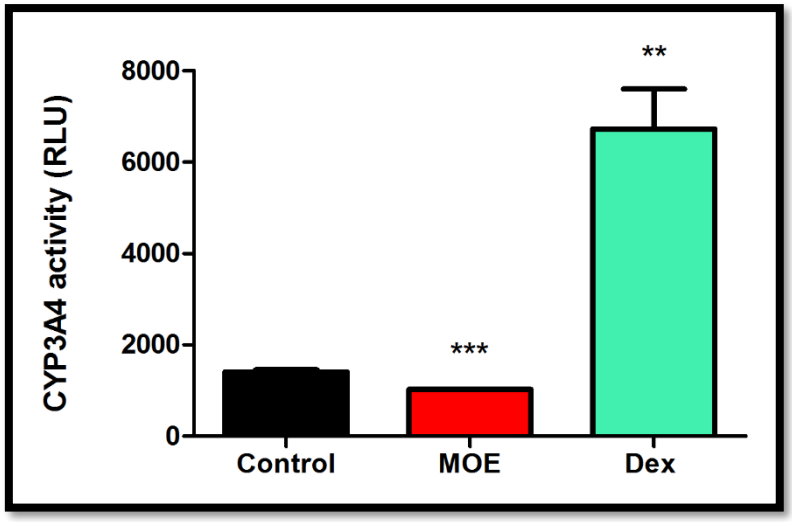

Figure 3.3: MOE decreased CYP3A4 activity in $HepG_2$ cells in comparison to the control following 72 h (*** $p < 0.0004$; ** $p < 0.0012$).

3.2 Oxidative stress

3.2.1 TBARS assay

Lipid peroxidation induced by ROS was assessed by quantification of MDA levels. The MDA levels were elevated in the MOE treated cells (0.3482 ± 0.013 µM, 1.23-fold) compared to the untreated cells (0.2821 ± 0.006 µM, $p < 0.05$) (Figure 3.4).

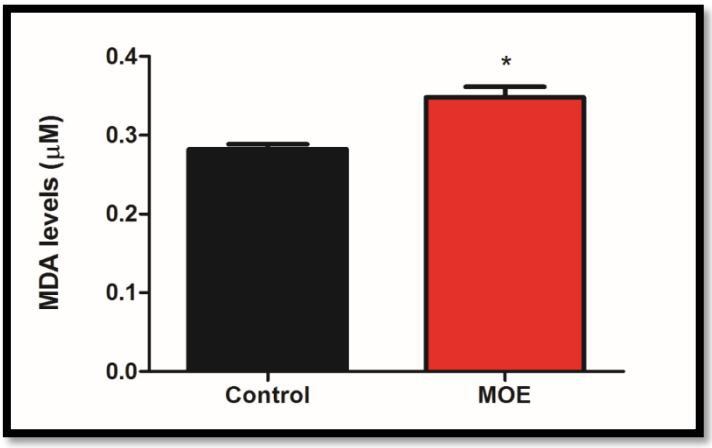

Figure 3.4: Extracellular MDA levels in Control and MOE treatment (* $p < 0.05$).

3.2.2 Nitrates and nitrites assay

The concentration of nitrates and nitrites was determined by extrapolation from a standard curve (Appendix C). Figure 3.5 shows a 1.17-fold increase ($p < 0.2905$) in nitrates and nitrites concentration in MOE treated cells (15.20 ± 2.694 µM) in comparison to the control (12.98 ± 0.2222 µM).

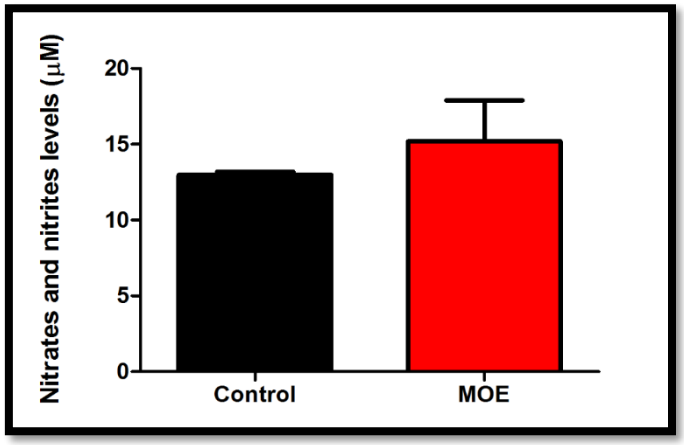

Figure 3.5: The nitrates and nitrites concentration in $HepG_2$ cells following treatment with MOE (72 h) ($p > 0.05$).

3.2.3 LDH assay:

Extracellular levels of LDH were quantified using a colorimetric assay. Results showed a 1.17 fold increase in LDH levels in the supernatant of the MOE treated cells (1.254 ± 0.008 OD, $p < 0.0035$) compared to that of the control supernatant (1.068 ± 0.017 OD) (Figure 3.6). Results are presented as mean optical density (OD).

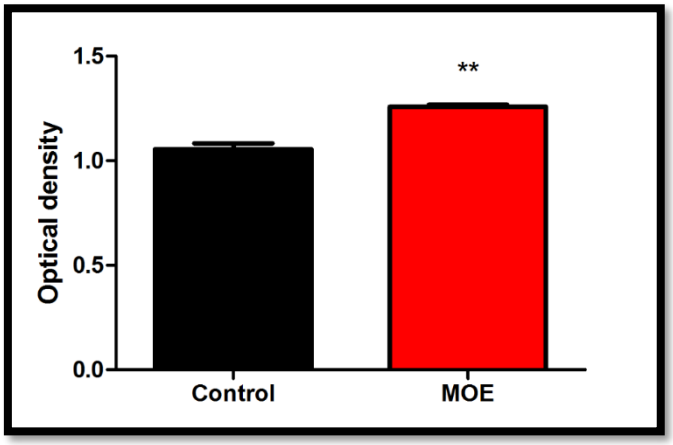

Figure 3.6: Extracellular LDH levels in MOE treated supernatant versus Control (** $p < 0.0035$).

3.2.4 SCGE Assay

The comet assay was performed to assess DNA fragmentation following treatment with MOE. Longer comet tail length is associated with higher DNA fragmentation. Figure 3.7 shows comet tails were significantly longer in the cells treated with MOE compared to the control cells indicating that MOE is genotoxic to $HepG_2$ cells (2.857 ± 0.6086 vs 1.394 ± 0.2236 μm, $p < 0.0001$).

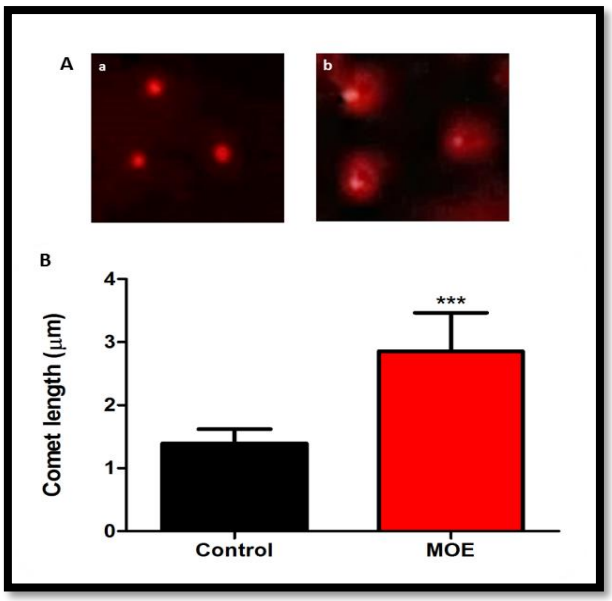

Figure 3.7: A. Comet tails of $HepG_2$ cells (a) prior to MOE exposure and (b) after 72 h MOE treatment ($p < 0.0001$). **B.** Comet tail length was significantly higher in MOE treated cells compared to control (*** $p < 0.0001$).

3.3 Inflammation

3.3.1 Western blot

Western blotting was used to determine the effects of MOE on protein expression of NF-kB p65, phospho-STAT3 (p-STAT3) and PARP-1. MOE induced significant 1.31-fold increase in expression of NF-kB p65 (1.317 ± 0.05767 vs control: 1.004 ± 0.005474 RFC, $p < 0.0112$) and 2.78-fold increase in p-STAT3 expression (3.786 ± 0.8184 vs control: 1.004 ± 0,005508 RFC, $p < 0.0277$). MOE induced the cleavage of PARP-1 to yield an 89 kDa and 24 kDA fragment (Figure 3.8). Analysis of the fragments showed a 1.17-fold decrease of 89 kDA fragment (1.004 ± 0.005474 vs control: 1.201 ± 0.05632 RFC, $p < 0.0263$) and a 1.11 fold increase in expression of the 24 kDA fragment (0.1.115 ± 0.008967 vs control: 1.001 ± 0.0006364 RFC, $p < 0.0354$). (Appendix F).

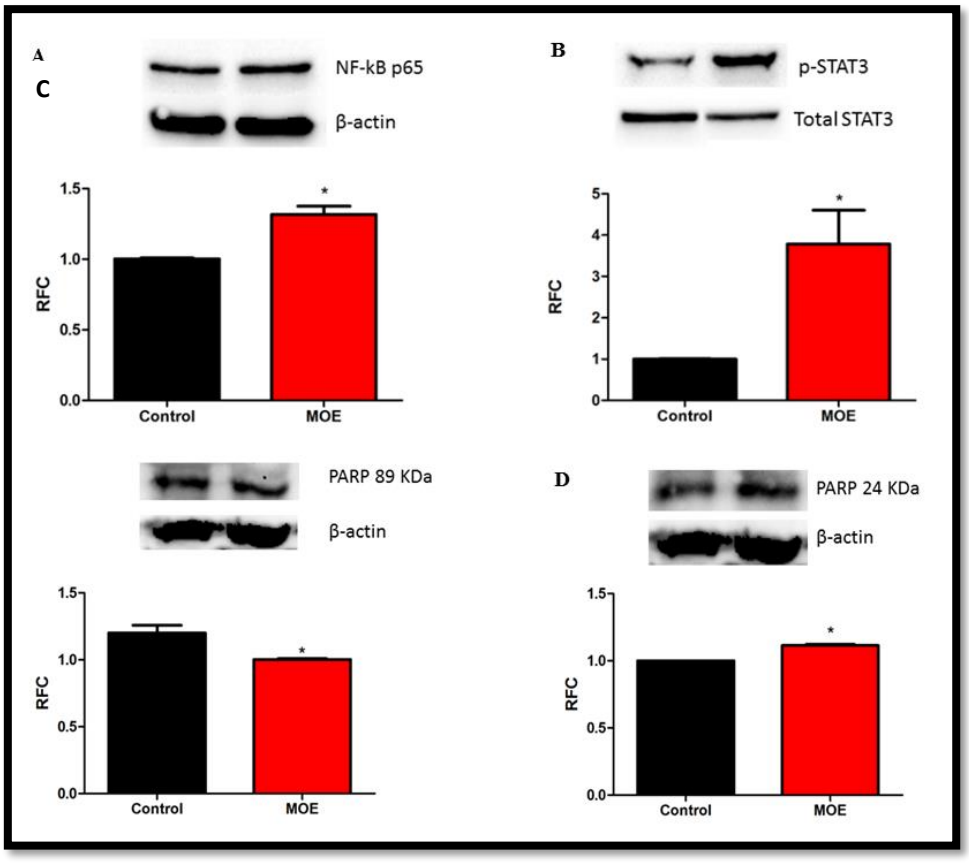

Figure 3.8: Western Blot images and graphs of NF-kB, p-STAT3 and cleaved PARP. Protein expression analysis showed a significant increase in **A.** NF-kB (* $p < 0.05$) and **B.** p-STAT3 (* $p < 0.05$) in MOE treatment. MOE treated cells depicted a significant decrease in **C.** 89 kDa fragment (* $p < 0.05$) and an increase in the **D.** 24 kDa fragment (* $p < 0.05$). RFC: Relative fold change.

3.3.2 ELISA

The effects of MOE on $HepG_2$ cells cytokine production was assessed using ELISA. There was a significant increase in IL-6 (1.2-fold) and a non-significant increase in TNF-α (1.03-fold), IL-10 (1.03-fold) and IL-1β (1.05-fold) cytokine concentration in MOE treated cells compared to untreated, controls cells (Table 3.1). (Appendix D).

Table 3.1: Cytokine concentrations in MOE treated cells.

Cytokine	Mean ± SD (pg/ml)		*p* value
	Control	MOE	
IL-6	145.5 ± 8.378	174.7 ± 2.734	0.0292*
TNF-a	52.43 ± 3.024	54.05 ± 1.859	0.4872
IL-10	294.3 ± 11.81	303.3 ± 2.417	0.3238
IL-1β	28.43 ± 0.9074	29.73 ± 0.4726	0.1151

SD: Standard deviation, *: significant

3.4 Cell death

3.4.1 Caspase activation

Intracellular activity of caspases 8, 9 and 3/7 was measured. Following MOE treatment, there was a 1.47-fold decrease in caspase 8 and a 1.34-fold decrease in caspase 9 activities (Table 3.2). A significant 2.83-fold increase of caspase 3/7 activity was observed in MOE treated compared to the control cells. (Appendix E).

Table 3.2: Intracellular caspase 8, 9 and 3/7 activities in MOE treated cells.

Caspase	Mean ± SD (RLU)		*p* value
	Control	MOE	
Caspase 8	61 450 ± 1 784	41 710 ± 2 732	0.0741
Caspase 9	685 200 ± 18 960	510 000 ± 10 730	0.0558
Caspase 3/7	63 350 ± 12 000	179 200 ± 1 535	* 0.0469

SD: Standard deviation, *: significant

3.4.2 Hoechst assay

Using the Hoechst 33342, the detection of morphological hallmarks of apoptosis were observed including cell shrinkage, nuclear condensation, apoptotic bodies and apoptotic cells (Figure 3.9:

B and C). This was compared to the control cells which showed cell division at various stages of the cell cycle (Figure 3.9: A). Cell density was reduced in the MOE treatment compared to the control.

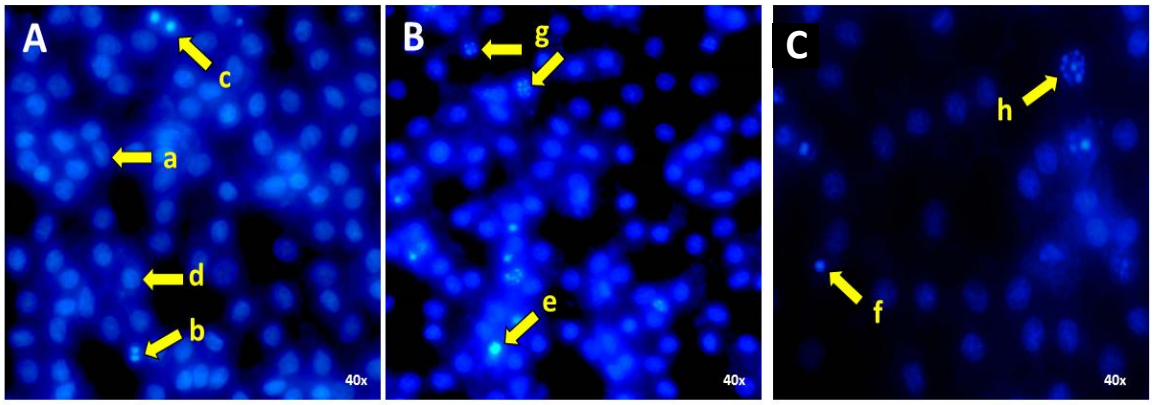

Figure 3.9: Hoechst 33342 stained $HepG_2$ cells displaying cell cycle morphology. **A.** $HepG_2$ control cells showing (a) metaphase, (b) anaphase, (c) early telophase and (d) interphase. **B and C.** MOE induced (e) chromatin hypercondensation, (f) cell shrinkage, (g) formation of apoptotic bodies and (h) apoptotic cells.

CHAPTER 4

Discussion

Moringa oleifera (MO) is a deciduous plant widely cultivated throughout tropical and sub-tropical countries of the world including Africa and Asia (Berkovich *et al.*, 2013). The plant has gained popularity due to its various medicinal properties attained by the bio-active phytochemical composition of its leaves. It is frequently used in the traditional treatment of a variety of illnesses such as anaemia, hypertension, hypercholesterolemia, diabetes mellitus type 2 and cancer (Koh *et al.*, 2013; Leone *et al.*, 2015). The biochemical effects of MOE on human HCC have not yet been fully elucidated. It was hypothesised that MOE induces cytotoxic effects on $HepG_2$ liver cancer cells upon chronic exposure (72 h).

The mitochondrion is a double-membrane organelle that plays a central role in cellular energy metabolism and is the major source of ROS production through oxidative phosphorylation (Gottlieb, 2001; Baynes and Dominiczak, 2007; Martinou and Youle, 2011). Normal cellular metabolism generates moderate levels of ROS which serves as an important stimulator of several signalling pathways involved in cell communication, immune responses and inflammation (Reuter *et al.*, 2010). ROS is directly generated as a by-product of the ETC within mitochondria of cells and is modulated by oxidative phosphorylation which involves the flow of electrons through the ETC complexes (Repetto *et al.*, 2012). Excessive production of ROS is implicated in a wide variety of diseases including chronic inflammation and subsequent cancer development (Poyton *et al.*, 2009; Reuter *et al.*, 2010). The chronic persistence of oxidative stress caused by the overproduction of ROS, predominantly $O_2^{\cdot -}$ and H_2O_2, has the capacity to damage cellular components and structure (Repetto *et al.*, 2012; Tiloke *et al.*, 2016). Cellular targets of ROS include DNA, lipids and proteins (Repetto *et al.*, 2012; Tiloke *et al.*, 2016).

The mitochondrion is not only the major source of ROS production, but it is also a highly susceptible target for ROS molecules and their damaging effects (Orrenius, 2007). The MTT assay indicated a dose dependent decrease in $HepG_2$ cell viability (Figure 3.1), thus demonstrating the cytotoxic potential of MOE. The decrease in cell viability is caused by reduced mitochondrial MTT conversion due to decreased enzymatic activity of mitochondrial succinate dehydrogenase and/or decreased availability of reducing equivalents such as co-enzyme NADH, (Stockert *et al.*, 2012). MOE also decreased intracellular ATP generation (Figure 3.2). Highly reactive ROS molecule $O_2^{\cdot -}$ can directly oxidise and inactivate iron-sulphur proteins such as NADH dehydrogenase and ATP synthase causing the loss of mitochondrial respiration and ATP generation ultimately resulting in mitochondrial dysfunction and decreased intracellular ATP concentrations (Orrenius, 2007). Additionally, glucose uptake is facilitated by carbohydrate digestive enzymes, α-glucosidase and α-amylase. Tannins, flavonoids and phenolic compounds present within the extract are responsible for inhibition of α-glucosidase and α-amylase enzyme activity thereby preventing glucose uptake and absorption. (Adisakwattana and Chanathong, 2011). This would result in decreased TCA cycle and glycolysis which is responsible for the production of reducing equivalents NADH and $FADH_2$. These co-enzymes supply electrons to the ETC in the mitochondria and facilitate ATP production via oxidative phosphorylation. Thus a decrease in the concentration of reducing equivalents would indicate decreased number of electrons entering the ETC and consequentially, ATP production would also decrease (Adeeyo *et al.*, 2013).

A major detrimental effect of ROS-induced oxidative stress is the induction of lipid peroxidation (Repetto *et al.*, 2012). Numerous end-products are produced following lipid peroxidation, such as aldehydes, more specifically MDA (Repetto *et al.*, 2012). The results from the study indicated that MOE increased MDA concentration (Figure 3.4) suggesting that MOE is a potent inducer of oxidative stress within $HepG_2$ cells, resulting in lipid peroxidation. This result is in agreement with a study conducted by Tiloke *et al* (2013) implicating MOE in the induction of ROS within

A549 lung cancer cells (Tiloke *et al.*, 2013). Although this study did not analyse each plant phytochemical compound within MO, a previous study conducted by Singh *et al*. (2009) identified the presence of quercetin and kaempferol, two flavonoids existing in substantial quantities within the crude aqueous extract (Singh *et al.*, 2009). This finding was further verified by Sreelantha *et al* (2009, 2011) and it was suggested quercetin and kaempferol may be inducers of elevated ROS production (Sreelatha and Padma, 2009; Sreelatha *et al.*, 2011).

Generally, cell membranes have a high content of PUFAs and is the main target of ROS-induced oxidative destruction, particularly due to its methylene group (=RH-). The physiological role of PUFAs include regulation of gene expression, cell signalling, selectively permeable barrier, a support system for membrane structure, flexibility and fluidity and providing of energy. Therefore lipid peroxidation induced by excessive ROS production is responsible for oxidative damage and reduced functionality of cell membranes (Repetto *et al.*, 2012). MOE significantly increased extracellular LDH levels (Figure 3.6), thereby strongly indicating $HepG_2$ cell membrane damage.

This study also investigated the production of RNS in response to MOE exposure. There was a non-significant increase in nitrates and nitrites levels (Figure 3.5) suggesting that the concentration of nitrates and nitrites was not affected by MOE. Since the nitrates and nitrite concentration was not depleted, and was evidently present, it still may contribute to oxidative stress to a small extent by providing substrates for RNS generation. MOE contains niacin as well as vitamin D3, vitamin C and magnesium, all of which stimulates NO production (Houston, 2013; Gopi *et al.*, 2016). In states of elevated ROS levels, NO combines with O_2^- to form OON^- which induces lipid peroxidation (Oboh *et al.*, 2015). Therefore, both ROS and RNS contribute to oxidative stress-induced lipid peroxidation (Dedon and Tannenbaum, 2004).

In the liver, constitutively activated NF-kB promotes cellular regeneration and inhibits apoptosis thus enabling cancer progression (Barkett and Gilmore, 1999). It is well-known that NF-kB expression is regulated by ROS (Wang *et al.*, 2015). This study showed MOE increased the expression of NF-kB in $HepG_2$ cancer cells (Figure 3.8). Previously it was observed that MOE increased ROS production, one source of ROS predominantly responsible for the activation of NF-kB is H_2O_2. It can directly exert its effect or through its transformation into $OH^\bullet$ whilst in the presence of Fe^{2+} in the Fenton reaction (Gloire *et al.*, 2006). These findings suggest MOE induced ROS-mediated pro-apoptotic NF-kB transcriptional activity in $HepG_2$ cells (Gloire *et al.*, 2006).

NF-kB transcriptional activity leads to the activation of various pro- and anti-inflammatory genes including TNF-α, IL-1β, IL-10 and IL-6 (Niemand *et al.*, 2003). TNF-α initiates and amplifies the inflammatory response (Hammam *et al.*, 2013), IL-1β is a major mediator of inflammation (Dinarello, 2009) and IL-10 is a potent anti-inflammatory cytokine capable of supressing pro-inflammatory cytokine release (Niemand *et al.*, 2003). MOE induced non-significant increases in the concentrations of TNF-α, IL-1β, IL-10 (Table 3.1).

TNF-α is also associated with activation of the extrinsic apoptotic pathway (Hammam *et al.*, 2013). In this pathway, caspase 8 is the main initiator caspase, functional in the cleavage and activation of caspase 3/7 (Elmore, 2007). In this study, $HepG_2$ cells exposed to MOE expressed a non-significant increase in TNF-α concentration (Table 3.1) and a non-significant decrease in caspase 8 activity (Table 3.2) and a significant increase in caspase 3/7 activity (Table 3.2). A second apoptotic pathway is the mitochondrial intrinsic pathway where cleavage and activation of caspase 3/7 is carried out by initiator caspase 9 (Elmore, 2007). Once again, it was observed that MOE exposed cells expressed a non-significant decrease in caspase 9 activity (Table 3.2). Collectively, these findings indicate that both the extrinsic and intrinsic apoptotic pathways were not activated by MOE and its likely caspase 3/7 activation occurred via another pathway.

Pleiotropic cytokine, IL-6 promotes cell survival and is the primary activator of STAT3 through IL-6 induced transcriptional phosphorylation of tyrosine 705 residue of STAT3 (Yu *et al.*, 2009; Wang *et al.*, 2011). MOE induced a significant increase in both IL-6 (Table 3.1) and protein

expression of p-STAT3 (Figure 3.8). Once STAT3 is activated, it induces further expression and subsequent production of IL-6 thereby creating a positive feedback mechanism causing excessive STAT3 activation and IL-6 production. Over activation of STAT3 induces apoptosis in cancer cells (Silva *et al.*, 2015; Rozovski *et al.*, 2016). Under normal conditions, IL-6 and activated STAT3 serves to inhibit apoptosis, promote malignant cell transformation and inflammation through the inhibition of pro-inflammatory proteins but excessive activation of STAT3 results in binding of activated STAT3 to STAT3-specific binding sites within caspase 3/7-gene promoter region causing increased transcription of procaspase 3/7. The high levels of activated STAT3 then binds with low affinity to STAT3-specific binding sites within the promoter region of procaspase 3/7 to initiate caspase activity (Silva *et al.*, 2015; Rozovski *et al.*, 2016).

In advanced cancers such as HCC, significantly reduced activity of CYP3A4 is often experienced. MOE induced a significant decrease in CYP3A4 activity (Figure 3.3). IL-6 cytokine release represses the hepatic *IL-6* gene transcription resulting in reduced *CYP3A4* mRNA, protein and activity (Morgan *et al.*, 2008). This suggests that $HepG_2$ cancer cells are highly susceptible and sensitive to the cytotoxicity of MOE due to their reduced capacity to metabolise MOE.

Caspase-dependent apoptosis involves PARP-1 cleavage by executioner caspase 3/7 at the aspartate-glutamine-valine-aspartate (DEVD) site located in the nuclear localisation signal (NLS) region of PARP-1. This cleavage generates two fragments of 89 kDa and 24 kDa. The 89 kDa fragment contains the auto-modification and catalytic domain whereas the 24 kDa fragment possess the DNA-binding domain and the double zinc fingers. Cleavage of PARP-1 is known to prevent repair of ds/ssDNA breaks and cell survival. MOE caused PARP-1 cleavage with a significant increase in the 24 kDa fragment (Figure 3.8). This further indicates MOE as an apoptotic inducer in $HepG_2$ cells. The 24 kDa fragment binds irreversibly to DNA strand breaks thus preventing DNA repair, eventually resulting in cell death. DNA damage induced by MOE was further validated by the presence of increased strand breaks represented by increased comet tail lengths (Figure 3.7). In combination, increased DNA strand breaks and PARP-1 cleavage signifies genotoxic potential of MOE resulting in cellular dysfunction and apoptosis.

Late stages of apoptosis can be identified by characteristic changes of the cell and nuclear morphology but overall the most prominent indicator of apoptosis is the formation of apoptotic bodies. Figure 3.9 (B and C) shows that MOE induced chromatin hypercondensation and shrinkage of cells, formation of apoptotic bodies were also seen in greater quantity in MOE treated cells compared to the untreated control cells (Figure 3.9 (A)). Apoptotic cells were also present in MOE exposed cells (Figure 3.9 (C)). Therefore MOE induces apoptosis in $HepG_2$ cancer cells.

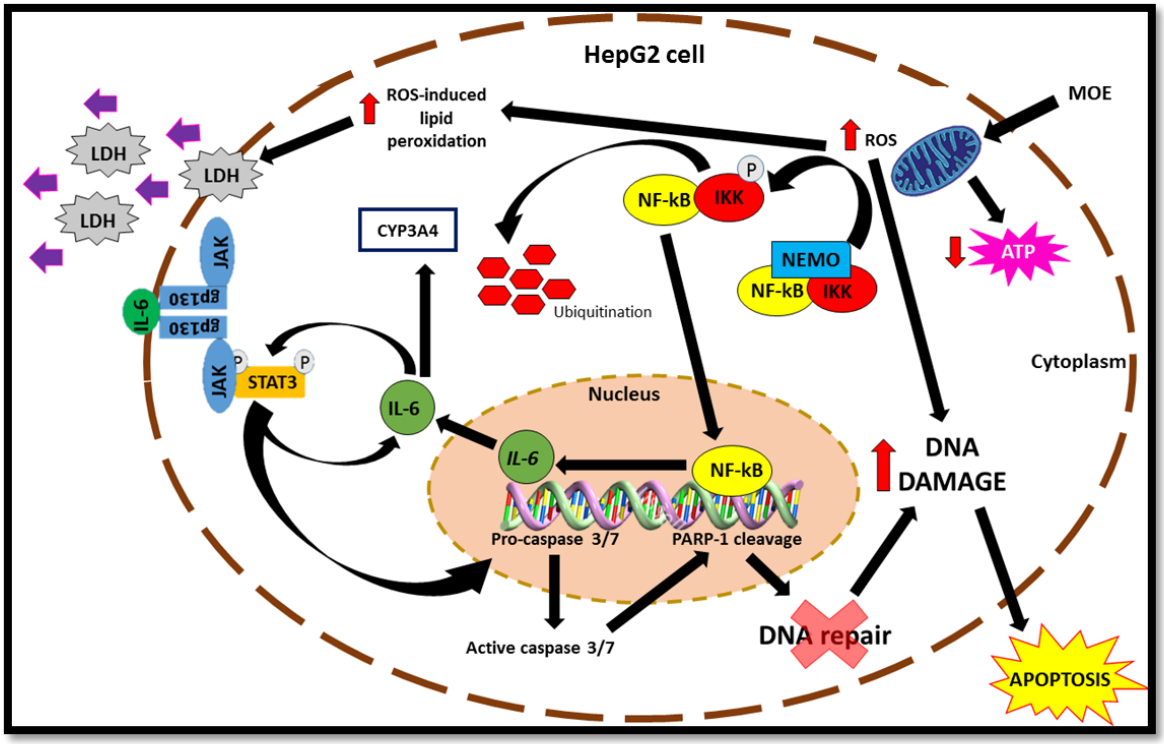

Figure 4.1: Schematic overview of the biochemical effects of MOE in human $HepG_2$ cells (Prepared by Author).

CHAPTER 5

Conclusion

MO is a highly nutritional plant, consumed worldwide. It possesses many medicinal properties and is associated with pharmacological activities that may aid in the development of new anticancer treatment modalities. However, the mechanism by which MOE causes cytotoxicity in human HCC has not yet been investigated and established. In this study, the cytotoxic effects of MOE on the $HepG_2$ cell line following chronic exposure (72 h) was determined (Figure 4.1).

The results from the study showed that MOE induced ROS-mediated lipid peroxidation causing reduced mitochondrial viability, ATP depletion, and membrane and DNA damage. MOE did not act via the typical NF-kB inflammatory pathway but instead induced the pro-apoptotic transcriptional activity of NF-kB through elevation of ROS levels thus triggering the IL-6/STAT3 pathway. The positive feedback loop that occurs between IL-6 and STAT3 results in STAT3 binding to STAT3-specific binding domains located on procaspase 3/7 to initiate caspase activity. Activated caspase 3/7 subsequently cleaves and inactivates PARP-1 leading to the inhibition of DNA repair, ultimately resulting in cell death. Taken together, MOE is an anti-proliferative, cytotoxic and genotoxic agent in human $HepG_2$ cancer cells. Understanding the underlying biochemical mechanism of toxicity of MOE on $HepG_2$ cells may aid in the development of new promising therapeutic treatments for HCC.

Phytochemical analysis of the bioactive compounds present in MOE is further recommended for future studies. It would be of interest to identify the compounds responsible for the cytotoxicity of MOE seen in the liver cell line. Further studies are also required to determine the effect of MOE on normal cell lines and an *in-vivo* model.

REFERENCES

Adeeyo, A. O., Adefule, A. K., Ofusori, D. A., Aderinola, A. A. and Caxton-Martins, E. A. (2013). Antihyperglycemic effects of aqueous leaf extracts of mistletoe and Moringa oleifera in streptozotocin-induced diabetes wistar rats. *Diabetologia Croatica, 42*(81-88).

Adisakwattana, S. and Chanathong, B. (2011). Alpha-glucosidase inhibitory activity and lipid-lowering mechanisms of Moringa oleifera leaf extract. *European review for medical and pharmacological sciences, 15*(7), 803-808.

Aggarwal, B. B., Shishodia, S., Sandur, S. K., Pandey, M. K. and Sethi, G. (2006). Inflammation and cancer: how hot is the link? *Biochemical pharmacology, 72*(11), 1605-1621.

Akhter, A. (2013). Development of a novel active targeting system for siRNA delivery to liver sinusoidal endothelial cell in vivo.

Álvarez, R., Vaz, B., Gronemeyer, H. and de Lera, A. R. (2013). Functions, therapeutic applications, and synthesis of retinoids and carotenoids. *Chemical reviews, 114*(1), 1-125.

Amabye, T. G. and Tadesse, F. M. (2016). Phytochemical and Antibacterial Activity of Moringa Oleifera Available in the Market of Mekelle. *Journal of Analytical & Pharmaceutical Research, 2*(1), 1-4.

Antonaki, A., Demetriades, C., Polyzos, A., Banos, A., Vatsellas, G., Lavigne, M. D., Apostolou, E., Mantouvalou, E., Papadopoulou, D., Mosialos, G. and Thanos, D. (2011). Genomic analysis reveals a novel nuclear factor-κB (NF-κB)-binding site in Alu-repetitive elements. *Journal of Biological Chemistry,, 286*(44), 38768-38782.

Anwar, F., Latif, S., Ashraf, M. and Gilani, A. H. (2007). Moringa oleifera: A Food Plant with Multiple Medicinal Uses. *Phytotherapy research, 21*(1), 17-25.

Ashe, P. C. and Berry, M. D. (2003). Apoptotic signaling cascades. *Progress in Neuro-Psychopharmacology & Biological Psychiatry, 27*(2), 199-214. doi: 10.1016/S0278-5846(03)00016-2

Auyang, S. Y. (2006). Cancer causes and cancer research on many levels of complexity.

Ayala, A., Muñoz, M. F. and Argüelles, S. (2014). Lipid peroxidation: production, metabolism, and signaling mechanisms of malondialdehyde and 4-hydroxy-2-nonenal. . *Oxidative medicine and cellular longevity, 2014*.

Badhani, B., Sharma, N. and Kakkar, R. (2015). Gallic acid: a versatile antioxidant with promising therapeutic and industrial applications. *RSC Advances, 5*(35), 27540-27557.

Barkett, M. and Gilmore, T. D. (1999). Control of apoptosis by Rel/NF-κB transcription factors. *Oncogene, 18*(49).

Basheer, L. and Kerem, Z. (2015). Interactions between CYP3A4 and dietary polyphenols. . *Oxidative medicine and cellular longevity, 2015*.

Baumann, E., Stoya, G., Völkner, A., Richter, W., Lemke, C. and Linss, W. (2000). Hemolysis of human erythrocytes with saponin affects the membrane structure. *Acta histochemica, 102*(1), 21-35.

Baynes, J. W. and Dominiczak, M. H. (2007). *Medical Biochemistry*: Elsevier Inc.

Beinke, S. (2004). Functions of NF-κB1 and NF-κB2 in immune cell biology. *Biochemical Journal, 382*(2), 393-409.

Ben-Neriah, Y. and Karin, M. (2011). Inflammation meets cancer, with NF-[kappa] B as the matchmaker. . *Nature immunology, 12*(8), 715-723.

Berg, J. M., Tymoczko, J. L. and Stryer., L. (2002). *Biochemistry,* .

Berkovich, L., Earon, G., Ron, I., Rimmon, A., Vexler, A. and Lev-Ari, S. (2013). Moringa Oleifera aqueous leaf extract down-regulates nuclear factor-kappaB and increases cytotoxic effect of chemotherapy in pancreatic cancer cells. *BMC complementary and alternative medicine, 13*(1), 212.

Bernhard, D., Schwaiger, W., Crazzolara, R., Tinhofer, I., Kofler, R. and Csordas, A. (2003). Enhanced MTT-reducing activity under growth inhibition by resveratrol in CEM-C7H2 lymphocytic leukemia cells. *Cancer letters,, 195*(2), 193-199.

Bishayee, A. (2014). *The inflammation and liver cancer. In Inflammation and Cancer*. Springer Basel.

Borel, P., Preveraud, D. and Desmarchelier, C. (2013). Bioavailability of vitamin E in humans: an update. *Nutrition reviews, 71*(6), 319-331.

Bouchard, V. J., Rouleau, M. and Poirier, G. G. (2003). PARP-1, a determinant of cell survival in response to DNA damage. *Experimental hematology, 31*(6), 446-454.

Brunelle, J. K. and Zhang, B. (2010). Apoptosis assays for quantifying the bioactivity of anticancer drug products. . *Drug Resistance Updates, 13*, 172-179.

Bryan, N. S. and Grisham, M. B. (2007). Methods to detect nitric oxide and its metabolites in biological samples. *Free Radical Biology and Medicine, 43*(5), 645-657.

Cali, J., Ma, D., Sobol, M., Simpson, D. J., Frackman, S., Good, T. D., Daily, W. J. and Liu, D. (2006). Luminogenic cytochrome P450 assays. *Expert opinion on drug metabolism & toxicology, 2*(4), 629-645.

Cali, J. J., Klaubert, D., Daily, W., Ho, S. K. S., Frackman, S., Hawkins, E. and Wood, K. V. (2012). U.S Patent No.: D. U. S. P. a. T. O. Washington.

Chambial, S., Dwivedi, S., Shukla, K. K., John, P. J. and Sharma, P. (2013). Vitamin C in disease prevention and cure: an overview. *Indian Journal of Clinical Biochemistry, 28*(4), 314-328.

Chan, F. K. M., Moriwaki, K. and De Rosa, M. J. (2013). Detection of necrosis by release of lactate dehydrogenase activity. *Immune Homeostasis: Methods and Protocols*, 65-70.

Charoensin, S. (2014). Antioxidant and anticancer activities of Moringa oleifera leaves. *Journal of Medicinal Plants Research, 8*(7), 318-325.

Chazotte, B. (2011). Labeling nuclear DNA with hoechst 33342. *Cold Spring Harbor Protocols, 2011*(1), pdb-prot5557.

Choi, I., Kang, H. S., Yang, Y. and Pyun, K. H. (1994). IL-6 induces hepatic inflammation and collagen synthesis in vivo *Clinical & Experimental Immunology, 95*(3), 530-535.

Choi, J. M., Chu, S.J ., Ahn, K. H., Kim, S. K., Ji, J. E., Won, J. H., Kim, H. C., Back, M. J. and Kim, D. K. (2011). C6-ceramide enhances phagocytic activity of Kupffer cells through the production of endogenous ceramides. *Molecules and cells, 32*(4),.325.

Choucroun, P., Gillet, D., Dorange, G., Sawicki, B. and Dewitte, J. D. (2001). Comet assay and early apoptosis. Mutation Research/Fundamental and Molecular Mechanisms of Mutagenesis,. *Mutation Research, 478*(1), 89-96.

Circu, M. L. and Aw, T. Y. (2010). REACTIVE OXYGEN SPECIES, CELLULAR REDOX SYSTEMS AND APOPTOSIS. *Free Radical Biology and Medicine, 48*(6), 749-762.

Collins, A. R. (2004). The comet assay for DNA damage and repair. . *Molecular biotechnology, 26*(3), 249-261.

Coppin, J. P., Xu, Y., Chen, H., Pan, M. H., Ho, C. T., Juliani, R., Simon, J. E. and Wu, Q. (2013). Determination of flavonoids by LC/MS and anti-inflammatory activity in Moringa oleifera. *Journal of Functional Foods, 5*(4), 1892-1899.

Cox, K. L., Devanarayan, V., Kriauciunas, A., Manetta, J., Montrose, C. and Sittampalam, S. (2014). Immunoassay methods.

Crouch, S. P. M., Kozlowski, R., Slater, K. J. and Fletcher, J. (1993). The use of ATP bioluminescence as a measure of cell proliferation and cytotoxicity. . *Journal of immunological methods, 160*(1), 81-88.

Dangi, S. Y., Jolly, C. I. and Narayanan, S. (2002). Antihypertensive activity of the total alkaloids from the leaves of Moringa oleifera. . *Pharmaceutical biology, 40*(2), 144-148.

Dedon, P. C. and Tannenbaum, S. R. (2004). Reactive nitrogen species in the chemical biology of inflammation. *Archives of biochemistry and biophysics, 423*(1), 12-22.

Devisetti, R., Sreerama, Y. N. and Bhattacharya, S. (2016). Processing effects on bioactive components and functional properties of moringa leaves: development of a snack and quality evaluation. *Journal of food science and technology, 53*(1), 649-657.

Dinarello, C. A. (2009). Immunological and inflammatory functions of the interleukin-1 family. *Annual review of immunology, 27*, 519-550.

Elmore, S. (2007). Apoptosis: A Review of Programmed Cell Death. *Toxicologic Pathology, 35*(4), 495-516. doi: 10.1080/01926230701320337

Erener, S., Pétrilli, V., Kassner, I., Minotti, R., Castillo, R., Santoro, R., Hassa, P. O., Tschopp, J. and Hottiger, M. O. (2012). Inflammasome-activated caspase 7 cleaves PARP1 to enhance the expression of a subset of NF-κB target genes. *Molecular cell, 46*(2), 200-211.

Esterbauer, H. (1993). Cytotoxicity and genotoxicity of lipid-oxidation products. *The American journal of clinical nutrition, 57*(5), 779S-785S.

Fahey, J. W. (2005). Moringa oleifera: a review of the medical evidence for its nutritional, therapeutic, and prophylactic properties. Part 1. . *Trees for life Journal, 1*(15), 1-15.

Fan, C., Zheng, W., Fu, X., Li, X., Wong, Y. S. and Chen, T. (2014). Strategy to enhance the therapeutic effect of doxorubicin in human hepatocellular carcinoma by selenocystine, a synergistic agent that regulates the ROS-mediated signaling. . *Oncotarget, 5*(9), 2853.

Fard, M. T., Arulselvan, P., Karthivashan, G., Adam, S. K. and Fakurazi, S. (2015). Bioactive extract from moringa oleifera inhibits the pro-inflammatory mediators in lipopolysaccharide stimulated macrophages. *Pharmacognosy magazine, 11*(Suppl 4), S556.

Ferreira, P. M. P., Farias, D. F., Oliveira, J. T. d. A. and Carvalho, A. d. F. U. (2008). Moringa oleifera: bioactive compounds and nutritional potential. *Revista de Nutrição, 21*(4), 431-437.

Fiume, L., M. Manerba, Vettraino, M. and Stefano, G. D. (2014). Inhibition of lactate dehydrogenase activity as an approach to cancer therapy. *Future medicinal chemistry, 6*(4), 429-445.

Forest, V., Figarol, A., Boudard, D., Cottier, M., Grosseau, P. and Pourchez, J. (2015). Adsorption of Lactate Dehydrogenase Enzyme on Carbon Nanotubes: How to Get Accurate Results for the Cytotoxicity of These Nanomaterials. . *Langmuir, 31*(12), 3635-3643.

Gerets, H. H. J., Tilmant, K., Gerin, B., Chanteux, H., Depelchin, B. O., Dhalluin, S. and Atienzar, F. A. (2012). Characterization of primary human hepatocytes, HepG2 cells, and HepaRG cells at the mRNA level and CYP activity in response to inducers and their predictivity for the detection of human hepatotoxins. *Cell biology and toxicology, 28*(2), 69-87.

Gloire, G., Legrand-Poels, S. and Piette, J. (2006). NF-κB activation by reactive oxygen species: fifteen years later. *Biochemical pharmacology, 72*(11), 1493-1505.

Gopi, S., Varma, K., Jude, S. and Divya, M. (2016). A Study on The Nitric Oxide (NO) Enhancing Ability of A Natural Phytochemical Formulation. *Asian Journal of Pharmaceutical Technology & Innovation, 4*(16), 1-6.

Goss, M. (2012). A study of the initial establishment of multi-purpose moringa (Moringa oleifera Lam) at various plant densities, their effect on biomass accumulation and leaf yield when grown as vegetable. *African Journal of Plant Science, 6*(3), 125-129.

Gottlieb, R. A. (2001). Mitochondria and Apoptosis. *Biological signals and receptors, 10*(3), 147-161.

Govender, R. (2012). *Silver nanoparticles of Albizia adianthifolia: The induction of apoptosis in a human lung carcinoma cell line.* (Master of Medical Science), University of KwaZulu-Natal, Journal of Nanobiotechnology. (MS 1840103851838905)

Grivennikov, S. I., Greten, F. R. and Karin, M. (2010). Immunity, inflammation, and cancer. *Cell 140*(6), 883-899.

Guengerich, F. P., 1-17. (1999). Cytochrome P-450 3A4: regulation and role in drug metabolism. *Annual review of pharmacology and toxicology, 39*(1-17).

Halliwell, B. (2006). Reactive species and antioxidants. Redox biology is a fundamental theme of aerobic life. *Plant physiology, 142*(2), 312-322.

Hammam, O., Mahmoud, O., Zahran, M., Sayed, A., Salama, R., Hosny, K. and Farghly, A. (2013). A possible Role for TNF-in coordinating inflammation and angiogenesis in chronic liver disease and hepatocellular carcinoma. . *Gastrointestinal Cancer Research, 6*(4), 107-114.

Hengartner, M. O. (2000). The biochemistry of apoptosis. *Nature, 407*(6805), 770-776.

Hoesel, B. and Schmid, J. A. (2013). The complexity of NF-κB signaling in inflammation and cancer. *Molecular Cancer 12*(86).

Houston, M. C. (2013). The role of nutrition and nutraceutical supplements in the prevention and treatment of hypertension.

Hunter, A. M., LaCasse, E. C. and Korneluk, R. G. (2007). The inhibitors of apoptosis (IAPs) as cancer targets. *Apoptosis, 12*(9), 1543-1568. doi: 10.1007/s10495-007-0087-3

Hunter, C. A. and Jones, S. A. (2015). IL-6 as a keystone cytokine in health and disease. *Nature immunology, 16*(5), 448-457.

Jaiswal, D., Rai, P. K., Kumar, A., Mehta, S. and Watal, G. (2009). Effect of Moringa oleifera Lam. leaves aqueous extract therapy on hyperglycemic rats. *Journal of ethnopharmacology, 123*(3), 392-396. doi: 10.1016/j.jep.2009.03.036

Janero, D. R. (1990). Malondialdehyde and thiobarbituric acid-reactivity as diagnostic indices of lipid peroxidation and peroxidative tissue injury. . *Free Radical Biology and Medicine, 9*(6), 515-540.

Jung, I. L., Lee, J. H. and Kang, S. C. (2015). A potential oral anticancer drug candidate, Moringa oleifera leaf extract, induces the apoptosis of human hepatocellular carcinoma cells. *Oncology letters, 10*(3), 1597-1604.

Kalra, B. S. (2007). Cytochrome P450 enzyme isoforms and their therapeutic implications: an update. *Indian journal of medical sciences, 61*(2), 102.

Kancheva, V. D. and Kasaikina, O. T. (2013). Bio-antioxidants-a chemical base of their antioxidant activity and beneficial effect on human health. *Current medicinal chemistry, 20*(37), 4784-4805.

Kasolo, J. N., Bimenya, G. S., Ojok, L., Ochieng, J. and Ogwal-Okeng, J. W. (2010). Phytochemicals and uses of Moringa oleifera leaves in Ugandan rural communities. *Journal of Medicinal Plants Research, 4*(9), 753-757.

Kew, M. C. (2010). Hepatocellular carcinoma in African Blacks: Recent progress in etiology and pathogenesis. *World Journal of Hepatology, 2*(2), 65-73.

Khalafalla, M. M., Abdellatef, E., Dafalla, H. M., Nassrallah, A. A., Aboul-Enein, K. M. and Lightfoot, D. A. (2010). Active principle from Moringa oleifera Lam leaves effective against two leukemias and a hepatocarcinoma. *African Journal of Biotechnology, 9*(49), 8467.

Kidmose, U., Yang, R. Y., Thilsted, S. H., Christensen, L. P. and Brandt, K. J. F. C. A. (2006). Content of carotenoids in commonly consumed Asian vegetables and stability and extractability during frying. *Journal of Food Composition and Analysis, 19*(562-571).

Kim, H. E., Du, F., Fang, M. and Wang, X. (2005). Formation of apoptosome is initiated by cytochrome c-induced dATP hydrolysis and subsequent nucleotide exchange on Apaf-1. . *Proceedings of the National Academy of Sciences of the United States of America, 102*(49), 17545-17550.

Kmieć, Z. (2001). Cooperation of Liver Cells in the Synthesis and Degradation of Eicosanoids. *In Cooperation of Liver Cells in Health and Disease*, 51-59.

Koh, W. P., Wang, R., Jin, A., Yu, M. C. and Yuan, J. M. (2013). Diabetes mellitus and risk of hepatocellular carcinoma: findings from the Singapore Chinese Health Study. *British journal of cancer, 108*(5), 1182-1188.

Kooltheat, N., Sranujit, R. P., Chumark, P., Potup, P., Laytragoon-Lewin, N. and Usuwanthim, K. (2014). An ethyl acetate fraction of Moringa oleifera Lam. inhibits human macrophage cytokine production induced by cigarette smoke. Nutrients. *6, 2*(697-710).

Kumar, M., Deepmala, J. and Sangeeta, S. (2012). Hepatoprotective Effects of Polygonum Bistorta and Its Active Principles on Albino Rats Intoxicated with Carbon Tetrachloride and Paracetamol. *1*, 226. doi: doi:10.4172/scientificreports.226

Kumar, S. and Pandey, A. K. (2013). Chemistry and biological activities of flavonoids: an overview. *The Scientific World Journal, 2013*.

Kuwana, T. and Newmeyer, D. D. (2003). Bcl-2 family proteins and the role of the mitochondria in apoptosis. *Current Opinion in Cell Biology, 15*(6), 691-699. doi: 10.1016/j.ceb.2003.10.004

Lakshminarayana, M., Shivkumar, H., Rimaben, P. and Bhargava, V. K. (2011). Antidiarrhoeal activity of leaf extract of Moringa Oleifera in experimentally induced diarrhoea in rats. *International journal of Phytomedicine, 3*(1), 68.

Leone, A., Spada, A., Battezzati, A., Schiraldi, A., Aristil, J. and Bertoli, S. (2015). Cultivation, genetic, ethnopharmacology, phytochemistry and pharmacology of Moringa oleifera leaves: An overview. *International journal of molecular sciences, 16*(6), 12791- 12835.

Liao, W., McNutt, M. A. and Zhu, W. G. (2009). The comet assay: a sensitive method for detecting DNA damage in individual cells. *Methods, 48*(1), 46-53.

Luedde, T. and Schwabe, R. F. (2011). NF-κB in the liver-linking injury, fibrosis and hepatocellular carcinoma. *Nature Reviews Gastroenterology and Hepatology,, 8*(2), 108-118.

Mahmood, T. and Yang, P. C. (2012). Western blot: technique, theory, and trouble shooting. *North American journal of medical sciences, 4*(9), 429.

Malarkey, D. E., Johnson, K., Ryan, L., Boorman, G. and Maronpot, R. R. (2005). New insights into functional aspects of liver morphology. *Toxicologic pathology, 33*(1), 27-34.

Martinou, J.-C. and Youle, R. J. (2011). Mitochondria in Apoptosis: Bcl-2 Family Members and Mitochondrial Dynamics. *Developmental Cell, 21*(1), 92-101. doi: 10.1016/j.devcel.2011.06.017

Matassov, D., Kagan, T., Leblanc, J., Sikorska, M. and Zakeri, Z. (2004). Measurement of apoptosis by DNA fragmentation. . *Apoptosis Methods and Protocols*, 1-17.

Mbikay, M. (2012). Therapeutic potential of Moringa oleifera leaves in chronic hyperglycemia and dyslipidemia: a review. *Frontiers in pharmacology, 3*(24). doi: 10.3389/fphar.2012.00024

McIlwain, D. R., Berger, T. and Mak, T. W. (2013). Caspase functions in cell death and disease. . *Cold Spring Harbor perspectives in biology,, 5*(4), a008656.

Mehta, K., Balaraman, R., Amin, A. H., Bafna, P. A. and Gulati, O. D. (2003). Effect of fruits of Moringa oleifera on the lipid profile of normal and hypercholesterolaemic rabbits. *Journal of Ethnopharmacology, 86*(2), 191-195.

Morgan, E. T., Goralski, K. B., Piquette-Miller, M., Renton, K. W., Robertson, G. R., Chaluvadi, M. R., Charles, K. A., Clarke, S. J., Kacevska, M., Liddle, C. and Richardson, T. A. (2008). Regulation of drug-metabolizing enzymes and transporters in infection, inflammation, and cancer. *Drug Metabolism and Disposition, 36*(2), 205-216.

Moses, T., Papadopoulou, K. K. and Osbourn, A. (2014). Metabolic and functional diversity of saponins, biosynthetic intermediates and semi-synthetic derivatives. *Critical reviews in biochemistry and molecular biology, 49*(6), 439-462.

Mosmann, T. (1983). Rapid colorimetric assay for cellular growth and survival: application to proliferation and cytotoxicity assays. *Journal of immunological methods, 65*(1-2), 55-63.

Moyo, B., Masika, P. J., Hugo, A. and Muchenje, V. (2011). Nutritional characterization of Moringa (Moringa oleifera Lam.) leaves. *African Journal of Biotechnology 10*(60), 1295-12933. doi: 10.5897/AJB10.1599

Mukherjee, P. K., Ponnusankar, S., Pandit, S., Hazam, P. K., Ahmmed, M. and Mukherjee, K. (2011). Botanicals as medicinal food and their effects on drug metabolizing enzymes. *Food and chemical toxicology: an international journal published for the British Industrial Biological Research Association,, 49*(12), 3142.

Mukhopadhyay, S., •, P. K. P., Sinha, N., Das, D. N. and Bhutia, S. K. (2014). Autophagy and apoptosis: where do they meet? *Apoptosis, 19*(4), 555-566. doi: 10.1007/s10495-014-0967-2

Muthu, C., Ayyanar, M., Raja, N. and Ignacimuthu, S. (2006). Medicinal plants used by traditional healers in Kancheepuram District of Tamil Nadu, India. *Journal of Ethnobiology and ethnomedicine, 2*(1), 1.

Nash, K. M., Rockenbauer, A. and Villamena, F. A. (2012). Reactive nitrogen species reactivities with nitrones: theoretical and experimental studies. *Chemical research in toxicology, 25*(8), 1581-1597.

Nebert, D. W. and Dalton, T. P. (2006). The role of cytochrome P450 enzymes in endogenous signalling pathways and environmental carcinogenesis. *NATURE REVIEWS| CANCER, 6*, 947.

Nebert, D. W. and Russell, D. W. (2002). Clinical importance of the cytochromes P450. *The Lancet, 360*(9340), 1155-1162.

Niemand, C., Nimmesgern, A., Haan, S., Fischer, P., Schaper, F., Rossaint, R., Heinrich, P. C. and Müller-Newen, G. (2003). Activation of STAT3 by IL-6 and IL-10 in primary human macrophages is differentially modulated by suppressor of cytokine signaling 3. *The journal of immunology, 170*(6), 3263-3272.

Niki, E., Yoshida, Y, Saito, Y. and Noguchi, N. (2005). Lipid peroxidation: mechanisms, inhibition, and biological effects. *Biochemical and biophysical research communications,, 338*(1), 668-676.

Nussbaum, R. L. (2005). Mining yeast in silico unearths a golden nugget for mitochondrial biology. *The Journal of Clinical Investigation, 115*(10), 2689-2691. doi: 10.1172/JCI26625.

Oboh, G., Ademiluyi, A. O., Ademosun, A. O., Olasehinde, T. A., Oyeleye, S. I., Boligon, A. A. and Athayde, M. L. (2015). Phenolic Extract from Moringa oleifera Leaves Inhibits Key Enzymes Linked to Erectile Dysfunction and Oxidative Stress in Rats' Penile Tissues. *Biochemistry research international, 2015*.

Olive, P. L. and Banáth, J. P. (2006). The comet assay: a method to measure DNA damage in individual cells. . *Nature Protocols-electronic edition, 1*(1), 23.

Orrenius, S. (2007). Reactive oxygen species in mitochondria-mediated cell death. *Drug metabolism reviews, 39*(2-3), 443-455.

Pamok, S., Vinitketkumnuen, S. S. U. and Saenphet, K. (2012). Antiproliferative effect of Moringa oleifera Lam. and Pseuderanthemum palatiferum (Nees) Radlk extracts on the colon cancer cells. *Journal of Medicinal Plants Research, 6*(1), 139-145.

Pandey, K. B. and Rizvi, S. I. (2009). Plant polyphenols as dietary antioxidants in human health and disease. *Oxidative medicine and cellular longevity, 2*(5), 270-278.

Parrotta, J. A. (1993). Moringa Oleifera Lam: Resedá, Horseradish Tree, Moringaceae, Horseradish-tree Family. *International Institute of Tropical Forestry, US Department of Agriculture, Forest Service.*

Pereira, F. S., Galvão, C. C., de Lima, V. F., da Rocha, M. F., Schuler, A. R., da Silva, V. L., & de Lima Filho, N. M. (2016). The versatility of the Moringa oleifera oil in sustainable applications. *OCL*, *23*(6), A601.

Pillay, P., Phulukdaree, A., Chuturgoon, A. A., Du Toit, K. and Bodenstein, J. (2013). The cytotoxic effects of Scilla nervosa (Burch.) Jessop (Hyacinthaceae) aqueous extract on cultured HepG2 cells. *Journal of ethnopharmacology*, *145*(1), 200-204.

Poyton, R. O., Ball, K. A. and Castello, P. R. (2009). Mitochondrial generation of free radicals and hypoxic signaling. *Trends in Endocrinology & Metabolism*, *20*(7), 332-340.

Prakash, D., Suri, S., Upadhyay, G. and Singh, B. N. (2007). Total phenol, antioxidant and free radical scavenging activities of some medicinal plants. *International Journal of Food Sciences and Nutrition*, *58*(1), 18-28.

Puntarulo, S. and Cederbaum, A. I. (1998). Production of reactive oxygen species by microsomes enriched in specific human cytochrome P450 enzymes. *Free Radical Biology and Medicine*, *24*(7), 1324-1330.

Rahman, K. (2007). Studies on free radicals, antioxidants, and co-factors. *Clinical interventions in aging*, *2*(2), 219.

Ramachandran, C., Peter, K. V. and Gopalakrishnan, P. K. (1980). Drumstick (Moringa oleifera): A Multipurpose Indian Vegetable. *Economic Botany*, *34*(3), 276-283.

Rathi, B. S., Bodhankar, S. L. and Baheti, A. M. (2006). Evaluation of aqueous leaves extract of Moringa oleifera Linn for wound healing in albino rats. *Indian journal of experimental biology*, *44*(11), 898.

Repetto, M., Boveris, A. and Semprine, J. (2012). *Lipid peroxidation: chemical mechanism, biological implications and analytical determination.* . INTECH Open Access Publisher.

Reuter, S., Gupta, S. C., Chaturvedi, M. M. and Aggarwal, B. B. (2010). Oxidative stress, inflammation, and cancer: How are they linked? *Free Radical Biology and Medicine*, *49*(11), 1603-1616.

Riss, T. L., Moravec, R. A., Niles, A. L., Benink, H. A., Worzella, T. J. and Minor, L. (2015). Cell viability assays.

Roloff, A., Weisgerber, H., Lang, U. and Stimm, B. (2009). Moringa oleifera LAM., 1785. . *Sea*, *10*(10).

Rozovski, U., Harris, D. M., Li, P., Liu, Z., Wu, J. Y., Grgurevic, S., Faderl, S., Ferrajoli, A., Wierda, W. G., Martinez, M. and Verstovsek, S. (2016). At High Levels, Constitutively Activated STAT3 Induces Apoptosis of Chronic Lymphocytic Leukemia Cells. . *The Journal of Immunology*, *196*(10), 4400-4409.

Sakpere, A. M. (2016). Effect of light regime and water stress on germination and seedling growth of moringa oleifera lam. *FUTA Journal of Research in Sciences*, *11*(2), 369-377.

Schmidt-Arras, D. and Rose-John, S. (2016). IL-6 pathway in the liver: From physiopathology to therapy. *Journal of hepatology*, *64*(6), 1403-1415.

Shanker, K., Gupta, M. M., Santosh K. Srivastava, Bawankule, D. U., Pal, A. and Khanuja, S. P. S. (2007). Determination of bioactive nitrile glycoside(s) in drumstick (Moringa oleifera) by reverse phase HPLC. *Food Chemistry*, *105*(1), 376-382.

Sherlock, S. and Dooley, J. (2008). *Diseases of the liver and biliary system*. : John Wiley & Sons.

Silva, K. A. S., Dong, J., Dong, Y., Dong, Y., Schor, N., Tweardy, D. J., Zhang, L. and Mitch, W. E. (2015). Inhibition of Stat3 activation suppresses caspase-3 and the ubiquitin-proteasome system, leading to preservation of muscle mass in cancer cachexia. . *Journal of Biological Chemistry, 290*(17), 11177-11187.

Singh, B. N., Singh, B. R., Singh, R. L., Prakash, D., Dhakarey, R., Upadhyay, G. and Singh, H. B. (2009). Oxidative DNA damage protective activity, antioxidant and anti-quorum sensing potentials of Moringa oleifera. *Food and Chemical Toxicology, 47*(6), 1109-1116.

Singh, N. P., McCoy, M. T., Tice, R. R. and Schneider, E. L. (1988). A simple technique for quantitation of low levels of DNA damage in individual cells. *Experimental cell research, 175*(1), 184-191

Soldatow, V. Y., LeCluyse, E. L., Griffith, L. G. and Rusyn, I. (2013). In vitro models for liver toxicity testing. *Toxicology research, 2*(1), 23-39.

Spandana, U. and Srikanth, P. (2016). A Review on Meracle tree: Moringa oleifera. *Journal of Pharmacognosy and Phytochemistry, 5*(6), 189.

Sreelatha, S., Jeyachitra, A. and Padma, P. R. (2011). Antiproliferation and induction of apoptosis by *Moringa Oleifera* leaf extract on human cancer cells. *Food and Chemical Toxicology, 49*(6), 1270-1275. doi: 10.1016/j.fct.2011.03.006

Sreelatha, S. and Padma, P. R. (2009). Antioxidant activity and total phenolic content of Moringa oleifera leaves in two stages of maturity. *Plant foods for human nutrition, 64*(4), 303-311.

Stevens, G. C., Baiyeri, K. P. and Akinnnagbe, O. (2013). Ethno-medicinal and culinary uses of Moringa oleifera Lam. in Nigeria. . *Journal of Medicinal Plants Research, 7*(13), 799-804.

Stockert, J. C., Blázquez-Castro, A., Cañete, M., Horobin, R. W. and Villanueva, Á. (2012). MTT assay for cell viability: Intracellular localization of the formazan product is in lipid droplets. *Acta histochemica, 114*(8), 785-796.

Stohs, S. J. and Hartman, M. J. (2015). Review of the safety and efficacy of Moringa oleifera. *Phytotherapy Research, 29*(6), 796-804.

Tarpey, M. M., Wink, D. A. and Grisham, M. B. (2004). Methods for detection of reactive metabolites of oxygen and nitrogen: in vitro and in vivo considerations. *American Journal of Physiology-Regulatory, Integrative and Comparative Physiology, 286*(3), R431-R444.

Tiloke, C., Phulukdaree, A. and Chuturgoon, A. A. (2013). The antiproliferative effect of Moringa oleifera crude aqueous leaf extract on cancerous human alveolar epithelial cells. *BMC complementary and alternative medicine, 13*(1), 226.

Tiloke, C., Phulukdaree, A. and Chuturgoon, A. A. (2016). The Antiproliferative Effect of Moringa oleifera Crude Aqueous Leaf Extract on Human Esophageal Cancer Cells. *Journal of medicinal food, 19*(4), 398-403.

Tsikas, D. (2007). Analysis of nitrite and nitrate in biological fluids by assays based on the Griess reaction: appraisal of the Griess reaction in the L-arginine/nitric oxide area of research. *Journal of Chromatography B, 851*(1), 51-70.

Wang, F., Yang, J. L., Yu, K. K., Xu, M., Xu, Y. Z., Chen, L., Lu, Y. M., Fang, H. S., Wang, X. Y., Hu, Z. Q. and Li, F. F. (2015). Activation of the NF-κB pathway as a mechanism of

alcohol enhanced progression and metastasis of human hepatocellular carcinoma. *Molecular cancer, 14*(1).

Wang, H., Lafdil, F., Wang, L., Park, O., Yin, S., Niu, J., Miller, A. M., Sun, Z. and Gao, B. (2011). Hepatoprotective versus oncogenic functions of STAT3 in liver tumorigenesis. *The American journal of pathology, 179*(2), 714-724.

Wang, X. (2001). The expanding role of mitochondria in apoptosis. *GENES & DEVELOPMENT, 15*(22), 2922-2933.

Waris, G. and Ahsan, H. (2006). Reactive oxygen species: role in the development of cancer and various chronic conditions. *Journal of carcinogenesis, 5*(1), 14.

Waterman, C., Cheng, D. M., Rojas-Silva, P., Poulev, A., Dreifus, J., Lila, M. A. and Raskin, I. (2014). Stable, water extractable isothiocyanates from Moringa oleifera leaves attenuate inflammation in vitro. *Phytochemistry, 103*, 114-122.

Wei, T., Chen, C., Hou, J., Xin, W. and Mori, A. (2000). Nitric oxide induces oxidative stress and apoptosis in neuronal cells. *Biochimica et Biophysica Acta (BBA)-Molecular Cell Research, 1498*(1), 72-79.

Westerink, W. M. and Schoonen, W. G. (2007). Cytochrome P450 enzyme levels in HepG2 cells and cryopreserved primary human hepatocytes and their induction in HepG2 cells. *Toxicology in Vitro, 21*(8), 1581-1591.

Yadav, S. and Srivastava, J. (2016). Moringa Oleifera: A Health Promising Plant with Pharmacological Characters. *Indo Global Journal of Pharmaceutical Sciences*, *6*(1), 24-33.

Yan, T., Lu, L., Xie, C., Chen, J., Peng, X., Zhu, L., Wang, Y., Li, Q., Shi, J., Zhou, F. and Hu, M. (2015). Severely Impaired and Dysregulated Cytochrome P450 Expression and Activities in Hepatocellular Carcinoma: Implications for Personalized Treatment in Patients *Molecular cancer therapeutics, 14*(12), 2874-2886.

Yin, H., Xu, L. and Porter, N. A. (2011). Free radical lipid peroxidation: mechanisms and analysis. . *Chemical reviews, 111*(10), 5944-5972.

Yu, H., Pardoll, D. and Jove, R. (2009). STATs in cancer inflammation and immunity: a leading role for STAT3. *Nature Reviews Cancer, 9*(11).

Yuan, C. H., Filippova, M. and Duerksen-Hughes, P. (2012). Modulation of Apoptotic Pathways by Human Papillomaviruses (HPV): Mechanisms and Implications for Therapy. *Viruses, 4*(12), 3831-3850. doi: 10.3390/v4123831

Zangar, R. C., Davydov, D. R. and Verma, S. (2004). Mechanisms that regulate production of reactive oxygen species by cytochrome P450. *Toxicology and applied pharmacology, 199*(3), 316-331.

Zatloukalová, J. (2008). *Deregulation of cell proliferation and apoptosis by xenobiotics and cytostatics*. (PřF D-BI4 Biologie Doktorský studijní program), Masarykova Univerzita.

Zhang, W.-l. (2011). The role of inflammation in breast cancer and prostate cancer *Clinical oncology and cancer research, 8*(2), 77-84.

APPENDICES

APPENDIX A

$HepG_2$ cells were treated with a range of MOE concentration (0 – 4 000 µg/ml) over a 72 h period. A dose-dependent decrease in $HepG_2$ cell viability was observed and an IC_{50} of 754.0 µg/ml was determined (Appendix Table 1).

Table 1: The determination of the IC_{50} using the cell viability (MTT) assay.

MOE Concentration (µg/ml)	Average Absorbance	% Viability	Log[MOE]
0	1.14533	100	
250	0.93600	82	2.39794
500	0.85867	75	2.69897
1 000	0.53333	47	3.00000
1 500	0.49633	43	3.17609
2 000	0.41433	36	3.30103
3 000	0.41467	36	3.47712
4 000	0.39733	35	3.60206

APPENDIX B

Table 1: Components Present in Eagles Minimum Essentials Media

COMPONENT	CONCENTRATION
Inorganic Salts	
CaCl2.2H2O	186.0
KCL	400.0
KH2PO4	60.0
MgSO4.7H2O	200.0
NaCl	8 000.0
NaHCO3	350.0
Na2HPO4.7H2O	90.0
Other Components	
Glucose	1 000.0
Phenol Red	20.0
Amino Acids	
L-Arginine-HCl	126.4
L-Cysteine	24.0
L-Histidine-HCl.H2O	42.0
L-Isoleucine	52.4
L-Leucine	52.4
L-Lysine-HCl	73.0
L-Methionine	15.0
L-Phenylalanine	33.0
L-Threonine	47.6
L-Tryptophan	10.2
L-Tyrosine	47.6
L-Valine	46.8
Vitamins	
D-Capantothenate	1.0
Choline Chloride	1.0
Folic acid	1.0
i-Inositol	2.0
Nicotinamide	1.0
Pyridoxine	1.0
Riboflavin	0.1
Thiamine-HCl	1.0

APPENDIX C

Table 1: The determination of the nitrates and nitrites standard reference curve.

Nitrite Standard Concentrations (µM)	OD1	OD2	OD3	Average OD
0	0.02	0.018	0.018	0.018667
12.5	0.074	0.068	0.071	0.071
25	0.153	0.14	0.137	0.143333
50	0.263	0.239	0.234	0.245333
100	0.484	0.434	0.455	0.457667
200	0.938	0.907	0.918	0.921

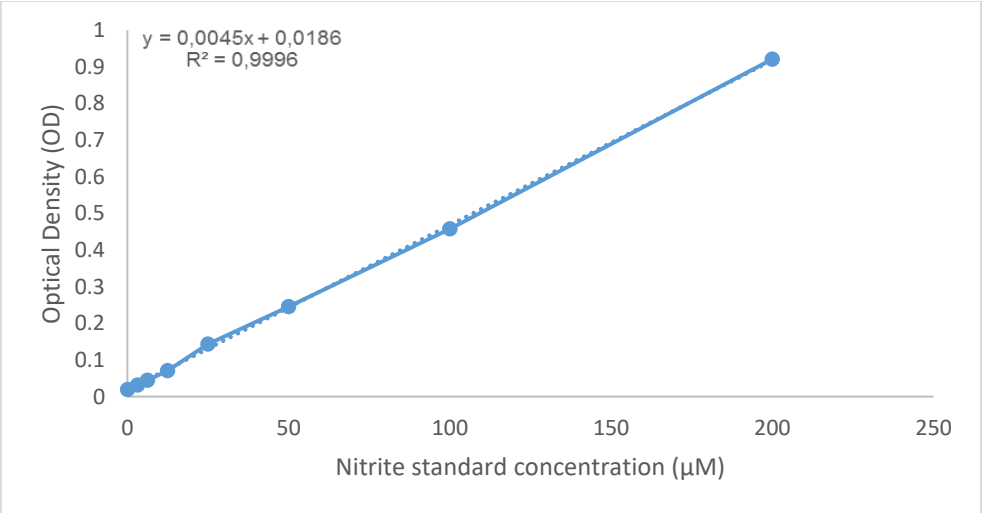

Figure 1: Nitrates and nitrites Standard reference curve used to determine nitrates and nitrites concentration in samples.

APPENDIX D

Table 1: Determination of the IL-6 standard reference curve.

Standard Concentration (pg/ml)	Average OD	Average OD - Average Blank OD
0	0.349	-1.003
4.7	0.3825	-0.9695
9.4	0.4165	-0.9355
18.8	0.5095	-0.8425
37.5	0.5755	-0.7765
75	0.8325	-0.5195
150	1.1975	-0.1545
300	2.0345	0.6825
Blank	1.003	

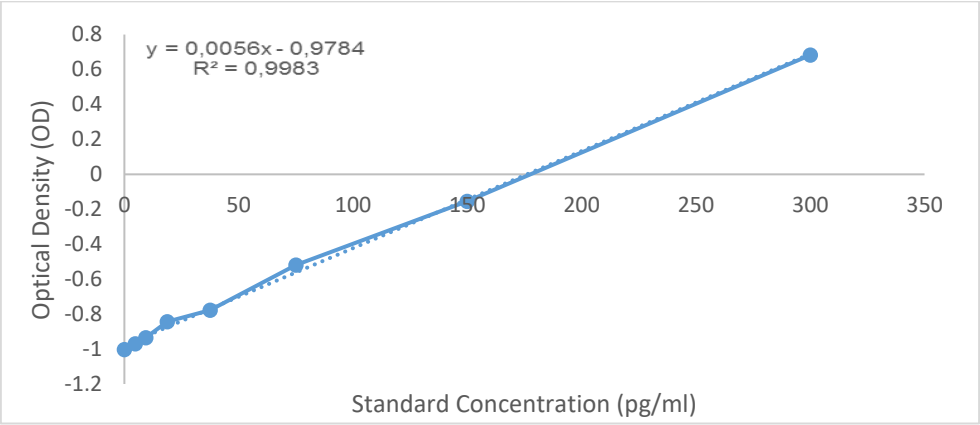

Figure 1: Standard reference curve using a range of known IL-6 concentrations for determination of sample cytokine concentrations using ELISA.

Table 2: Determination of the TNF-α standard reference curve.

Standard Concentration (pg/ml)	Average OD	Average OD - Average Blank OD
0	0.147	-0.2605
7.8	0.146	-0.2615
15.6	0.168	-0.2395
31.3	0.232	-0.1755
62.5	0.3715	-0.036
125	0.585	0.1775
250	1.0505	0.643
500	1.8785	1.471
Blank	0.2605	

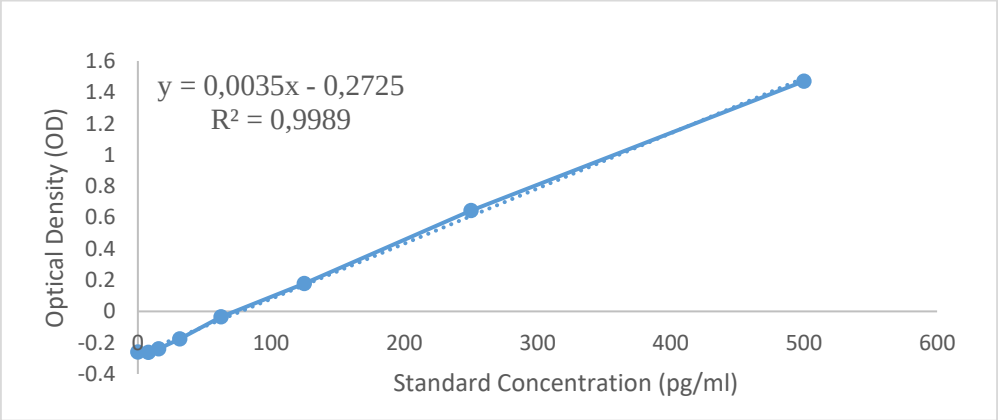

Figure 2: Standard reference curve using a range of known TNF-α concentrations for determination of sample cytokine concentrations using ELISA.

Table 3: Determination of the IL-10 standard reference curve.

Standard Concentration (pg/ml)	Average OD	Average OD - Average Blank OD
0	0.258	-0.6825
7.8	0.177	-0.7635
15.6	0.2965	-0.644
31.3	0.223	-0.7175
62.5	0.3455	-0.595
125	0.4745	-0.466
250	0.774	-0.1665
500	1.012	0.0715
Blank	0.6825	

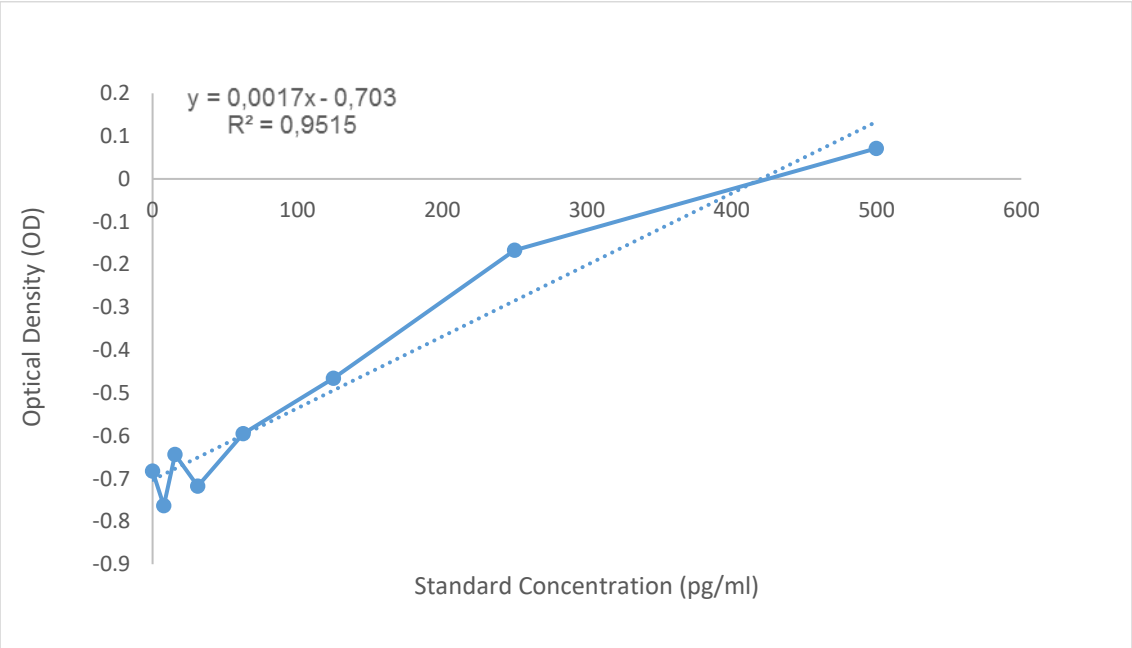

Figure 3: Standard reference curve using a range of known IL-10 concentrations for determination of sample cytokine concentrations using ELISA.

Table 4: Determination of the IL-1β standard reference curve.

Standard Concentration (pg/ml)	Average OD	Average OD - Average Blank OD
0	0.106	-0.2605
3.9	0.1115	-0.255
7.8	0.161	-0.2055
15.6	0.218	-0.1485
31.3	0.351	-0.0155
62.5	0.594	0.2275
125	1.0335	0.667
250	1.8205	1.454
Blank	0.2605	

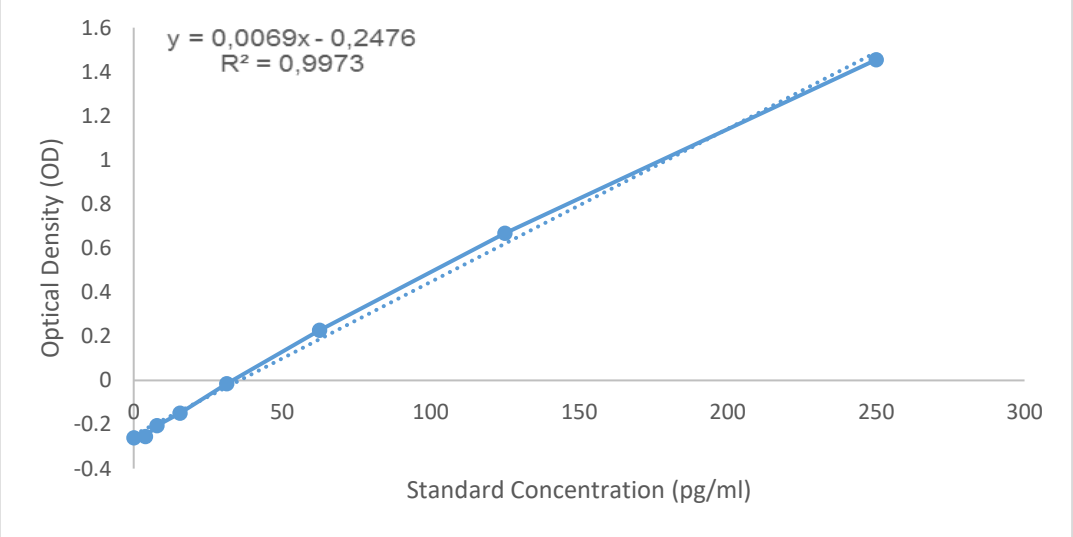

Figure 4: Standard reference curve using a range of known IL-1β concentrations for determination of sample cytokine concentrations using ELISA.

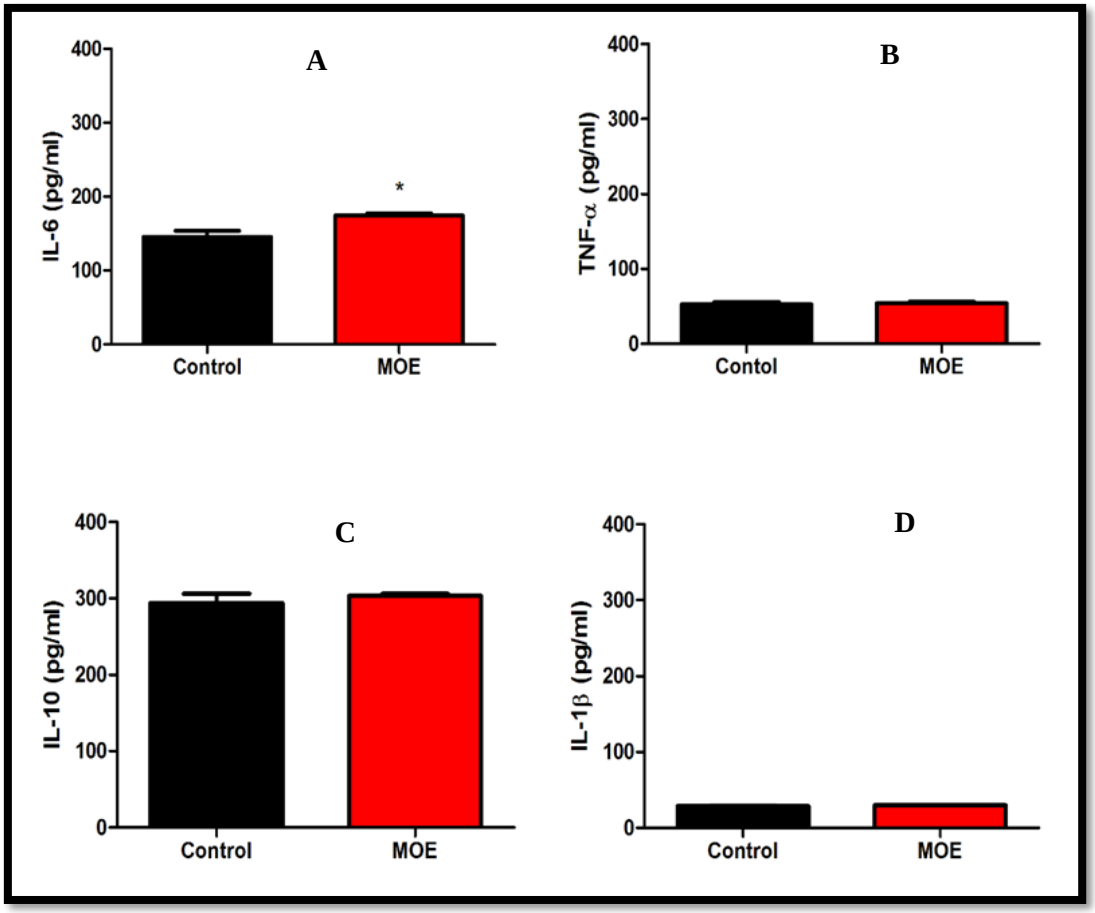

Figure 5: **A.** IL-6 concentration was significantly higher in cells exposed to MOE compared to control cells ($p < 0.05$). There was a non-significant increase in **B.** TNF-α, **C.** IL-10 and **D.** IL-1β ($p > 0.5$).

APPENDIX E

Caspase Activity

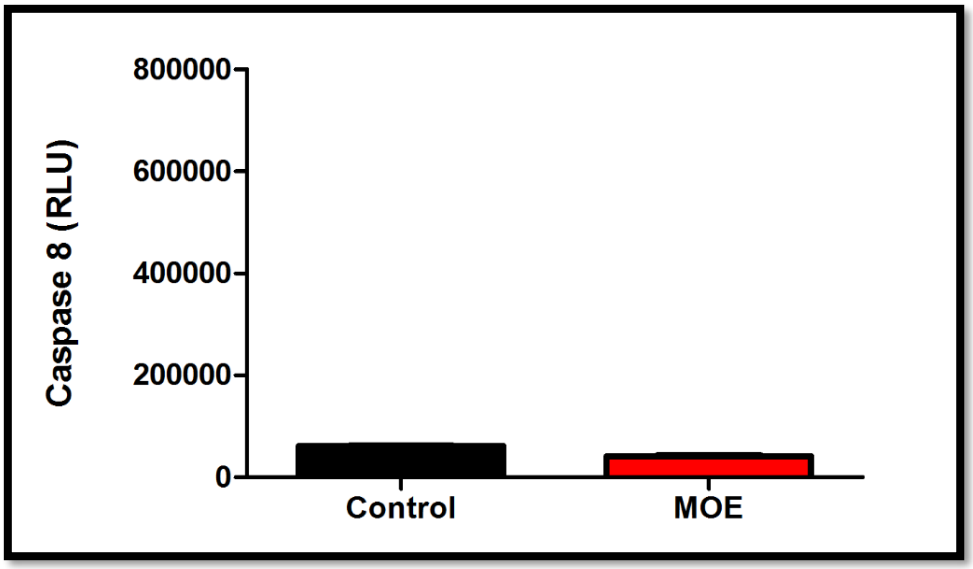

Figure 1: The activity of caspase 8 was non-significantly decreased in cells exposed to MOE compared to control cells ($p > 0.05$).

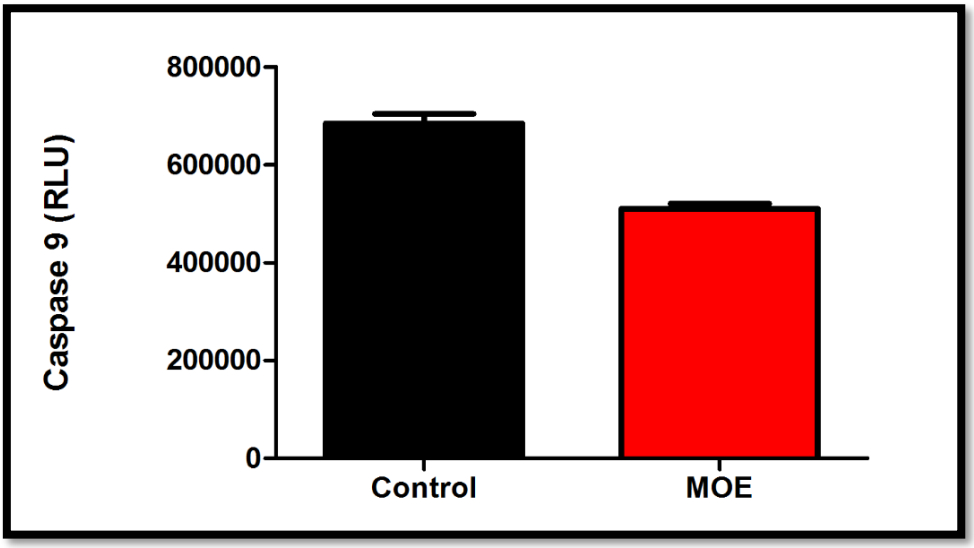

Figure 2: The activity of caspase 9 was non-significantly decreased in cells exposed to MOE compared to control cells ($p > 0.05$).

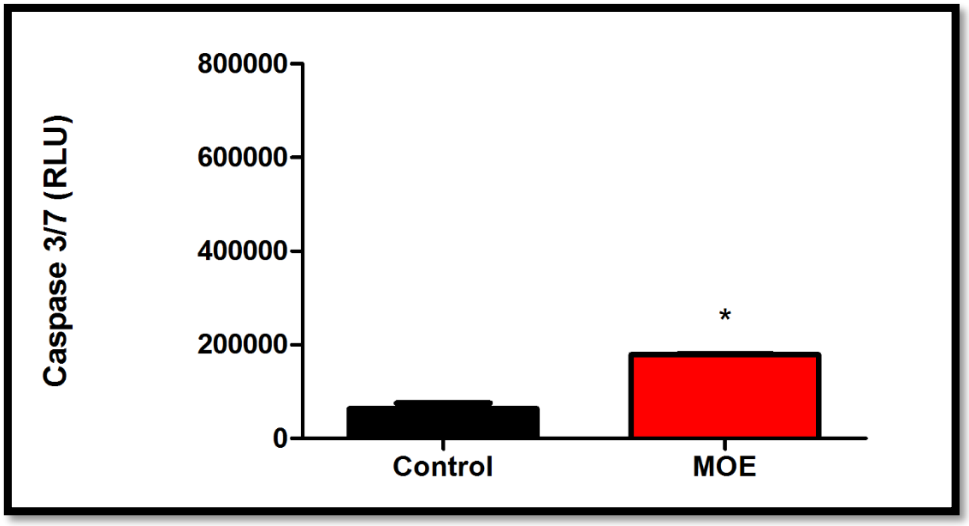

Figure 3: Caspase 3/7 activity was significantly higher in cells exposed to MOE compared to control cells (* $p < 0.05$).

APPENDIX F

Table 1: Protein Quantification and Standardisation using Bovine Serum Albumin (BSA).

Protein Standard (mg/ml)	OD1	OD2	OD3	Average OD
0	0	0.114	0.112	0.075333333
0.2	0.498	0.502	0.591	0.530333333
0.4	0.8	0.831	0.72	0.783666667
0.6	1.071	1.055	1.135	1.087
0.8	1.471	1.396	1.347	1.404666667
1	1.725	1.549	1.67	1.648

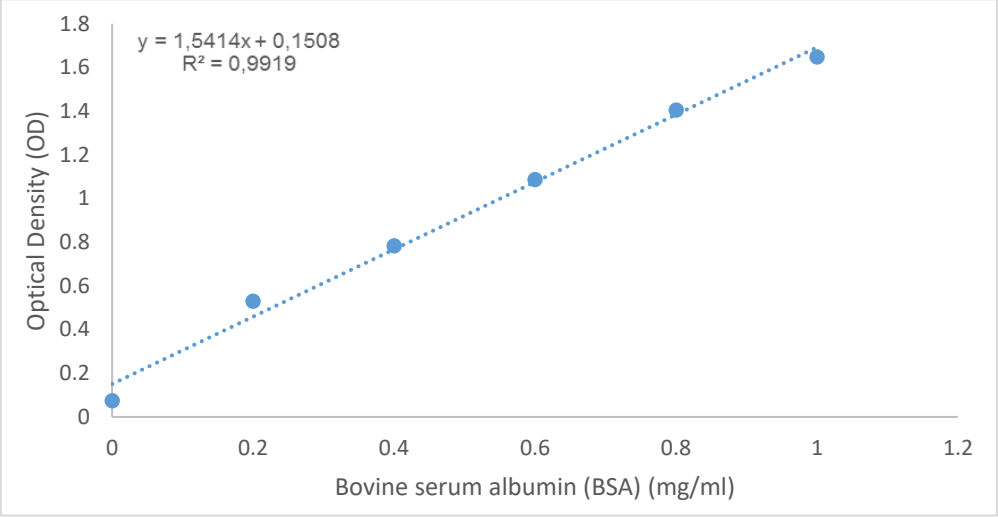

Figure 1: Standard calibration curve using a range of known bovine serum albumin concentrations for determination of sample protein concentrations using the bicinchoninic acid assay.

Table 2: Standardisation of protein using the standard calibration curve for Sodium dodecyl sulphate polyacrylamide gel electrophoresis.

	Average OD	Protein (mg/ml)	C2 (mg/ml)	V2 (µl)	V1 (µl)
Control	3.8535	2.4	1.5	150	93.75
MOE	3.6945	2.3	1.5	150	97.83